To the Graduate Council:

I am submitting herewith a thesis written by Robert M. Dean entitled "Water and Solute Transporting Properties of Soybean Nodulin 26: an Integral Symbiosome Membrane Protein". I have examined the final copy of this thesis for form and content and recommend that it be accepted in partial fulfillment of the requirements for the degree of Master of Science, with a major in Biochemistry.

Daniel M. Roberts, Major Professor

We have read this thesis
and recommend its acceptance:

Elizabeth E Howell

Accepted for the Council:

Associate Vice Chancellor and
Dean of the Graduate School

Water and Solute Transporting Properties of Soybean Nodulin 26: an Integral Symbiosome Membrane Protein

A Thesis

Presented for the

Master of Science

Degree

The University of Tennessee, Knoxville

Robert M. Dean

December 1997

ACKNOWLEDGEMENTS

I would like to express the much deserved gratitude owed to my major professor, Dr. Daniel M. Roberts. He put in the extra time and effort to assure that I developed the mental and technical skills required in the discipline of biochemistry. He taught me to approach a problem not with an "assembly line approach" but meticulously and thoroughly. It was through his guidance that I learned the importance of aggressively pursuing the problem at hand and putting it above all other priorities. This aggressive solution to a scientific problem is key to success in this line of work and enabled me to be productive as a graduate student and will ensure my future successes in this vocation. Additionally he taught me that nothing less than "top quality" is acceptable. For these things I am grateful.

I would also like to thank Dr. Elizabeth Howell and Dr. Jim Hall from my Master's committee for their helpful comments and highly constructive criticisms. I would like to further thank Dr. Elizabeth Howell for the use of her stopped-flow fluorimeter and spectrofluorimeter which were crucial to the completion of this work. Also I would like to thank the members of her laboratory, Fred West, Brad Hamilton, and Brad Strader for their help and hospitality during the times that I worked in their laboratory. I would also like to thank both the faculty and graduate students of the Department of Biochemistry at The University of Tennessee, Knoxville for the times they provided help over the last few years.

I would like to thank Dr. Evans Roth, University of Tennessee, Knoxville for the electron micrograph of the soybean nodule infected and uninfected cell. I would like to thank James Guenther, Dick Williams, and Dr. John Dunlap for providing electron micrographs of liposomes which I could use to determine the liposome diameters and also for their photography assistance in developing several of the proofs displayed in this manuscript. I would like to thank Dr. Peter Gresshoff, The University of Tennessee, Knoxville for providing greenhouse space for the cultivation of soybeans.

I would like to acknowledge my collaborators. Dr. Grischa Chandy and Dr. James Hall at the University of California, Irvine who conducted the oocyte experiments discussed here. I would like to acknowledge Dr. Ricky Rivers and Dr. Mark Zeidel from the University of Pittsburgh, who collaborated with us on the SM vesicle studies and who acted as gracious and instructional hosts when I visited their laboratory to learn the stopped-flow fluorimetry technique. I would especially like to thank Dr. Ricky Rivers who allowed me to reside in his home during my trips to the University of Pittsburgh.

I would like to thank the members of our laboratory, both current and past, James Guenther, Jennifer Dodd, Damon Patterson, Kathy Brooks, Dr. Scott Harding, Dr. Chang Hoon Han, and Jung Weon Lee for their advice and help throughout my graduate career. I would like to thank Dr. David Weaver and his

fellow lab workers for their help when I visited Vanderbilt University to learn *Xenopus* oocyte microinjection.

Finally, and most importantly, I would like thank my parents Gwen and Robert P.E. Dean for their encouragement, guidance, love, and support. The values, work ethic, and importance of education that they instilled in me allowed me to become what I am today (for better or for worse). I would also like to thank my sisters, Sarah and Michelle, my Grandmother Irene Jenkins, my Aunt Nancy Reddish, and the rest of my family and friends who believed in me and supported me all these years. You know who you are.

ABSTRACT

Infection of soybean roots by nitrogen fixing *Bradyrhizobium japonicum* leads to expression of plant nodule-specific genes known as nodulins. Nodulin26 is a major component of the symbiosome membrane that encloses the rhizobium bacteroid. Nodulin 26 constitutes 10-15% of the total symbiosome membrane protein and is a member of the aquaporin water channel family. Expression of nodulin 26 and the phosphorylation site mutants S262A and S262D in *Xenopus laevis* oocytes resulted in a 4-fold increase in osmotic water permeability (P_f) over control uninjected oocytes. The addition of 3 mM $HgCl_2$, a known water channel blocker, reduced the P_f to the levels of control oocytes and this inhibition was reversed upon addition of 5 mM β-mercaptoethanol. To further define the biophysical and biochemical properties of nodulin 26 water channels we studied its transport properties in the native symbiosome membrane and in liposomes containing purified, reconstituted nodulin 26. Permeabilities were determined by use of stopped-flow spectrofluorimetry with symbiosome membrane vesicles or nodulin 26 proteoliposomes loaded with the fluorescent indicator dye carboxyfluorescein.

Symbiosome membrane vesicles exhibited a high P_f (0.05 ± 0.003 cm/s, n=15) that was inhibited 92 % upon addition of 0.1 mM $HgCl_2$. This water transport was characterized by a low Arrhenius E_a (3.3 ± 0.4 kcal/mole, n=3) indicating a facilitated means of water transport. Diffusive water permeability (P_d) was

0.0024 ± 0.0002 cm/s (n =3) and the resulting P_f / P_d ratio was 18.3. If water transport is single file through nod26, than the P_f / P_d value of 18.3 suggests 18 water molecules line up single file within the lumen of the pore and estimates the channel length at 49.8 Å. Symbiosome membrane vesicles are also highly permeable to small nonelectrolytes such as formamide and glycerol, but not urea. The formamide and glycerol flux was inhibited 85-90% by $HgCl_2$ suggesting that these solutes are transported through nodulin 26.

To determine if purified nodulin 26 was capable of mediating the water and solute fluxes observed for symbiosome membrane vesicles, nodulin 26 was purified from soybean symbiosome membranes and was reconstituted into liposomes for permeability measurements by stopped-flow spectrofluorimetry. Liposomes containing nodulin 26 exhibited a high P_f (0.012 ± 0.001 cm/s, n=4) which was 4-fold over control pure lipid liposomes. This water permeability was characterized by a low E_a (3.5 ± 1.3 kcal/mole, n=3) and was reduced 67 % upon addition of 1 mM $HgCl_2$. Reconstituted nodulin 26 exhibited a single channel conductance of $3.0 \pm 2.9 \times 10^{-15}$ cm^3/s (n=2) similar to the calculated value for nodulin 26 in symbiosome membrane vesicles of $3.2 \pm 1.2 \times 10^{-15}$ cm^3/s (n=3). This suggests that purified reconstituted nod26 can mediate water flux at levels similar to those observed in the symbiosome membrane. This unit conductance value for nodulin 26 is approximately 30-fold lower than the corresponding value for the "archetypal" water channel aquaporin 1 from red blood cells suggesting that nodulin 26 is an

aquaporin of modest conductance. Reconstituted nodulin 26 was also able to facilitate glycerol transport 40-fold over control liposomes and this glycerol flux was inhibited 94 % upon addition of 1 mM $HgCl_2$ consistent with the glycerol flux properties of symbiosome membrane vesicles. Nodulin 26 appears to be a mulitifunctional aquaporin with water and solute transporting capabilities similar to aquaporin 3, the only other water channel shown to facilitate both water and solute flux.

Overall the data show that symbiosome membrane vesicles contain a mercuric chloride sensitive water and solute transporter and that purified reconstituted nodulin 26 possesses the properties of this transporter.

TABLE OF CONTENTS

CHAPTER PAGE

I. INTRODUCTION....1

Nitrogen fixation and legume nodulation....1

Nodule metabolism and physiology....6

The symbiosome and symbiosome membrane....9

The major intrinsic protein / aquaporin family....14

Structural properties of the MIP family....14

Functional properties of the MIP family....18

The MIP family channel and phosphoprotein, nodulin 26...28

II. MATERIALS AND METHODS....34

Materials....34

Cloning of nod26 constructs into the *Xenopus* expression vector, pXBG-ev1....35

In vitro transcription of nod26 cRNA and expression in *Xenopus laevis* oocytes....35

Bacterial culture and plant growth....38

Soybean SM isolation for permeability measurements....39

Modifications of SM prep for nod26 purification....41

Purification of native nod26 from soybean root nodules....42

Proteoliposome reconstitution....44

Membrane permeability measurements....45

Osmotic water permeability (P_f)....47

Unit conductance (pf)....49

Small nonelectrolyte permeability (P_{solute})....51

CHAPTER PAGE

Diffusive water permeability (P_d) for SM vesicles.....52
Electrophoresis and immunochemical techniques.....53

III. RESULTS.....54
Expression of nod26 confers water permeability to *Xenopus* oocyte membranes.....54
In situ analysis of nod26 water channel properties in isolated SM vesicles.....54
Size distribution of SM vesicles.....59
Osmotic water permeability (P_f) of SM vesicles.....59
Diffusive water permeability (P_d) of SM vesicles.....65
Solute permeability (P_{solute}) of SM vesicles.....66
Water permeability of reconstituted nod26.....69
Proteoliposomes and control liposomes are osmotically sensitive.....73
Osmotic water permeability determinations of nod26 proteoliposomes.....77
Single channel conductance (pf) of nod26 proteoliposomes.....81
Glycerol permeability of nod26 proteoliposomes 84

IV. DISCUSSION.....88
Nod26 and the aquaporin family.....89
Role of nod26 in symbiosis and symbiosome membrane transport.....96

CHAPTER PAGE

LIST OF REFERENCES.....101

VITA.....115

LIST OF TABLES

TABLE PAGE

I. Summary of permeability values for SM vesicles and nod26-containing proteoliposomes.....91

II. Summary of glycerol transport values for SM vesicles and nod26-containing proteoliposomes.....94

LIST OF FIGURES

FIGURE		PAGE
1.	Electron micrograph of infected and uninfected cells from soybean nodules	4
2.	Diagram of a representative soybean nodule infected and uninfected cells	12
3.	Topology and hourglass model of AQP1	16
4.	Deduced amino acid sequence and proposed membrane topology of nodulin 26 (nod26)	19
5.	Partial map of the *Xenopus* expression vector pXBG(nod26)	36
6.	cRNA of nod26 wild type and phosphorylation site mutants confers water channel activity to the *Xenopus* oocyte membrane	55
7.	Nod26 is a major symbiosome membrane protein	57
8.	Representative Western blot used for determination of the concentration of nod26 in SM	58
9.	Representative quasielastic light scattering profile of SM vesicles	60
10.	Illustration of stopped-flow fluorimetry technique used to measure water efflux from carboxyfluorescein loaded vesicles	61
11.	Time course of water efflux from SM vesicles	63
12.	Representative Arrhenius E_a plot of SM water flux as a function of temperature	64
13.	Diffusive water permeability measurements of SM vesicles	67

FIGURE PAGE

14. Illustration of stopped-flow fluorimetry technique used to measure solute efflux from carboxyfluorescein loaded vesicles.....68
15. Representative plots of solute efflux from SM vesicles.....70
16. Histogram of solute permeabilities in both the presence (unfilled bars) and absence (dark bars) of 0.1 mM $HgCl_2$.....71
17. Coomassie-Blue stained gel of purified nod26.....72
18. Coomassie-Blue stained gel of a representative nod26 proteoliposome preparation.....74
19. Electron micrographs of representative nod26 proteoliposome and control liposome preparations.....75
20. Fluorimeter test to verify integrity of vesicle preparations.....76
21. Time course of water efflux from nod26 proteoliposomes and control liposomes.....78
22. Full time course of water efflux from nod26 proteoliposomes and control liposomes.....79
23. Representative Arrhenius plots for water efflux from nod26 proteoliposomes and control liposomes.....80
24. Representative Coomassie-Blue stained gel used for determinations of protein concentrations in nod26 proteoliposomes.....82
25. Determination of unit proteoliposome volume.....83
26. Time course of glycerol efflux from nod26 proteoliposomes and control liposomes.....85

FIGURE PAGE

27. Full time course of glycerol efflux from nod26 proteoliposomes and control liposomes.....86

LIST OF ABBREVIATIONS

ANTS, aminonaphthalenetrisulfonic acid; **AQP**, aquaporin; **AVP**, arginine vasopressin; **BCA**, bicinchronic acid; **BIB**, *Drosophila* big brain protein; **βME**, β-mercaptoethanol; **BSA**, bovine serum albumin; **cAMP**, cyclic adenosine monophosphate; **CCCP**, carbonyl-cyanide; **CDPK**, calmodulin-like domain protein kinase; **CHIP28**, channel forming integral protein of 28,000 molecular weight (same as AQP1); **CF**, carboxyfluorescein; **DEAE**, diethylaminoethyl; **DTT**, dithiothreitol; $\mathbf{E_a}$, Arrhenius activation energy; **EDTA**, ethylenediaminetetraacetic acid; **EGTA**, ethylene glycol bis (ß-amino ethyl ether)-N,N,N',N'-tetraacetic acid; **ENOD**, early nodulin; **FPLC**, fast protein liquid chromatography; **HDS mixer**, high density solution mixer; **HEPES**, N-(2-hydroxyethyl)piperazine-N'-(2-ethanesulfonic acid); **LLC-PK1**, porcine renal epithelial cells; **MES**, 2-(N-morpholino) ethanesulfonic acid; **MIP**, major intrinsic protein (or polypeptide); **Ngm**, nodulin in *Glycine max*; **NMDG**, N-methyl-D-glucamine chloride; **NOD**, late nodulin protein; **nod26**, nodulin 26; **OG**, 1-O-n-octyl-ß-D-glucopyuranoside; $\mathbf{P_d}$, diffusive water permeability; $\mathbf{P_f}$, osmotic water permeability (cm/s); **pf**, unit conductance (cm^3/s); $\mathbf{P_{gly}}$, osmotic glycerol permeability (cm/s); **PKA**, protein kinase A (or cAMP dependent protein kinase); **PIP**, plasma membrane intrinsic protein; **PMSF**, phenylmethylsulfonyl fluoride; $\mathbf{P_{solute}}$, osmotic solute permeability (cm/s); **PVP-40**, polyvinylpyrrolidone (average MW = 40,000); **S262A**, recombinant nodulin 26 with an alanine residue substituted for a serine residue at position 262; **S262D**, recombinant nodulin 26 with an aspartic acid residue substituted for a serine residue at position 262; **SDS-PAGE**, sodium dodecyl sulfate polyacrylamide gel electrophoresis; **SM**, symbiosome membrane; **SuD**, density of nod26 channels per unit suface area; **TIP**, tonoplast intrinsic protein; **Tris**, tris (hydroxymethyl) aminoethane.

CHAPTER I

INTRODUCTION

Nitrogen fixation and legume nodulation.

Successful crop-based agriculture or plant growth in general, is dependent upon the quality of the soil. Fixed nitrogen is a key nutrient without which plants would be unable to thrive. Plants of the family Leguminosae possess the ability to fix atmospheric nitrogen under conditions of limiting soil nitrogen. The ability to fix nitrogen results from a symbiotic relationship between the host legume and its diazotrophic (nitrogen-fixing) symbiont. These diazotrophs are soil bacteria of the family Rhizobiaceae including the generas *Rhizobium*, *Bradyrhizobium*, *Sinorhizobium*, and *Azorhizobium* (Stacey et al., 1992). The establishment of this symbioses involves the formation of a novel plant root organ, the nodule (Govers et al., 1987; Franssen et al., 1992; Kijne, 1992; Mylona et al., 1995; Long, 1996).

Nodulation is governed by a complex exchange of molecular signals between the plant root and the rhizobia bacterium. Flavonoid compounds are secreted by the plant root into the soil (Kijne, 1992; Mylona et al., 1995; Stokkermans, et al., 1995; Long, 1996). These compounds are encountered by rhizobia and induce the transcription of the bacterium nodulation genes (Kijne, 1992;

Mylona et al., 1995; Long, 1996). The product of these nodulation genes are bio-synthetic enzymes which synthesize lipo-oligosaccharides (nod factor) consisting of a tetramer of ß-1,4-linked N-acetylglucosamine residues containing a fatty acid component and other moieties such as fucosyl or sulfate groups (Kijne, 1992; Long et al., 1992; Mylona et al., 1995; Long, 1996). These modifications are proposed to lead to specific interactions between the legume species and a given bacterium species (Long et al., 1992; Mylona et al., 1995; Long, 1996). "Nod factor" is able to induce early nodulation events such as curling of root hairs and cortical cell divisions. Purified nod factor has been shown to induce root hair curling at concentrations as low as 10^{-12} M and can also induce the expression of certain plant genes (Mylona et al., 1995). These processes are necessary for the entrapment of the bacteria and formation of the nodule structure (Faucher et al., 1988, Faucher et al., 1989; Kijne, 1992; Mylona et al., 1995; Long, 1996).

Infection and nodulation process can be divided into three stages : (1) the preinfection stage, (2) infection and nodule organogenesis, and (3) nodule function and maintenance (Libbenga et al., 1973; Newcomb, 1981; Bauer, 1981; Govers et al., 1985; De Lajudie & Huguet, 1988; Franssen et al., 1992; Mylona et al., 1995; Long, 1996). During the preinfection process, rhizobia interact with growing root hairs, producing nod factor, which induces root hair curling and the beginning of the infection process (Turgeon & Bauer, 1982; Turgeon & Bauer, 1985). In *Vicia sativa* nod factor leads to changes in calcium flux, proton efflux,

rearrangements of actin filaments, and increased cytoplasmic streaming (Mylona et al., 1995) These changes occur 5 to 30 minutes after addition of nod factor and are thought to eventually lead to root hair deformation (Mylona et al., 1995). During infection and nodule organogensis, the bacterium partially dissolves the plant cell wall, the plasma membrane invaginates, and new plant cell wall material is deposited leading to the formation of the tubular infection thread (Kijne, 1992; Mylona, 1995). Rhizobia invade the root hair cell and root cortex through the infection thread which grows in the direction of the expanding nodule primordium (Franssen et al, 1992; Mylona et al., 1995; Long, 1996). This nodule primordia arises independently from dedifferentiating root cortex cells. From the tip of the infection thread the bacteria, through endocytosis, are released into the host cell cytoplasm.

The bacteria become surrounded by the plant derived symbiosome membrane (SM) (Roth et al., 1988) (Figure 1). The SM is a membrane specific to the symbiosis and mediates communication and metabolic flux between the plant host and endosymbiont (Streeter, 1995; Day & Udvardi, 1997). The SM also appears to protect the enclosed bacteroid since bacterial mutants that have defective SM undergo premature senescence (Werner et al., 1984; Werner et al., 1985). During the final stage, the rhizobia differentiate into nitrogen fixing bacteroids (Franssen et al., 1992; Mylona et al., 1995; Long et al., 1996).

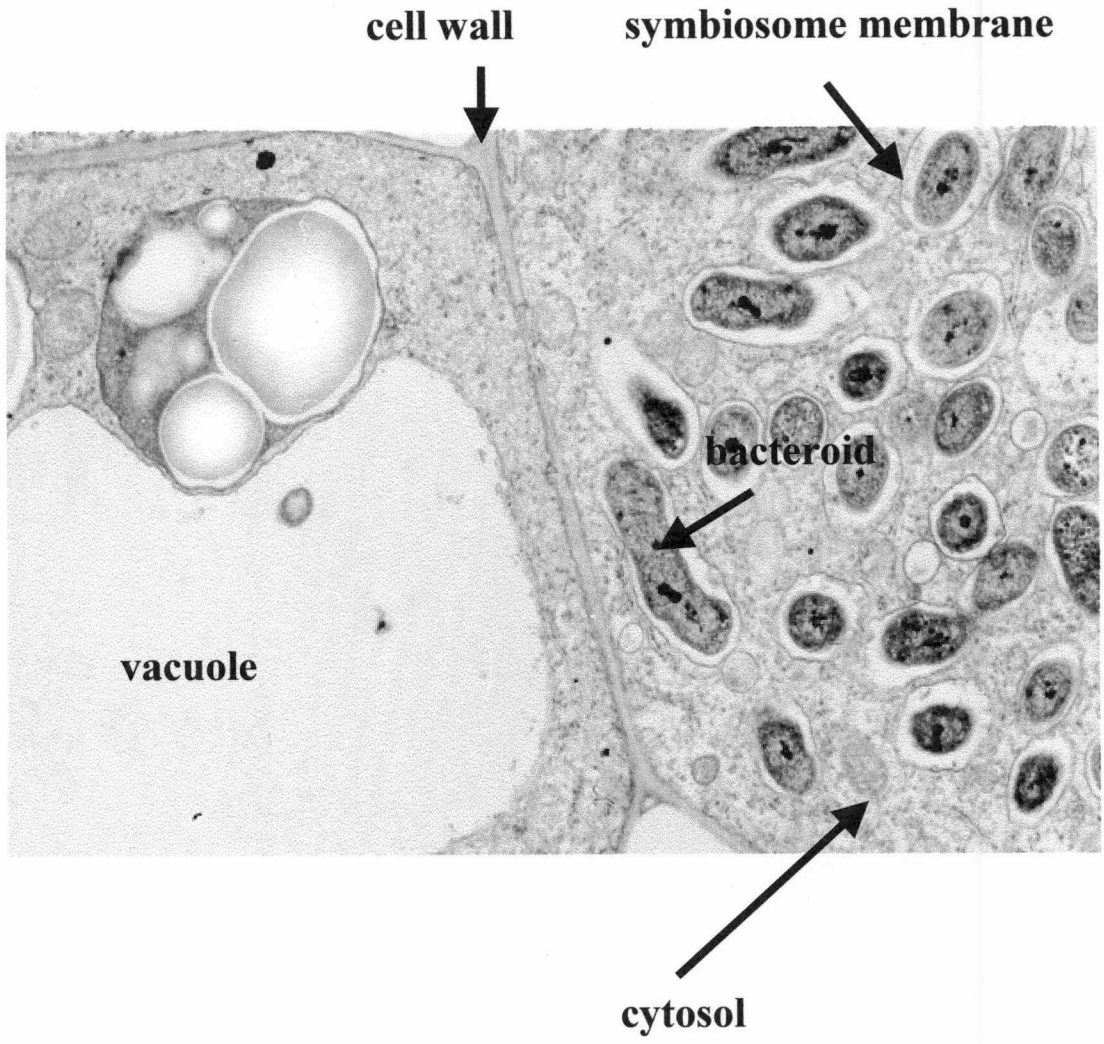

Figure 1. Electron micrograph of infected and uninfected cells from soybean nodules. The infected cell is distinguished by the presence of symbiosomes which enclose *Bradyrhizobium japonicum* bacteroids. The uninfected cell lacks symbiosomes and contains a large vacuole. Electron micrograph was provided by Dr. Evans Roth, University of Tennessee, Knoxville. Final magnification is 12,200 x.

Two types of nodules, determinate or indeterminate, are found on legumes (Newcomb, 1976; Newcomb, 1981; Corby et al., 1983). These classes differ in overall morphology and by the presence or absence of an apical meristem (Franssen et al., 1992) Generally, temperate legumes such as *Pisum*, *Vicia*, *Trifolium*, and *Medicago* possess indeterminate nodules whereas tropical legumes such as *Glycine*, *Phaseolus*, and *Vigna* form determinate nodules (Franssen et al., 1992).

Indeterminate nodules, possess a persistent apical meristem and therefore can be separated into different developmental stages (Newcomb, 1976). The apical meristem is found in the most distal portion of the nodule. This followed by the infection zone, the early symbiotic zone, the late symbiotic zone (area of nitrogen fixation), and finally most proximal to the root, the senescent zone.

In contrast to indeterminate nodules, determinate nodules lack a persistent apical meristem (Newcomb et al., 1979). In determinate nodules growth occurs through cell expansion whereas in indeterminate nodules growth is focused at apical meristem (Franssen et al., 1992). As discussed above, prior to infection by the bacteria, root cortex cells dedifferentiate forming the nodule primordia (Calvert et al., 1984; Franssen et al., 1992). Once infected with rhizobia, determinate nodules continue to divide for approximately one week after the onset of nitrogen fixation (Franssen et al., 1992). Once this mitotic activity has ceased, nodule growth occurs primarily through cell expansion (Franssen et al., 1992).

Morphologically, determinate nodules are composed of three distinct tissue layers: exoderm, central tissue, and endodermis (Newcomb 1976; Newcomb, 1979; Newcomb et al., 1981; Van de Wiel et al., 1990). The central tissue, or the nodule cortex, is the site of nitrogen fixation and consists of both infected and un-infected cells. Infected cells are characterized by diazotrophic bacteroids enclosed within the symbiosome (Roth et al., 1988) (see Figure 1). The innermost layer, the endodermis, is comprised of nodule parenchyma tissue and is the location of the oxygen barrier in the nodule (Tjepkema & Yocum, 1974; Witty et al., 1986; Mylona et al., 1995). The oxygen tension must remain low in the nodule since oxygen will inhibit the bacterial nitrogenase and the fixation of nitrogen (Mylona et al., 1995). The nodule parenchyma contains vascular bundles and differs from the cortical tissue in that it possesses smaller intercellular spaces (Franssen et al., 1992; Mylona et al., 1995).

Nodule metabolism and physiology.

Nodule formation and nitrogen fixation are accompanied by the expression of the host nodulin genes (Legocki et al., 1980). These genes are necessary for the establishment and maintenance of the symbiosis (Legocki et al., 1980; Van Kammen et al., 1984). Nodulin genes are defined *stricto senso* as nodule-specific and are expressed exclusively during the symbiosis, thereby being absent from uninfected roots or other plant organs (Franssen et al., 1992). Nodulins have been

categorized into two types that differ in temporal expression, the early nodulins (ENODs) and late nodulins (NODs).

ENODs are produced early during the nodulation process and are proposed to be involved in the preinfection stage as well as the the infection and nodulation processes (Franssen et al., 1992; Mylona et al., 1995; Long, 1996). Some ENODs are cellular proteins induced by nod factor while other are cell wall components (Franssen et al., 1992; Mylona et al., 1995; Long, 1996). In soybean, GmENOD13, appears to be a cell wall component in the nodule parenchyma. This is the location of the oxygen barrier, in the nodule, which is essential for nitrogen fixation. GmENOD2, similar to GmENOD13, is another cell wall component (Gloudemans et al., 1989). ENODs do not require full nodulation for expression and many can be induced by nod factor alone (Franssen et al., 1992; Mylona et al., 1995; Long, 1996; Minami et al., 1996). The function of most ENOD proteins is unknown (Franssen et al., 1992; Mylona et al., 1995; Long, 1996). A possible exception is the soybean early nodulin, ENOD40. This product is expressed in all cells in the nodule primordia and is also induced in the pericycle of the nodule vascular bundle opposite to the diving cortical cells (Franssen et al., 1992; Mylona et al., 1995; Minami et al., 1996). ENOD40 possesses a phytohormone effect when introduced into the nonlegume tobacco (Van de Sande, 1996). Since ENOD40 has phytohormone activity in tobacco and its induction in the pericycle proceeds the first cortical cell divisions, Bisselling's group propose

that ENOD40 can cause the cytokinin / auxin ratio to change in cortical cells leading to cell division (Mylona et al., 1995; Van de Sande, 1996).

In contrast to ENODs, late nodulins show expression coinciding with the onset of nitrogen fixation, and many have been implicated in the metabolism and transport of carbon, oxygen, and nitrogen (Franssen et al., 1992; Mylona et al., 1995; Day & Udvardi, 1997). The most abundant late nodulin is leghemoglobin, which is present in the cytosol conferring nodule cells their red color. Leghemoglobin constitutes 20% to 30% of the total soluble protein and is responsible for maintaining low oxygen tension in the nodule and providing a facilitated oxygen carrier supporting bacteroid respiration (Wittenberg et al., 1974; Sheehy, et al., 1985; Govers et al., 1986; Fransseen et al., 1992; Werner, 1992). Other late nodulins include a uricase (Ngm-35) in uninfected cells (Bergmann et al., 1983), a catabolic sucrose synthase (Ngm-100) (Thummler & Verma, 1987), and several genes of unknown function.

The SM is the site of several of these late nodulin gene products (Franssen et al., 1992; Mylona et al., 1995; Day & Udvardi, 1997). For example, the soybean SM contains a nodule-specific isoform of choline-kinase I (Mellor et al., 1986). In addition, several cDNA's encoding proteins of unknown function have been found by differential cDNA screening (Fortin et al., 1987; Franssen et al., 1992). For example, the nodulin Ngm-24 has been identified in the SM and is thought to reside on the surface of the SM facing the peribacteroid space (Fischer

& Hennecke, 1987; Fortin et al., 1987; Franssen et al., 1992). Therefore it is not thought to be a membrane transport molecule (Fischer & Hennecke, 1987; Fortin et al., 1987). Another SM nodulin, Ngm23 (Jacobs et al., 1987), is a member of a small gene family and it has been suggested that it may be a metal binding protein based on the occurrence of four highly conserved cysteine residues (Franssen et al., 1992). Perhaps the most well studied SM nodulin is the integral membrane protein nodulin 26 (Fortin et al., 1987; Shiels et al., 1988; Sandal & Marcker, 1988; Weaver et al., 1991). Nodulin 26 and its structure and function are discussed in greater detail below. These proteins likely play a role in maintenace of symbiosis and SM function. Below I discuss further the fuctional properties of this membrane.

The symbiosome and symbiosome membrane.

As discussed earlier, the symbiosome is a nodule-specific organelle delimited by a membrane of plant origin, the symbiosome membrane (SM), that serves as a protective barrier mediating communication and metabolic flux between the plant host and its diazotrophic endosymbiont (Roth et al., 1988; reviewed in Franssen et al., 1992, Streeter, 1995, and Day & Udvardi, 1997).

The primary metabolic exchange across the SM is reduced carbon for reduced nitrogen. Fixed carbon as photosynthate (sucrose) is transported into the cytoplasm of the infected cells where it is metabolized to glucose-6-phosphate by

the actions of the late nodulin catabolic sucrose synthase, Ngm-100 (Thummler & Verma, 1987). Glucose-6-phosphate enters glycolysis and is converted to phosphoenolpyruvate, which is in turn converted into the four carbon dicarboxylate malate, by phosphoenolpyruvatecarboxylase (Werner, 1992). Experimental evidence suggests malate is the primary source of fixed carbon supporting nitrogen fixation. For example, the SM has low permeabilities to mannitol, glucose, fructose, sucrose, glutamate, and proline (Day et al., 1990; Udvardi et al., 1990; Day & Udvardi, 1993) suggesting carbohydrates and amino acids are not the source of fixed carbon driving bacteroid nitrogen fixation. However, dicarboxylates, such as malate and succinate, are readily transported across the SM with rates sufficient to support the fixation of nitrogen (Udvardi et al., 1988; Ou Yang et al., 1990; Li & Day, 1991; Streeter, 1995; Udvardi & Day, 1997). The proposed utilization of malate as a carbon source is supported by the observation that bacterial strains that are defective in dicarboxcylic acid transport (*dct*$^-$) form nodules that are unable to fix nitrogen (*fix*$^-$) (Finan et al., 1981; Ronson et al., 1981; Bolton et al., 1986). However, these bacteria survive within the symbiosomes suggesting malate is not necessary for bacteroid survival but rather is the fuel needed to drive the fixation of nitrogen. Additionally, a promoter regulated by one of the bacteroid nitrogen fixation genes, *nif A*, exists upstream of the *dct* gene suggesting there may be coordinate control of genes involved in nitrogen fixation and the ability of the bacteroid to transport dicarboxylic acids (Ronson & Astwood, 1985; Streeter, 1995).

This fixed carbon provides the endosymbiont with energy that enables nitrogen fixation. Atmospheric nitrogen, at the cost of sixteen ATPs, undergoes reduction to ammonia by the rhizobium nitrogenase (Dean & Jacobson, 1992; Werner, 1992). As illustrated in Figure 2, ammonia is transported out of the symbiosome and is converted to glutamine in the infected cell cytoplasm by the host glutamine synthetase (Dean & Jacobson, 1992; Werner, 1992). Glutamine is incorporated into purines in the plastid and is transported via the plasmodesmata into uninfected cells (Werner, 1992). In the uninfected cell, the fixed nitrogen is incorporated into allantoin in the peroxisomes by the nodulin uricase, Nmg-35, and then finally to allantoic acid which is transported to other plant tissues by the vascular xylem (Bergmann et al., 1983; Mellor & Werner, 1990; Werner, 1992).

The activities of the symbiosome membrane and its components are necessary for the transport of reduced carbon for reduced nitrogen as well as other symbiotic functions (Streeter, 1995; Day & Udvardi, 1997). Characterized transport processes include an inward proton translocating ATPase capable of generating an electrochemical gradient across the SM (Udvardi & Day, 1989; Udvardi et al., 1991; Udvardi & Day, 1997); a dicarboxylate transporter with malate as the preferred substrate (Udvardi et al., 1988; Ou Yang et al., 1990; Li & Day, 1991; Streeter, 1995; Udvardi & Day, 1997); a cation ion channel that is proposed to mediate fixed ammonium efflux (Whitehead et al., 1995; Tyerman et al., 1995; Udvardi & Day, 1997); iron transport (Moreau, 1995; Wittenberg et al., 1996;

LeVier et al., 1996; Udvardi & Day, 1997); and a general anion transport activity (Udvardi et al., 1991; Udvardi & Day, 1997). In addition to these transporters, a calmodulin-like domain protein kinase (CDPK) has been localized on the SM (Weaver et al., 1991; Weaver et al., 1992)

The electrochemical gradient generated by the proton translocating ATP-ase, as well as a concentration gradient generated by the consumption of malate during bacteroid respiration, are thought to drive malate transport (Price et al., 1987; Udvardi et al., 1988; Ou Yang et al., 1990; Li & Day, 1991). This proposal is supported by the finding that the protonophore CCCP which uncouples proton transport and dissipates the proton gradient, also inhibits malate transport (Ou Yang et al., 1990). In addition, respiratory poisons such as KCN destroy malate transport without affecting the electrochemical gradient (Ou Yang et al., 1990) suggesting the electrochemical gradient is not sufficient for transport, and that bacteroid consumption of malate, which establishes a concentration gradient, is also necessary.

To fully understand the intricacies of the symbiosis and the nitrogen fixation process, the proteins associated with nodule formation must be rigorously characterized. None of the symbiosome membrane proteins have been purified and biochemically characterized with the exception of the soybean late nodulin, nodulin 26 (nod26) (Weaver et al., 1991; Miao et al., 1992; Weaver & Roberts, 1992; Weaver et al., 1994; Lee et al., 1995). Comparison of the deduced amino

acid sequence of nod26 with other proteins indicates that it is a member of the major intrinsic protein (MIP) family (Sandal & Marcker, 1988; Shiels et al, 1988; Reizer et al., 1993). Below I summarize the features of this family, and our current understanding of the structure and function of these proteins.

The major intrinsic protein / aquaporin family.

The MIP family is named after the first member to be identified and characterized, major intrinsic polypeptide (MIP) or aquaporin 0 (AQP0) from lens membranes (Takemoto & Hansen, 1981; Gorin et al., 1984). As discussed in detail below, several of the MIP family proteins function as water transporters and the term "aquaporin" was coined for them (Agre et al., 1993). The ubiquitous MIP family dates back 2.5 to 3.0 million years in evolutionary time and is characterized by more than 50 homologous integral membrane channel proteins, each sharing about 30% - 40% identity (Pao et al., 1991; Reizer et al., 1993; Saier, 1994; Park & Saier, 1996).

Structural properties of the MIP family.

Members of the MIP family possess symmetry, with the carboxyl and amino halves showing sequence similarity (Chrispeels & Agre, 1994; Park & Saier, 1996; King & Agre, 1996). In each half of the molecule an invariant asparagine-proline-alanine (NPA) motif is found within a loop region (Chrispeels &

Agre, 1994; Park & Saier, 1996; King & Agre, 1996) (Figure 3). Multiple alignments on MIP family members revealed two regions of sequence similarity encompassing these NPA motifs: (HQA)-(LIVF)-N-P-(AS)-(LIVMF)-(TS)-(LIVFW) and (LIVM)-N-(PL)-A-(LIVR)-(SATD)-(LIVFT)-(GAM)-(LIVPSTA)-(ASKR)-(LIVMF) (Park & Saier, 1996). Hydropathy analysis on various MIP family members predicts hydrophilic (likely cytoplasmic) amino and carboxyl termini that flank six hydrophobic membrane spanning domains (Gorin et al., 1984; Agre et al., 1995; King & Agre, 1996) (Figure 3). This observation is supported by numerous studies as summarized below.

Biochemical and immunoelectron microscopy studies have established that the amino and carboxyl termini of AQP1 project into the cytosol (Smith & Agre, 1991; Nielsen et al., 1993; Zeidel et al., 1994; Agre et al., 1995). The N-glycosylation site in loop A for AQP1 and loop C for AQPs 2-5 establish the extracellular location of these domains (Agre et al., 1995) (Figure 3). Circular dichroism (CD) studies on AQP0 revealed approximately 50% α-helix (α-helixes are common motifs in bilayer spanning proteins) and approximately 20% β-structure (Horwitz & Bok, 1987) and CD studies on the 28,000 MW channel forming integral protein (CHIP28 or AQP1) from red cells showed a similar composition (Van Hoek et al., 1993).

Jung et al. (1994) have proposed the hourglass structural model for the most characterized MIP family member, AQP1. The hourglass model exhibits 2-

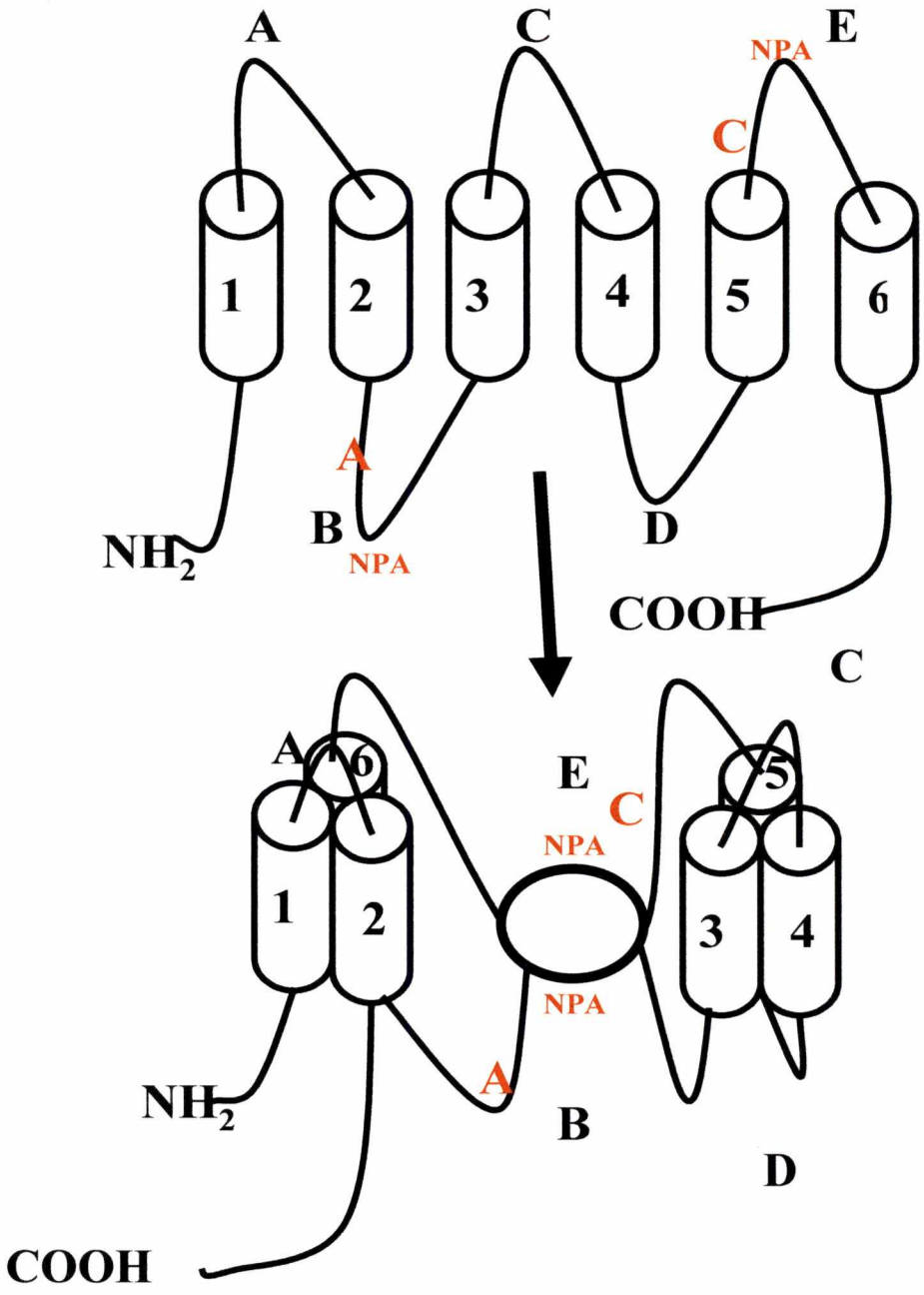

Figure 3. Topology and hourglass model of AQP1. Six bilayer spanning model of AQP1 folding into proposed hourglass structural model. Shown are six transmembrane domains 1-6, extracellular loops (A, C, and E), intracellular loops (B and D), intracellular amino (NH_2) and carboxyl (COOH) termini, mercuric chloride sensitive site cysteine 189 (**C**), and alanine 73 (**A**) which when changed to a cysteine residue also results in mercuric chloride sensitivity. Loops B and E are proposed to form a single aqueous pathway. Adapted from Jung et al. (1994).

fold symmetry with each half containing three membrane spanning regions connected by extracellular loops A,C, and E and intracellular loops B and D while the amino and carboxyl termini project into the cytoplasm (Figure 3). A juxtaposition of the amino and carboxyl halves of the molecule is predicted, resulting in an hourglass structure forming a single aqueous pore involving the NPA motifs in loops B and E (Figure 3). This model is based upon the finding that a cysteine residue (cys189) located in loop C is responsible for inhibition of water flux through the channel upon the addition of mercury and the engineering of another cyteine (ala73cys) residue in a homologous position in the first half of the molecule (loop B) also results in mercury sensitivity (Jung et al., 1994; King & Agre, 1996) (Figure 3). This observation led to the proposal that these residues (each of which is located near the two NPA motifs) are near the channel pore (Jung et al., 1994).

Numerous studies, including freeze fracture on both AQP1 and AQP0 and two and three dimensional crystallography studies on AQP1, indicate that members of the MIP family are present in a tetrameric state in the membrane (Zampighi et al., 1989; Ehring et al., 1990; Verbavatz et al., 1993; Mitra & Yeager, 1994; Walz et al., 1994; Jap & Li, 1995; Cheng et al., 1997; Walz et al., 1997). A recent high resolution (7 Å) three dimensional structure published by Cheng et al. (1997) shows that the AQP1 monomer is composed of six tilted α-helices that span the membrane and verifies that the molecule contains a 2-fold symmetry.

These conclusions are supported by Walz et al. (1997) who have obtained a three dimensional structure for AQP1 at 6 Å resolution. This structure identifies a central region of high density (the X density) that is proposed to contain the regions of loops E and B encompassing the NPA motifs (Walz et al., 1997), and is postulated to be the area of water permeation. Thus, since the six bilayer model (shown for AQP 1 in Figure 3 and nod26 in Figure 4) was proposed by Gorin et al. (1984), a multitude of studies have arisen strongly strengthening the case for such a topology.

Functional properties of the MIP family.

Water is capable of crossing lipid bilayers by simple diffusion with a diffusional water permeability coefficient (P_d) of <0.01 cm/s for most membranes, and a high Arrhenius activation energy (E_a >10 kcal/mole) (Finkelstein, 1987; Chrispeels & Agre, 1994; Brown et al., 1995; Agre et al., 1995; Maurel, 1997). However, it was observed that certain membranes (i.e. erythrocyte membranes) have a water conductance that is too high to be accounted for by simple diffusion and it was postulated that a proteinaceous water transporter must be located in these membranes that facilitates this enhanced activity.

Xenopus laevis oocytes provide a useful system for the study and identification of water channels (Preston et al., 1992; Chrispeels & Agre, 1994; Agre et al., 1995). The oocyte membrane has a very low water permeability, even under

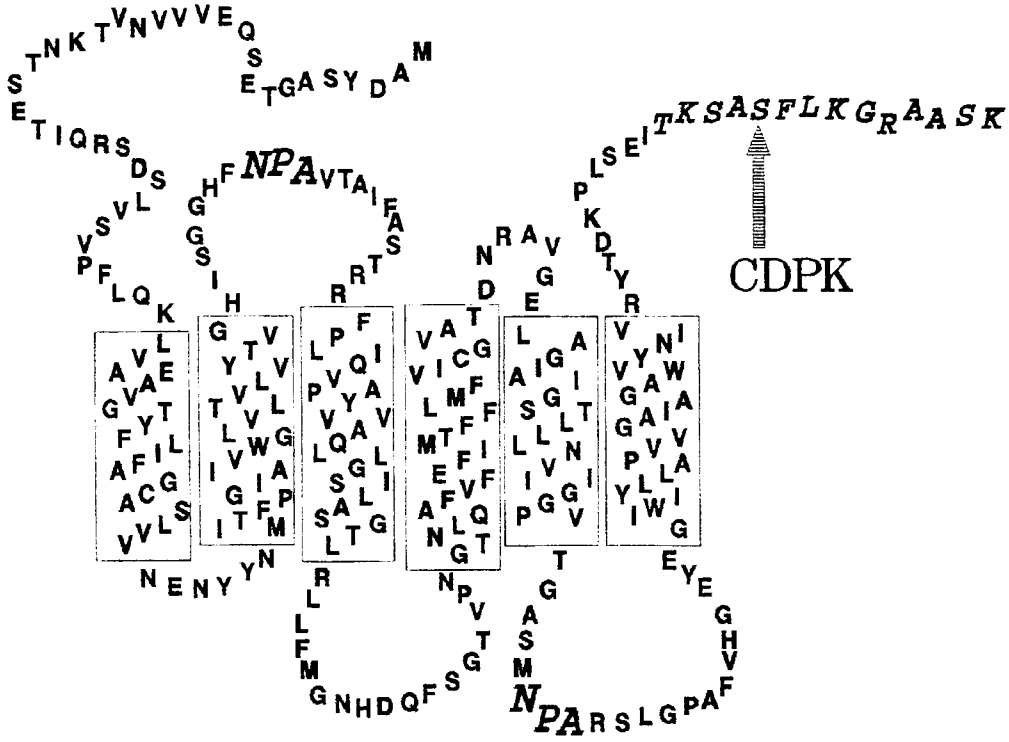

Figure 4. Deduced amino acid sequence and proposed membrane topology of nodulin26 (nod26). The proposed topology is based on hydropathy analysis (Kyte & Doolittle, 1982) assuming a cytosolic localization of the COOH- and NH2-terminal domains based on Miao et al. (1992). Highly conserved "NPA" motifs characteristic of the MIP family are indicated (Reizer et al., 1993) along with the unique site of CDPK phosphorylation (Weaver et al., 1991, 1992).

severe osmotic conditions. The cRNA encoding the protein of interest can be injected into the oocyte and the translation machinery of the oocyte produces the desired gene product. Upon incorporation of the translated protein into the oocyte membrane, evidence for a water channel is an enhanced rate of oocyte swelling under hypoosmotic conditions (Preston et al., 1992; Chrispeels & Agre, 1994; Zampighi et al., 1995; Mulders et al., 1995; Agre et al., 1995; Chandy et al., 1997).

By using this method, the erythrocyte membrane protein AQP1 was first shown to facilitate water flux in a specific manner, leading to a breakthrough in the understanding of how water crosses biological membranes (Preston et al., 1992). More biochemical studies followed in which it was shown that proteoliposomes containing purified AQP1 facilitate an osmotically driven water flux that was as high as 50-fold greater than control lipid vesicles (Zeidel et al., 1995). Purified AQP1 showed an osmotic water permeability coefficient (P_f) of 0.05 cm/s at 37 ° C, an E_a of 3 kcal/mole, and inhibition by 1 mM $HgCl_2$ (Zeidel et al., 1992). The site of mercuric chloride inhibition was later determined to be cysteine 189 by site-directed mutagenesis suggesting this residue is near the pore of the channel (Preston et al., 1993).

Water transporting members of the MIP family are referred to as aquaporins (the official name designated by the Human Genome Nomenclature

Committee) and the mammalain members are numbered AQP0, AQP1, AQP2, etc., based on the order of their identification as water transporters (Agre et al., 1993; Agre et al., 1995). Aquaporins, as demonstrated for AQP1, are "water selective" channels characterized by a high osmotic water permeability (P_f), a low Arrhenius activation energy, an osmotic to diffusive water permeability ratio (P_f / P_d) > 1, and inhibition by mercurial reagents (Finkelstein, 1987; Stein et al., 1990; Chrispeels & Agre, 1994; Brown et al., 1995; Agre et al., 1995; Maurel, 1997). The P_f / P_d ratio is proposed to be equivalent to the number of water molecules which line up single file within the pore of the channel (Finklestein, 1987; Stein et al., 1990; Mathai et al., 1996). The discovery of AQP1 lead to an explosion of research in the area of water transport, and to the identification of a growing list of animal, microbial, and plant water channels and other facilitators.

In addition to AQP1, there are five other known mammalian water channels (for a recent review see King & Agre, 1996). These include the lens fiber protein MIP or AQP0 for which the protein family is named (Mulders et al., 1995; Zampighi et al., 1995; Chandy et al., 1997). The vasopressin-regulated water channel, AQP2 is present in the apical membranes of the kidney collecting duct, and is responsible for concentration of urine (Katsura et al., 1996; Nielsen et al., 1996; Yasui et al., 1997; Fushimi et al., 1997; Knepper, 1997). Individuals with mutations in AQP2 are inflicted with hereditary nephrogenic diabetes insipidus (Van Lieburg et al., 1994; Deen et al., 1995). The unique water channel, AQP3, is lo-

calized on the basolateral membrane of kidney collecting duct cells and possesses water, glycerol, and urea transport activities (Ishibashi et al., 1994; Frigeri et al., 1995; Echevarria et al., 1996; Ishibashi et al., 1997). The mercury insensitive water channel, AQP4, is predominantly located in brain but is also found in epithelial cells and kidney and is thought to be responsible for spinal fluid reabsorption and osmoreception (Jung et al., 1994; Frigeri et al., 1995; Shi & Verkman, 1996; Terris et al., 1995). AQP5 has been found in salivary glands, lacrimal glands, and lung (Raina et al., 1995; Lee et al., 1996; Delporte et al., 1996). As stated above, AQP3 is multifunctional and transports water, glycerol, and urea. It is the only known water channel to exhibit this promiscuous behavior (Ishibashi et al., 1994; Frigeri et al., 1995; Echevarria et al., 1996; Ishibashi et al., 1997)

To date there is one known bacterial water channel, AQPZ (Calamita et al., 1995). AQPZ was found in *Escherichia coli* by homology cloning, and exhibited water channel activity upon expression in *Xenopus* oocytes (Calamita et al., 1995). Another MIP family member encoded by the *glp*F gene is present in the inner membrane of *E. coli.* (Heller et al., 1980; Sweet et al., 1990; Maurel et al., 1994). The GlpF protein is selective for glycerol transport, does not facilitate water flux, and shows inhibition by mercuric ion upon expression in *Xenopus* oocytes (Heller et al., 1980; Sweet et al., 1990; Maurel et al., 1994). Such glycerol transport activity has also been implicated for the *Saccharomyces cerevisiae* MIP family member, Fps1 (a suppressor of a growth defect on fermentable sugars) (Van

Aelst et al., 1991; Luyten, et al., 1995). Yeast mutants lacking Fps1 are though to be defective in their ability to export glycerol and are characterized by an intracellular buildup of glycerol (Van Aelst et al., 1991; Luyten, et al., 1995). Fps1 differs from most other MIP family members in that it possesses long hydrophilic N- and C- terminal extensions (Luyten et al., 1995). The only other MIP member known to possess such extensions is the *Drosophila* BIB (big brain) protein whose function remains unknown (Rao et al., 1990)

In plants, water transport is crucial for maintaining homeostasis. Water enters the roots and follows a transpiration stream up the plant were it exits through stomata (Chrispeels & Agre, 1994). No doubt water channels play an important role in regulating water balance in plant tissues (Steudle & Henzler, 1995; Maurel, 1997). Evidence for this is the diversity of aquaporins being identified in plant tissues. For instance, twenty-three MIP family aquaporins have been identified in *Arabidopsis thaliana* alone (Weig et al., 1997)! Sequence relationships between all plant MIP-like proteins indicate the existence of three sequence subclasses: tonoplast intrinsic proteins (TIP) located within plant vacuoles, plasma membrane intrinsic proteins (PIP) present in plant plasma membranes, and a third class comprised of nod26 and the recently discovered At-NLM1 from *Arabidopsis thaliana* (Robinson et al., 1996; Weig et al., 1997; Maurel, 1997).

As reviewed in Maurel (1997), the tonoplast intrinsic protein (TIP) subfamily includes: α-TIP from seeds and seedlings of *Phaseolus vulgaris* (Johnson

et al., 1989; Melroy & Herman, 1991); γ and δ-TIP detected in roots, shoots, and flowers of *Arabidopsis thaliana* (Höfte et al., 1992; Ludevid et al., 1992; Daniels et al., 1994); and the *Nicotiana tabacum* homolog, pRB7, involved in root-knot nematode infection (Opperman et al., 1994). Upon nematode infection, pRB7 is expressed in nearby cells and leads to cell swelling (Opperman et al., 1994). The nematode is thought to feed off these swollen cells (Opperman et al., 1994). The plasma membrane intrinsic protein (PIP) subfamily is the largest subclass including PIP1a, PIP1b (AthH2), and PIP1c which are expressed throughout the tissues of the *Arabidopsis thaliana* plant (Robinson et al., 1996; Weig et al., 1997; Maurel, 1997) . PIP2 or RD28, first identified by Daniels et al. (1994), is found within all *Arabidopsis thaliana* organs except seeds. The *Mesembryanthemum crystallinum* (common ice plant) aquaporins MIPA and MIPB are PIPs as well (Yamaguchi-Shinozaki et al., 1992; Yamada et al., 1995; Maurel et al., 1997).

The expression of several plant aquaporins are induced in response to hormonal or environmental stimuli. For example, γ-TIP induction is controlled by the plant hormone giberellic acid which promotes cell enlargement (Höfte et al., 1992; Ludevid et al., 1992). Since γ-TIP is expressed in the elongating zone of roots and shoots and is under control of giberellic acid it may poteintially be envolved in growth and / or expansion (Höfte et al., 1992; Ludevid et al., 1992). As discussed above, pRB7 is expressed upon nematode infection (Opperman, 1994), RD28 is up-regulated upon dessiccation (Daniels et al., 1994), MIPA is down-

regulated by salt stress (Yamada et al., 1995), while PIP1b expression is controlled by blue light, abscisic acid, and giberellic acid (Kaldenhoff, et al., 1993, 1995, & 1997; Maurel et al., 1997).

Two post translational modifications are known to occur on MIP family members: glycosylation and phosphorylation (King & Agre, 1996; Maurel, 1997). AQP 1-5 are N-glycosylated on an asparagine residue in loop A for AQP1 and loop C for AQP 2-5 (King & Agre, 1996). The role of the glycosylation has not been elucidated but is proposed to be related to membrane trafficking (Preston et al., 1994). Biochemical analysis of AQP1 revealed that only one of the four sub-units in the tetramer was glycosylated (Smith & Agre, 1991). Also, elimination of the N-glycosylation site on AQP1 did not affect its function or trafficking in *Xenopus* oocytes suggesting that N-glycosylation is not necessary for membrane targetting (King & Agre, 1996).

Phosphorylation is a common post translational modification of proteins and known to be involved in the regulation of a wide spectrum of polypeptides. Several plant and animal aquaporins possess phosphorylation consensus sequences and / or have been shown to be specifically phosphorylated. Protein kinase A (PKA) phosphorylates AQP0 specifically on serine243 (Lampe & Johnson, 1990). In addition, PKA consensus site are present in C-terminus for AQP2, loop B for AQP4, and loop D for AQP5 (King & Agre, 1996). Nodulin 26 is phosphorylated on serine262 *in vitro* and *in vivo* (Weaver et. al., 1991; Weaver & Roberts, 1992),

and the significance of this will be discussed below. In addition, other plant aquaporins have have been found to be phosphorylated including α-TIP (Johnson & Chrispeels, 1992) and PM28A (Johansson et al., 1996). PM28A is a spinach leaf putative aquaporin was shown to be phosphorylated in response to Ca^{+2} and apoplastic water potential (Johansson et al., 1996).

Phosphorylation, among aquaporins, has three proposed affects: (1) directly affecting the proteins transport (Maurel et al., 1995); (2) serving as a signal for membrane targetting of the protein (Kuwahara et al., 1995; Fushimi et al., 1997); or (3) results in channel gating (Ehring et al., 1991; Lee et al., 1995).

α-TIP is proposed to contain three putative phosphorylation sites on the cytoplasmic surface of the membrane (Maurel et al., 1995). Mutation of these sites, followed by expression in *Xenopus* oocytes, reduced the apparent water transport activity of α-TIP (Maurel et al., 1995). Incubation of the oocytes with cAMP analogs, which should increase the endogenous activity of the ooctye PKA, correlated with a 80 – 100 % increase in water transport (Maurel et al., 1995). However, the amount of α-TIP in the plasma membrane was not quantitated. Immunoblots were done on whole oocytes and therefore the amount of protein in the plasma membrane, in comparison to other oocyte membranes, is unknown. This raises the possibility that the observed water flux enhancement may be a result of the amount of α-TIP targetted to the oocyte plasma membrane rather than an enhancement resulting from phosphorylation. Additionally, α-TIP was proposed to

be phosphorylated at three sites in oocytes while only one phosphorylation site (serine7) was detected in the tonoplast and it is not clear whether these other sites are ever phosphorylated *in planta* (Johnson & Chrispeels, 1992; Maurel et al., 1995). Mutation of the site determined to be phosphorylated in the tonoplast (serine7) only resulted in a 42 % decrease in water channel acitivity in *Xenopus* oocytes (Maurel et al., 1995). Because of these discrepancies more detailed studies with α-TIP are needed to determine the specific role that phosphorylation plays on this aquaporin.

As stated above, AQP2 is an arginine vasopressin (AVP) sensitive water channel in the principle cells of the kidney collecting duct where it is found primarily in the apical membrane and intracellular vesicles and is involved in concentration of urine (King & Agre, 1996). Recent studies have established that AQP2 is capable of "shuttling" between the apical membrane (resulting in increased water permeability) and intracellular vesicles in response to AVP (King & Agre, 1996). This AVP-induced shuttling has been proposed to be a result of phosphorylation of AQP2 on S256 (Kuwahara et al., 1995; Fushimi et al., 1997). Fushimi et al. (1997) have demonstrated this affect by expressing both wild type AQP2 and the phosphorylation site mutant S256A in LLC-PK1 cells and comparing the osmotic water permeability (P_f), of these two constructs, by measurement using stopped-flow light scattering. The wild type AQP2 expressing cells showed increased water permeabiliy over the mutant with an 85% stimulation of P_f

achieved by addition of a cAMP analog (Fushimi et al., 1997). The mutant (S256A) showed a significant decrease in water permeability, in comparison to the wild type, and showed no enhanced activity upon addition of the cAMP analog (Fushimi et al., 1997). Also biotin labeling revealed that the surface expression of wild type AQP2 was approximately 80% higher than that for the S256A mutant after cAMP analog stimulation (Fushimi et al., 1997). Thus experimental evidence supports phosphorylation as a signal for fusion of AQP2 containing vesicles to the apical membrane and thereby conferring increased water permeability upon this membrane (Kuwahara et al., 1995; Fushimi et al., 1997).

In addition to these studies a substantial amount of work has been done on the phosphorylation of nodulin 26. Below I have summarized our present knowledge of the MIP family channel protein nodulin 26.

The MIP family channel and phosphoprotein, nodulin 26.

Nodulin 26 (nod26) was first identified as a nodule specific cDNA by Fortin et al. (1987) through differential screening of soybean nodule and root libraries. The full length sequence of nod26 was later published by Shiels et al. (1988) and Sandal & Marcker (1988), who noted its similarity to AQP0. As mentioned earlier, nod26 is a late nodulin located only within the SM of the infected cells of soybean root nodules (Weaver et al., 1991). Based upon hydropathy analysis, nod26, similar to other MIP family members, possesses six putative hy-

drophobic regions long enough to span a membrane with hydrophilic amino and carboxyl terminal regions that project into the cytosol (Figure 4) (Sandal & Marcker, 1988; Shiels et al., 1988; Miao et al., 1992; Verma, 1992). The location of the phosphorylation site in the carboxyl terminus of nod26 and its accessibility to alkaline phosphatase lend credence to its cytoplasmic location (Ou Yang et al., 1991; Weaver, et al., 1991, 1992; Lee et al., 1995). Additionally, Miao et al. (1992) performed topological studies on *in vitro* translated nod26 inserted into canine pancreatic microsomal membranes to investigate the sensitivity of certain regions of the molecule to trypsin digestion. The amino and carboxyl termini of nod26 were sensitive to trypsin placing them outside the membrane (Miao et al., 1992; Verma, 1992). Deletion analysis revealed the first two transmembrane domains are sufficient for incorporation of nod26 into the membrane (Miao et al., 1992; Verma, 1992).

Since nod26 belongs to a structurally homologous membrane protein family with diverse transport functions it has been proposed to be involved in transport across the symbiosome membrane. Previous studies have identified possible transport roles for the nod26 channel. When incorporated into planar lipid bilayers, nod26 forms a high conductance ion channel with a single channel conductance of 3.1 nanosiemens in 1.0 M KCl (Weaver et al., 1994; Roberts et al., 1997). The channel is non-rectifying and transports K^+ and Cl^- across the bilayer showing a weak selectivity for the anion (Weaver et al., 1994; Roberts et al., 1997).

As illustrated in Figure 4, nod26 is phosphorylated in the carboxyl terminal region on serine262 by a Calmodulin-like Domain Protein Kinase (CDPK) (Weaver et al., 1991; Weaver & Roberts, 1992). CDPK activities and immunoreactive bands are found in both soluble and membrane-bound forms in the nodule (Weaver et al., 1991; Roberts et al., 1993; Roberts et al., 1997). Nod26 is phosphorylated by a SM-associated CDPK (Weaver et al., 1991; Weaver & Roberts, 1992; Weaver et al., 1994; Roberts et al., 1997).

CDPKs are a novel class of protein kinases present in plants (Roberts & Harmon, 1992) and protist species (Gunderson & Nelson, 1987; Son et al., 1993). They are stimulated by micromolar amounts of Ca^{+2} and show no dependence on calmodulin and lipid effectors for activity (Roberts & Harmon, 1992; Roberts et al., 1993). From the deduced amino acid sequence, CDPKs consist of a carboxyl-terminal, calmodulin-like regulatory domain containing four EF-hand calcium binding sites, and amino-terminal protein kinase catalytic and autoinhibitory domains sharing highest sequence identity (39%) with the respective domains from calmodulin-dependent protein kinase II (Harper et al., 1991; Roberts & Harmon, 1992; Roberts, 1993; Harmon et al., 1997). CDPK and calmodulin-dependent protein kinase II possess similar catalytic properties and phosphorylate some of the same substrates *in vitro* (Roberts & Harmon, 1992). CDPK recognizes the concensus sequence, hydrophobic-Xaa-basic-Xaa-Xaa-serine (Bachmann et al., 1996), which is similar to the smaller calmodulin-dependent protein kinase II con-

sensus site, basic-Xaa-Xaa-serine (Roberts & Harmon, 1992). The site on nod26 recognized by CDPK is serine262 (Figure 4) (Weaver & Roberts, 1992). This is found in a consensus CDPK motif (ITKSAS) (Figure 4).

Similar to nod26, AQP0 forms single channels in planar lipid bilayers with a high conductance (approximately 3 nS), exhibits lower subconductance states that are preferentially occupied at higher voltage potentials, and shows a weak selectivity for anions (Gorin et al., 1984; Zampighi et al., 1985; Ehring et al., 1990; Shen et al., 1991). AQP0 also is phosphorylated on serine243 in its C-terminus by cAMP-dependent protein kinase (Lampe & Johnson, 1990). Phosphorylated AQP0 shows an enhanced voltage sensitivity compared to the unphosphorylated protein (Ehring et al., 1991). Native soybean nod26 also shows voltage sensitivity. Lower voltages (30 mV) have no affect on nod26 ion channel activity (Weaver et al., 1994). However, at higher applied voltages (70 - 100 mV), the nod26 channel exhibits "gating behavior" with a selectivity for lower subconductance states (Weaver et al., 1994; Roberts et al., 1997).

To determine whether phosphorylation effects voltage sensitivity of the nod26 channel, wild type recombinant nod26, as well as several site directed mutants (S262A & S262D) of the phosphorylation site, were expressed in *E. coli* and purified for planar lipid bilayer studies (Lee et al., 1995). Recombinant wild type nod26 shows a high conductance channel activity but shows no sensitivity to voltage (Lee et al., 1995). The serine to alanine mutant also shows no voltage sensi-

tivity. The serine to aspartic acid mutant behaves as the phosphorylated channel showing gating behavior at higher applied voltage potentials (Lee et al., 1995). *In situ* phosphorylation of the wild type recombinant nod26 by CDPK in planar lipid bilayers results in the acquistion of voltage dependent gating behavior (Lee et al., 1995). These results suggest that phosphorylation on serine262 modulates the channel activity by conferring voltage sensitivity. This effect has been shown to be reversible (Lee et al., 1995). Upon addition of alkaline phosphatase, which dephosphorylates the protein, the channel activity is restored to that of the un-phosphorylated protein (Lee et al., 1995).

This gating effect is similar to that observed for the Shaker potassium channel (Zaggota et al., 1990) which exhibits channel closure, upon phosphorylation. This has been proposed to be a result of the pore being blocked by a "charged ball" (ball & chain model) (Bezanilla & Armstrong, 1977). This voltage gated ion channel activity, if occurring *in vivo*, may be modulated by the symbiosome membrane ATPase, which is capable of establishing a voltage potential across this membrane (Udvardi & Day, 1989; Udvardi et al., 1991; Udvardi & Day, 1997). An *in situ* study, using intact isolated symbiosomes, showed that phosphorylation of nod26 is associated with changes in malate transport across the symbiosome membrane (Ou Yang et al., 1991).

Though ion channel activity has been demonstrated for several MIP family members in planar lipid bilayers, it remains a controversial issue. AQP0, Nod26,

and AQP1 all demonstrate ion channel activity upon incorporation into planar lipid bilayers (Ehring et al., 1990; Weaver et al., 1994; Lee et al., 1995; Agre et al., 1995). However, upon expression of these proteins in *Xenopus* oocytes, ion channel activity has not been detected across the oocyte membrane (Agre et al., 1995) except for one report for AQP1 (Yool et al., 1996). This study reported that forskolin stimulated both water and cation permeability in oocytes. However, this finding has failed to be reproduced by several laboratories (Agre et al., 1997). In addition, AQP0, originally proposed to be an ion channel forms a low activity aquaporin upon expression in *Xenopus* ooctyes (Mulders et al., 1995; Zampighi et al., 1995; Agre et al., 1995). The finding that AQP0 forms a low activity water channel upon expression in *Xenopus* oocytes (Mulders et al., 1995; Agre et al., 1995; Zampighi et al., 1995; Zamphighi et al., 1997), and that several members of the MIP family are aquaporins, led us to evaluate the potential role of nod26 as a SM-specific aquaporin.

In the present work, by using *Xenopus* oocyte expression techniques and fluorimetric analyses of SM vesicles and liposomes containing purified nod26 it is shown that nod26 exhibits a complex aquaporin and solute transport function.

CHAPTER II

MATERIALS AND METHODS

Materials.

pXBG-ev1 was a kind gift from Dr. Peter Agre, Johns Hopkins University. Restriction enzymes and DNA ligase were purchased from New England Biolabs. 1-O-n-octyl β-D-glucopyranoside (OG) was purchased from Alexis Corporation. DEAE fast flow resin, protease inhibitors, antibiotics, Dnase I, and Percoll were purchased from Sigma. Soybean seeds (*Gycine max,* cv. Essex) were a kind gift from Dr. Peter Greshoff, The University of Tennessee, Knoxville. Vermiculite was purchased from Knoxville Seed and Greenhouse. Bradford reagent and nitrocellulose were purchased from BioRad. BCA assay reagents and the protein standards bovine serum albumin (BSA) and γ-globulin were purchased from Pierce Chemical Company. Horseradish peroxidase coupled goat-anti-rabbit IgG was purchased from Vector Laboratories. The fluorescent indicator dyes carboxyfluorescein (CF) and aminonaphthalenetrisulfonic acid (ANTS) were purchased from Molecular Probes. Miracloth was purchased from Calbiochem. Anti-carboxyfluorescein antibodies (Kuypers et al., 1984; Lande et al., 1995) were a

kind gift from Dr. Mark Zeidel, University of Pittsburgh. Lipids were purchased from Avanti Polar Lipids, Inc. All other reagents were of reagent grade or higher.

Cloning of nod26 constructs into the Xenopus expression vector, pXBG-ev1.

Full length nod26 and the phosphorylation site mutants (S262A & S262D) were cloned into a pRSETA expression vector as previously described (Lee et al., 1995). Full length constructs were excised from the pRSETA expression vector by *BamH*I restriction enzyme digestion and the nod26 fragment was isolated by electrophoresis on a 0.8% (w/v) low melting point agarose gel by the method of Sambrook et al. (1988). The nod26 cDNA was inserted into the *Xenopus* expression vector, pXBG-ev1 (Preston et al., 1992) into the *Bgl*II site of the *Xenopus* β-globin gene downstream of the T3 promoter. The resulting plasmid, pXBG-ev1(nod26) (Figure 5), was transformed into *E. coli* strain JM101 competent cells prior to *in vitro* transcription experiments and *Xenopus laevis* oocyte expression.

In vitro transcription of nod26 cRNA and expression in Xenopus laevis oocytes.

Capped nod26 cRNA's (flanked by 3'- and 5'- untranslated regions of the *Xenopus* β-globin mRNA) were synthesized by *in vitro* transcription of the *Xba*I lineralized plasmid by T3 RNA polymerase according to the manufacturers protocol (Stratagene).

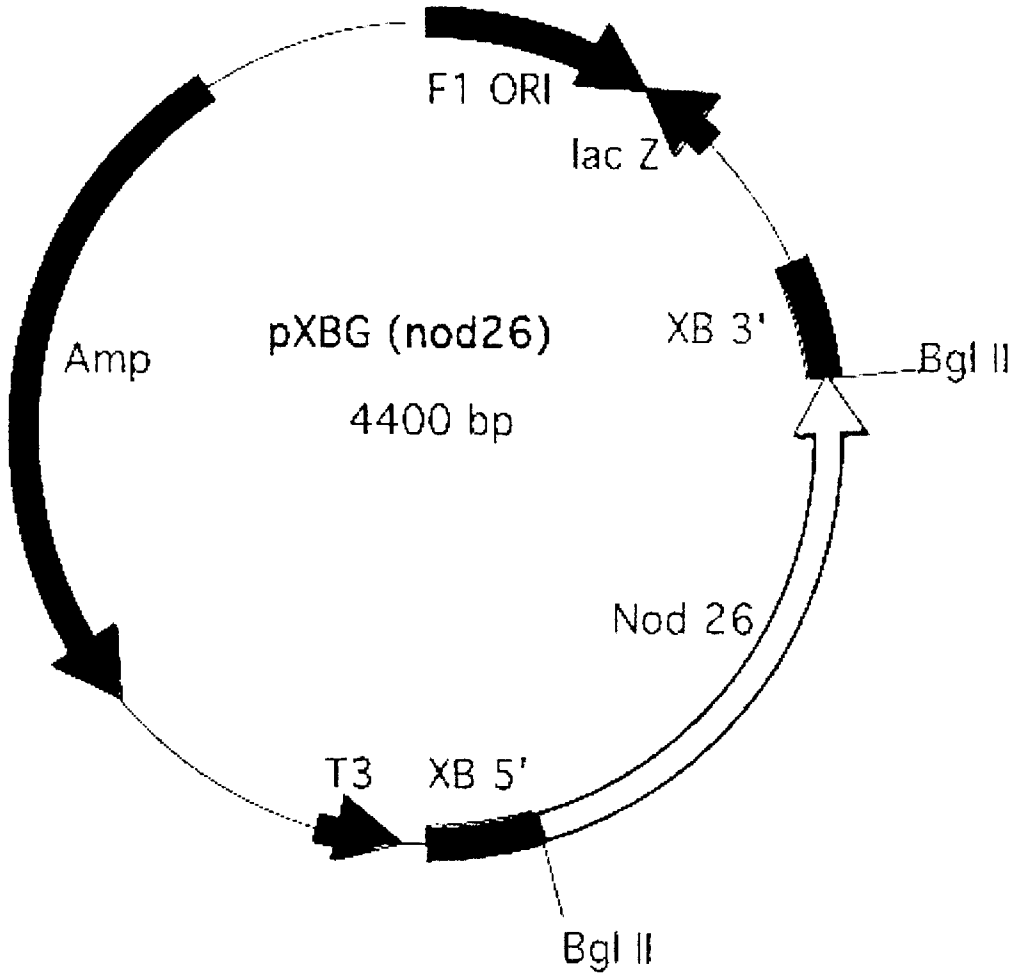

Figure 5. Partial map of the *Xenopus* expression vector pXBG(nod26). Full length nod26 (Zhang & Roberts, 1995) was cloned into the *Bgl*II site under control by the T3 promoter. **F1 ORI**, origin of replication; **Amp**, ampicillin resistance gene; **T3**, bacteriophage T3 RNA polymerase promoter; **lacZ**, lactose operon for blue/white colony screening; **XB 3' & 5'**, *Xenopus* β-globin gene.

Xenopus laevis oocytes (stage VI) were prepared as previously described (Zampighi et al., 1995) and were injected with 50 nl of water (control) or 50 nl of 1 mg/ml nod26 cRNA. Oocytes were then incubated at 18 °C in ND96 (96 mM NaCl, 2 mM KCl, 1.8 mM $CaCl_2$, and 5 mM HEPES-NaOH, pH 7.4) media plus supplements (2.5 mM sodium pyruvate, 10 μg/ml aminobenzylpenicillin, and 10 μg/ml streptomycin) for 24 hours prior to analysis (Zampighi et al., 1995).

Osmotic water permeability (P_f) of the nod26 cRNA injected and control oocytes was determined by monitoring the change in cross-sectional area of the oocyte upon 70% dilution as described previously (Zampighi et al., 1995; Mulders et al., 1995; Chandy et al., 1997). The relative change in volume (V/V_0) was calculated as shown in Equation 1.

$$(A/A_0)^{3/2} = V/V_0 \qquad \textit{(Equation 1)}$$

A_0 and V_0 are the cross-sectional area and cell volume, respectively, at time 0, and A and V are the cross-sectional area and cell volume, respectively, at time = t. P_f was calculated as shown in Equation 2.

$$P_f = \{d(V/V_0)/dt\}\{V_0/S_0)\} \div \{\Delta_{osm} \times V_w \times (S_{real} / S_{sphere})\} \qquad \textit{(Equation 2)}$$

S_0 is the geometric surface area of the oocyte at time 0, Δ_{osm} is the osmotic gradient, V_w is the partial molar volume of water, S_{real} is the actual area of the oolemma, and S_{sphere} is the surface area of the oocyte assuming it is a sphere. An S_{real} / S_{sphere} value of 9 was used for all P_f calculations. This factor corrects for the in-

crease in surface area due to the presence of folds and microvilli in the oolemma (Zampighi et al., 1995).

For measurements of reversible $HgCl_2$ inhibition, oocytes were incubated in ND96 media containing 3 mM $HgCl_2$ for 4 minutes. P_f was then remeasured in diluted ND96 media containing 3 mM $HgCl_2$. Reversibility was shown by then incubating the same oocyte in ND96 media containing 5 mM 2-mercaptoethanol for 15 minutes prior to a third P_f determination. Between each measurement, oocytes were rinsed and incubated in ND96 medium containing no agents for 20 minutes.

Bacterial culture and plant growth.

Bradyrhizobium japonicum strain USDA 110 were cultured at 30°C with constant shaking in Bergenson's minimial medium : $NaH_2PO_4 \cdot 7H_2O$, 270 mg/L; $MgSO_4 \cdot 7H_2O$, 80 mg/L; $FeCl_3 \cdot 6H_2O$, 3 mg/L; ferric monosodium EDTA, 3.7 mg/L; $CaCl_2 \cdot 2H_2O$, 30 mg/L; $MnSO_4 \cdot 4H_2O$, 0.0025 mg/L; H_3BO_3, 0.03 mg/L; $ZnSO_4 \cdot 7H_2O$, 0.03 mg/L; $NaMoO_4 \cdot 2H_2O$, 0.0025 mg/L; $CuSO_4 \cdot 5H_2O$, 0.0025 mg/L; $CoCl_2 \cdot 6H_2O$, 0.0025 mg/L; biotin, 0.1 mg/L; thiamine, 1 mg/L; mannitol, 10 g/L; sodium glutamate, 0.5 g/L; yeast extract, 0.5 g/L, pH 6.8-7.0. Bacterial cultures were grown until they reached an $A_{600} > 1.0$ (approximately 5 to 7 days for a 0.5 L culture volume).

Soybean seeds (*Glycine max,* cv. Essex) were planted in 10 inch pots (10

seeds/pot, approximately 1.5 inches deep) filled with medium vermiculite. Before planting the vermiculite is thoroughly soaked with Herridges solution (K_2HPO_4, 22 mg/L; KH_2PO_4, 17 mg/L; KCl, 19 mg/L; $MgSO_4 \cdot 7H_2O$, 250 mg/L; $CaCl_2 \cdot 2H_2O$, 37 mg/L; ferric monosodium EDTA, 9 mg/L; H_3BO_3, 0.71 mg/ml; $MnCl_2 \cdot 4H_2O$, 0.45 mg/L; $ZnCl_2$, 0.03 mg/L; $CuCl_2 \cdot 2H_2O$, 0.01 mg/L; $NaMoO_4 \cdot 2H_2O$, 0.005 mg/L). After planting a culture of *Bradyrhizobium japonicum* (100 ml) was diluted with 3 gallons of water in a watering can and this solution was spread evenly over 30 pots. The inoculation was repeated 1 week later. The plants were grown in a greenhouse with natural lighting supplemented to 16 hours with 400 watt multivapor metal-halide lamps. Plants were watered approximately every 4-5 days alternately with water and Herridges solution.

Soybean SM isolation for permeability measurements.

Nodules (20 - 40 g) were harvested from 28 - 40 day old soybean plants (*Glycine max,* cv. Essex), and symbiosomes were isolated by a modification of a previous procedure (Udvardi & Day, 1989; Weaver et al., 1991; Weaver & Roberts, 1992). The nodules were washed twice on a sieve (200 ml/wash) with symbiosome wash buffer (25 mM MES-bis-trispropane, 3 mM $MgSO_4$, 350 mM mannitol, 1 % (w/v) BSA, 1 μM leupeptin, pH 7.0). Nodules were gently crushed in a glass mortar with a pestle in 20 mM MES-NaOH, pH 7.0, 20 mM sodium isoascorbate, 1% (w/v) BSA, 1% (w/v) PVP-40, 10 mM $MgSO_4$, 10 mM EGTA, 5

mM DTT, 1 μM leupeptin, 350 mM mannitol (1.5 ml/g of nodules). The crushed nodules were filtered through Miracloth (soaked in extraction buffer) and re-extracted as just described. The combined extracts were filtered through Miracloth and were layered on a Percoll step gradient (7 ml of extract on a 15 ml of gradient consisting of 5 ml each of 30, 60, and 80% (v/v) Percoll in 10 mM MOPS-NaOH, pH 7.0, 3 mM $MgSO_4$, 350 mM mannitol, 1μM leupeptin). The gradients were centrifuged without braking (5,550 rpm, 15 minutes, in a Sorvall HS-4 rotor at 4 °C). Isolated symbiosomes were collected from the 60/80% Percoll interface with a wide mouth glass pipette. The symbiosomes were washed in 200 ml of symbiosome wash buffer and centrifuged at 650 x g for 3.5 minutes at 4 °C in a Sorvall GSA-3 rotor. The final washed symbiosome pellet was suspended in 3-4 ml of symbiosome wash buffer containing 20 mM CF (for P_f determinations) or 10 mM ANTS (for P_d measurements) and the symbiosomes were ruptured by vortexing for 2 minutes. SM vesicles were separated from bacteroids by differential centrifugation. Bacteroids were pelleted at 6000 rpm for 10 minutes at 4°C in a Sorvall HS-4 rotor. The pelleted bacteroids were resuspended, vortexed and the centrifugation was repeated. The supernatants were combined and centrifuged at 100,000 x g for 1 hour at 4°C in a Beckman Ti60 rotor. The final SM vesicle pellet was suspended in 25 mM MES-bis-trispropane, 3 mM $MgSO_4$, 2 μg/ml leupeptin, pH 7.0 (final resuspension buffer) and either 20 mM CF (for P_f determinations) or 10 mM ANTS (for P_d determinations). SM vesicles were

washed 3 times in 25 mM MES-bis-trispropane, pH 7.0, 3 mM $MgSO_4$, 45 mOsm/Kg or until no extravesicular CF was detected. The purity of the preparation was verified by SDS-PAGE and protein concentration was determined by BCA assay using BSA as a standard protein.

Modifications of SM prep for nod26 purification.

For purification of nod26, SM were isolated according to the above protocol with the following modifications. Nodules were washed in a modified wash buffer (20 mM MOPS-NaOH, pH 7.0, 350 mM mannitol, 3 mM $MgSO_4$, 1 μM pepstatin A, 1 mM PMSF, and 1 μM leupeptin). Nodules were crushed in 20 mM MOPS-NaOH, pH 7.0, 350 mM mannitol, 10 mM EDTA, 10 mM $MgSO_4$, 10 mM DTT, 1% (w/v) BSA, 1% (w/v) PVP-40, 20 mM sodium isoascorbate, 1 μM pepstatin A, 1 mM PMSF, and 1 μM leupeptin (1 ml buffer / g nodules). Symbiosomes isolated from the Percoll step gradient were washed in a modified wash buffer (20 mM MOPS-NaOH, pH 7.0, 350 mM mannitol, 3 mM MgSO4, 1 μM pepstatin A, 1 mM PMSF, and 1 μM leupeptin). The washed symbiosomes were resuspended in 20 mM MOPS-NaOH, pH 7.0, 150 mM KCl, 1 μM pepstatin A, 1 mM PMSF, and 1 μM leupeptin (8 ml) and were ruptured by extruding them twice through a 25 gauge hypodermic needle connected to a 10 ml syringe (rather than by vortexing as above). Bacteroids were pelleted at 6000 rpm for 10 minutes at

4°C in a Sorvall HS-4 rotor. The pelleted bacteroids were resuspended, reextruded through the needle, and the centrifugation was repeated. The pelleted SM were resuspended in 1.0 ml of 10 mM sodium phosphate, 1 μM pepstatin A, 1 mM PMSF, and 1 μM leupeptin and stored at -80°C until needed. Prep purity was verified by SDS-PAGE and protein concentration was determined by BCA assay using BSA as a standard protein.

Purification of native nod26 from soybean root nodules.

Native nod26 was purified by a modified protocol of Weaver et al. (1994). Five SM preps (5-6 mg of total protein) were diluted to 15 ml in ice-cold 10 mM sodium phosphate buffer (pH 7.5) containing 1 μM pepstatin A, 1 mM PMSF, 1 μM leupeptin, and was centrifuged at 100,000 x g for 1 hour at 4°C in a Beckman Ti60 rotor. The pellet was resuspended in 20 ml of 7.5 mM sodium phosphate, pH 7.5, 1.0 M KI, 1 mM EDTA, 1 mM DTT, 1 μM pepstatin A, 1 mM PMSF, 1 μM leupeptin, and was incubated at 4°C for 30 minutes with occasional gentle mixing. The sample was then centrifuged at 100,000 x g for 1 hour at 4°C in a Beckman Ti60 rotor. The pellet was rinsed twice with two 5 ml portions of 10 mM Tris-HCl, pH 8.0. The pellet was suspended in 10 ml of 10 mM Tris-HCl, pH 8.0, 1 μM pepstatin A, 1 mM PMSF, 1 μM leupeptin, and was centrifuged at 100,000 x g for 1 hour at 4°C in a Beckman Ti60 rotor. The pellet was then solu-

bilized in 10 ml of 10 mM Tris-HCl, pH 8.0, 2% (w/v) OG, 1 μM pepstatin A, 1 mM PMSF, and 1 μM leupeptin at 4 °C with constant shaking (200 rpm) for 12-14 hours. The sample was centrifuged at 100,000 x g for 1 hour at 4 °C in a Beckman Ti60 rotor and the supernatant fraction was collected and filtered through a 0.2 micron filter.

The supernatant fraction was applied at a flow rate of 0.25 ml/min. to a 1.8 ml DEAE fast flow column attached to a Pharmacia FPLC system controlled through a computer interface (FPLC assistant software, Pharmacia). The column was pre-equilibrated in column buffer A (10 mM Tris-HCl, pH 8.0, 1% (w/v) OG, and 1 μM leupeptin). The column was washed at a flow rate of 0.5 ml/min with 20 ml of column buffer A and then with 20 ml of column buffer B (20 mM MES-NaOH, pH 6.2, 1% (w/v) OG, and 1 μM leupeptin). The column was eluted with a biphasic salt gradient. First, a 15 ml linear gradient of 0 - 0.2 M NaCl in column buffer B was applied, and was then immediately followed by a second, steeper 8.0 ml linear gradient of 0.2 - 0.4 M NaCl in column buffer B. Pure nod26 (250-300 μg) elutes between 0.2 to 0.3 M NaCl. One ml fractions were collected and screened for nod26 by SDS-PAGE and Western blot with anti-nod26 antibodies (Weaver et. al., 1991; Zhang & Roberts, 1995). The column was stripped in 20 mM Tris-HCl, pH 8.0, 1.0 M NaCl between runs.

Fractions containing purified nod26 were concentrated 6 to 10-fold, to a final concentration of 0.5 to 1.0 mg/ml, using an Amicon Centricon-10 ultrafiltra-

tion device. The concentrated nod26 was then dialyzed 12 hours at 4 °C against 100 ml of 20 mM Tris-HCl, pH 7.8, 0.9% (w/v) OG, 0.1 mM βME, and 1 μM leupeptin in a Pierce Microdialyzer (100 μl/well) and was stored at -80°C. Protein concentrations were determined using the BCA method with BSA (0.5 mg/ml, Pierce) used as a protein standard.

Proteoliposome reconstitution.

Proteoliposome reconstitution was done by a previously described protocol (Kasahara & Hinkle, 1977; Zeidel et al., 1992). *E. coli* total phospholipid (acetone/ether washed to remove neutral lipid, 22.5 mg) was suspended in 10 mM Tris-HCl (pH 7.5) in a 13 x 100 mm borosilicate glass test tube. The phospholipid mixture was flushed with nitrogen gas and was covered with parafilm. The phospholipid mixture was placed in a bath-type sonicator (Model G112SPIG, Laboratory Supplies Co., Inc.) filled with 0.02% (v/v) TritonX-100 and sonicated until the solution clarified (approximately 40 minutes).

Reconstitution was carried out by combining 200-250 μg of nod26, 9 mg of bath sonicated *E. coli* phospholipid, 50 mM Tris-HCl, pH 7.5, and 1.25% (w/v) OG in a final volume of 1.0 ml. Control liposomes were prepared in a similar manner except nod26 was omitted. The mixture was vortexed briefly and incubated on ice for 30 minutes. Liposomes were formed by rapidly injecting the mixture (using a 1.0 ml syringe fitted with a 20 gauge needle) into 25 ml of 50

mM MOPS, pH 7.5, 150 mM NMDG, 10 mM CF, 1 mM DTT, 0.5 mM PMSF, 300 mOsm/Kg, at room temperature (22-25°C). The suspension was incubated for 20 minutes at room temperature and was centrifuged at 120,000 x g for 1 hour at 4 °C in a Beckman Ti60 rotor. The pelleted CF-loaded liposomes were washed in 8 ml of 50 mM MOPS, pH 7.5, 150 mM NMDG, 300 mOsmole/Kg (hypotonic buffer) and were centrifuged at 120,000 x g for 1 hour at 4°C in a Beckman Ti50 rotor. The washing step was repeated 3 times or until no CF was detected in the supernatant. After the final wash, the vesicles were resuspended in 300 µl of hypotonic buffer and stored at 4°C until analysis.

Membrane permeability measurements.

Permeabilities measurements of SM vesicles and reconstituted liposomes were performed by CF self-quenching by a stopped-flow fluorimetric approach (Zeidel et al., 1992; Zeidel et al., 1994; Lande et al., 1995; Negrette et al., 1996). Prior to permeability measurements anti-CF Ab was added to completely quench any residual extravesicular CF fluorescence (Zeidel et al., 1992; Zeidel et al., 1994; Kuypers et al., 1984; Lande et al., 1995). Fluorimetry measurements were done with an excitation wavelength of 490 nm with the emission filtered with a 515 nm cutoff filter. Experiments were performed on one of two stopped-flow spectrofluorimeters.

Initial SM experiments (University of Pittsburgh) were done on a Applied Photophysics Model SF.17MV (Leatherhead, UK) with a measured dead time of 0.7 ms. Fluorescence data from 5 to 10 individual determinations were averaged and fit to single exponential curves using software supplied by Applied Photophysics. The software utilizes a nonlinear regression (Equation 3) (Marquardt) algorithm calculated from the time course using the "Curfit" routine.

Later experiments (Universtiy of Tennessee, Knoxville) were performed on a Bio-Logic Model SFM-3 with MPS-51 power supply fitted with a TC-100/10 cuvette, 15 ml syringes, HDS mixer, running at a total flow rate of 3 ml/second (80 μl / injection) with a measured dead time of 7 ms. The fluorimeter was controlled by the Bio-Kine Software V3.20. Fluorescence data were collected (1000 points) at time intervals of 0.1 ms and 0.5 ms (or for glycerol permeablilities at time intervals of 1.0 ms and 10 ms) and individual traces of >10 were averaged to reduce the signal to noise ratio. The averaged curves were fitted to a single exponential (Equation 3) by the software program SigmaPlot provided by Jandel Scientific.

$$\textit{Relative Fluorescence} = Aexp(-B(t))+C \qquad \textit{(Equation 3)}$$

A is the amplitude of the curve, B is the rate constant (s^{-1}), and C is the endpoint of the fluorescene trace.

Osmotic water permeability (P_f).

Osmolarities of all the solution were checked by freezing point depression by using either an Advanced Osmometer Model 3D3 (Advanced Instruments, Inc.) or an Osmette A Osmometer (Precision Instruments). Liposomes in hypotonic buffer (50 mM MOPS, pH 7.5, 150 mM NMDG, 300 mOsm/Kg) or SM vesicles in final resuspension buffer (25 mM MES-bis-trispropane, 3 mM $MgSO_4$, 2 μg/ml leupeptin, pH 7.0, 45 mOsm/Kg) with entrapped CF (10-15 mM for liposomes; 20 mM for SM vesicles), were rapidly injected into identical buffers containing sucrose concentrations adjusted to triple the osmolarity to 135 mOsm/Kg for SM vesicles and 900 mOsm/Kg for liposomes (1 mM sucrose = 1 mOsm/Kg). After mixing the extravesicular osmolarity (C_{out} = 600 mOsm/Kg for liposomes; C_{out} = 90 mOsm/Kg for SM vesicles) was double that of the intravesicular osmolarity (C_{in} = 300 mOsm/Kg liposomes; C_{in} = 45 mOsm/Kg for SM vesicles). Since the volume inside the vesicle is small compared to the volume outside it was assumed that the outside volume remained constant throughout the experiment. As water effluxes out of the vesicles the internal CF concentration increases and time-dependent fluorescence-monitored self-quenching is recorded. P_f was calculated from the time course of relative fluorescence by comparing single exponential time constants fitted to simulated curves where P_f was varied (Zeidel et al., 1992, 1994; Lande et al., 1995; Negrette et al.,1996). Simulated curves were calculated

using the software package (MathCad) from the osmotic permeability equation (Equation 4).

$$dV(t)/dt = (P_f)(SAV)(MVW) \bullet \{[C_{in}/V(t)] - C_{out}\} \qquad \textit{(Equation 4)}$$

V(t) is the relative volume of the vesicles at time t, P_f is the osmotic water permeability, SAV is the vesicle surface area-to-volume ratio, MVW is the molar volume of water (18 cm^3/mole), C_{in} and C_{out} are the total osmolarity inside and outside the vesicle, respectively. SAV was calculated from the average vesicle diameter measured by quasielastic light scattering (Nicomp Model 270 submicron particle analyzer) or by negative staining of liposomes (1:100 dilution) with 1% (w/v) uranyl acetate, and visualization at 50,000x magnification with a transmission electron microscope (Hitach H-800, 100 kV). From the EM micrographs the diameters of 30-100 liposomes from each preparation were measured and an average diameter was calculated. Both methods showed excellent agreement.

Based on the difference between C_{in} and C_{out}, an assumption is made that the relative volume at time (t=0) will be 1 and will decrease over time till an equilibrium is reached at a relative volume of 0.5 at the end of the experiment (Zeidel et al., 1992; Zeidel et al., 1994; Lande et al., 1995; Negrette et al., 1996). Parameters from the exponential fit (amplitude and endpoint, Equation 3) are used to normalize the data from relative fluorescence to relative volume using the as-

sumptions described above (initial volume = 1 and final volume = 0.5) (Zeidel et al., 1992; Zeidel et al., 1994; Lande et al., 1995; Negrette et al., 1996).

Unit conductance (pf).

Unit conductance for nod26 was determined by estimating the nod26 content per unit surface area of either proteoliposomes or SM vesicles by the approach described previously (Zeidel et al., 1992). The total surface area (SA) of the liposomes was based on the surface area to volume ratio (SAV) calculated from the vesicle diameter ($SAV = 4\pi r^2 / (4/3\pi r^3) = 3/r$, r = vesicular radius) and the total internal vesicle volume. The total intravesicular volume was measured by lysing the vesicles with TritonX-100 and measuring spectrofluorimetrically the total CF flourescence released per unit volume of vesicles. The total CF fluorescence released from the vesicles was compared to a standard curve of known CF standard solutions (measured on the same instrument at identical time and settings) to allow a determination of the concentration of CF within the cuvette. Based on the determined CF concentration, the solution volume, and the concentration of CF entrapped within the vesicles (20 mM for SM vesicles and 10-15 mM for proteoliposomes), a total intravesicular volume was calculated.

The concentration of nod26 within SM vesicles was determined utilizing two methods. First, the total protein content of SM vesicles was estimated by the method of Bradford (1976). The proportion of the SM protein which was nod26

was estimated by densitometry (BioRad Model GS-670 Imaging Densitometer) of a Coomassie Blue-stained SDS-polyacrylamide gel of the SM vesicle preparation. The density of the nod26 band was compared to the total density of all SM protein bands and the concentration of nod26 in the SM prep was determined from the total protein content determined by the Bradford (1976) assay described above.

In a second method, a quantitative Western blot method was used in which the densitometry value of the immunoreactive nod26 band (using nod26 specific antibodies, Zhang & Roberts, 1995) was compared to densitometry determinations of immunoreactive bands of a purified nod26 standard protein. Determinations of nod26 concentration by both methods showed excellent agreement.

The protein concentration of purified nod26 incorporated into liposomes was estimated by densitometry of a Coomassie Blue-stained SDS-polyacrylamide gel of the proteoliposome preparation, as discussed above, and comparison to a purified nod26 standard protein.

Based on the density of nod26 per unit surface area, and the P_f determination (at 20°C), a unit conductance (pf) for nod26 could then be calculated based on Equation 5.

$$pf = P_f \div SuD \qquad \textit{(Equation5)}$$

P_f is the calculated osmotic water permeability in cm/s at 20°C, and SuD is the number of nod26 molecules per unit vesicle surface area (nod26 molecules/cm^2).

Small nonelectrolyte permeability (P_{solute}).

Permeabilities of SM vesicles and liposomes for various uncharged solutes were determined as previously described (Lande et al., 1995; Negrette et al, 1996). Vesicles or liposomes were loaded with the test solute by incubation at room temperature (22-25 °C) for 15 minutes.

For SM vesicles, the test solute (90 mM, either formamide, glycerol, acetamide, or urea) was added to the final resuspension buffer (25 mM MES-bis-trispropane, 3 mM $MgSO_4$, 2 μg/ml leupeptin, pH 7.0, 45 mOsm/Kg) resulting in a final osmolarity of 135 mOsm/Kg. SM vesicles were rapidly injected into an isoosmotic medium identical to this buffer except containing an impermeant solute (sucrose, 90 mM) in place of the test solute. After mixing, the conditions remain isotonic (C_{in} = 90 mOsm/Kg test solute and 45 mOsm/Kg impermeant solute; C_{out} = 45 mOsm/Kg test solute and 90 mOsm/Kg impermeant solute) but a solute concentration gradient is now in place.

Glycerol (permeant test solute) permeability was determined for liposomes as described above. Glycerol (600 mM) was added to hypotonic buffer (50 mM MOPS, pH 7.5, 150 mM NMDG, 300 mOsm/Kg) bringing the final osmolarity of the solution to 900 mOsm/Kg. Liposomes are incubated in this buffer for 15 minutes at room temperature (22-25 ° C) prior to permeability measurements and are then rapidly injected into an identical, isoosmotic buffer (900 mOsm/Kg) containing 600 mM added sucrose (an impermeant solute) in the place of glycerol.

After mixing C_{in} = 600 mOsm/Kg glycerol and 300 mOsm/kg impermeant solute and C_{out} = 300 mOsm/Kg glycerol and 600 mOsm/Kg impermeant solute.

The permeant test solute effluxes out of the vesicles, driven by the solute concentration gradient, and water follows leading to vesicular shrinkage and CF self-quenching. The CF self-quenching is monitored spectrofluorimetrically as a time dependent CF quench curve. Calculations of solute permeabilities (P_{solute}) were performed, in MathCad, using the parameter from the single exponential fit (Equation 3) and Equation 6.

$$dV_{rel}/dt = P_{solute}(SA/V_0)(1/141)(188/V_{rel} - 235) \qquad \textit{(Equation 6)}$$

P_{solute} is the permeability coefficient (cm/s) for the permeant solute, V_{rel} is the relative volume of the vesicles at a given time, V_0 is their relative volume at time 0, and SA is the vesicle surface area. The other parameters are values calculated in MathCad for these experimental conditions and have been derived and validated as described previously (Lande et al., 1995; Negrette et al., 1996).

Diffusive water permeability (P_d) for SM vesicles.

P_d was measured as described (Ye & Verkman, 1989), using the fluorophore ANTS (10 mM) (loaded into SM vesicles instead of CF) which exhibits enhanced fluorescence when exposed to deuterium. ANTS loaded vesicles were prepared in the H_2O based final resuspension buffer (25 mM MES-bis-trispropane, 3 mM $MgSO_4$, 2 μg/ml leupeptin, pH 7.0, 45 mOsm/Kg) and rapidly injected, via

stopped-flow, into an isoosmotic buffer, which is identical to the just described buffer except containing 50% deuterium oxide (D_2O). The time course of enhanced ANTS fluorescence was recorded spectrofluorimetrically. Because the time course of these experiments were so fast, P_d measurements were done at 12°C instead of 20°C to slow the rate and permit maximal definition of the time course of water diffusion. The ANTS fluorescence trace was fitted to a single exponential equation and P_d was calculated using Equation 7 (Ye & Verkman, 1989).

$$P_d = 1 / (B \bullet SAV) \qquad \textit{(Equation 7)}$$

P_d (cm/s) is the diffusive water permeability, B (s^{-1}) is the single exponential rate constant, and SAV (cm^{-1}) is the surface area to volume ratio.

Electrophoresis and immunochemical techniques.

SDS-PAGE was performed by the method of Laemmli (1970) on 15% (w/v) polyacrylamide gels.

Nod26 anti-sera against gel-purified nod26 isolated from purified SM were prepared as described previously (Zhang & Roberts, 1995). Anti-nod26 IgG was purified on protein A-agarose (Pierce) by the manufacturer's protocol. Western blotting was done with anti-nod26 IgG (3 mg/ml) used at a 1:1000 dilution by the procedure of Zhang & Roberts (1995). Westerns were developed by use of a horseradish peroxidase coupled goat-anti-rabbit IgG secondary antibody. Preimmune rabbit IgG was used as a control.

CHAPTER III

RESULTS

Expression of nod26 confers water permeability to Xenopus oocyte membranes.

Expression of nod26 in *Xenopus* oocytes results in enhanced water permeability that is 4-fold higher than controls (Figure 6). Incubation of oocytes that express nod26 with 3 mM $HgCl_2$ inhibits water flux to the levels of untransformed control oocytes while addition of βME returns water permeability values to normal (Figure 6). Since phosphorylation was shown to modulate the channel activity of nod26 in planar lipid bilayer recording experiments (Lee et al., 1995), it was determined whether expression of the wild type or phosphorylation site mutants (S262A & S262D) alter the water permeability properties in oocytes (Figure 6). The site-directed mutants of nod26 show significant P_f values that are only slightly lower than wild type, show typical inhibition by $HgCl_2$, and are reversed by incubation with βME.

In situ analysis of nod26 water channel properties in isolated SM vesicles.

Based on the oocyte experiments, we wished to further characterize the water-fluxing properties of the nod26 channel in its native state in the symbiosome membrane. Highly purified symbiosome membrane vesicles were prepared (Day

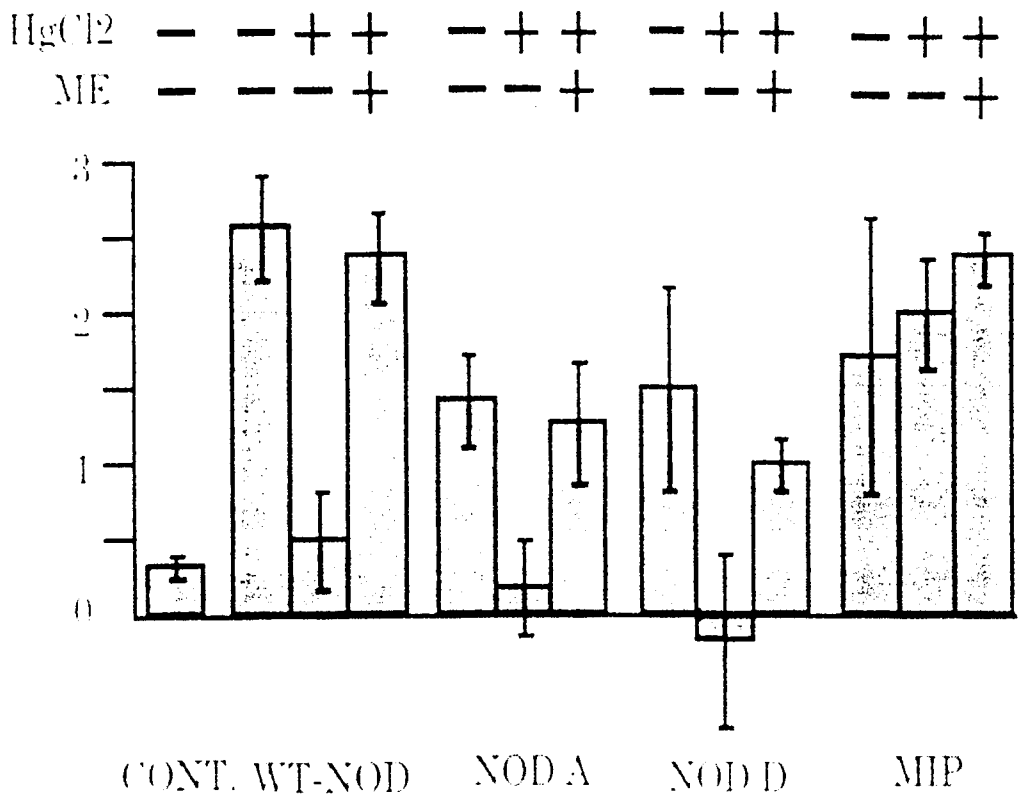

Figure 6. cRNA of nod26 wild type and phosphorylation site mutants confers water channel activity to the *Xenopus* oocyte membrane. Histogram of osmotic water permeabilities (P_f) of *Xenopus* oocytes expressing wild type nod26 or phosphorylation site mutants determined as described under "Materials & Methods". **CONT**, control oocyte injected with 50 nl of water; **WT-NOD** (wild type nod26), **NODA** (S262A nod26), **NOD D** (S262D nod26), and **MIP (AQP0)**, injected with 50 nl of 1 mg/ml AQP0 cRNA. P_f was measure either with no addition or in the presence of 3 mM $HgCl_2$ or 3 mM $HgCl_2$ followed by incubation with 5 mM β-mercaptoethanol (βME). This figure was provided by Dr. Grischa Chandy and Dr. James E. Hall and was a result of a collaboration with their laboratory (University of California, Irvine). Reproduced with permission of Dr. Grischa Chandy.

& Udvardi, 1989) and used for these *in situ* studies. To standardize and verify the purity of the SM vesicle preparation, SDS-PAGE (Figure 7) and Western blotting were performed. This analysis verifies the presence of nod26 as a major protein component (Figure 7). Preps were also standardized for total protein content by the method of Bradford (1976) yielding total protein concentrations in the range of 2-4 mg/ml.

For single channel conductance measurements, the concentration of nod26 within SM vesicles must be determined. Two methods were used to generate this value. First, a quantitative Western blotting method was established (Figure 8) in which the densitometry of the nod26 band (Figure 8B) was compared to the densitometry values of various loadings of a purified nod26 standard protein (Figure 8A, lanes 1-4). A standard curve was then constructed and used to determine the concentration of nod26.

Secondly, densitometry of a Coomassie Blue-stained SDS-PAGE gel of the vesicle preparation and the total prep protein concentration, estimated by the method of Bradford (1976), were used to determine the nod26 concentration in the SM. The molar concentration was estimated using a molecular weight of 28,887 (calculated from the deduced amino acid sequence of nod26, Sandal & Marcker, 1988). Both methods showed excellent agreement and the nod26 concentration within SM vesicles was calculated to be between 3 to 4 nmoles / mg SM protein. This represents approximately 10-15% of the total SM protein.

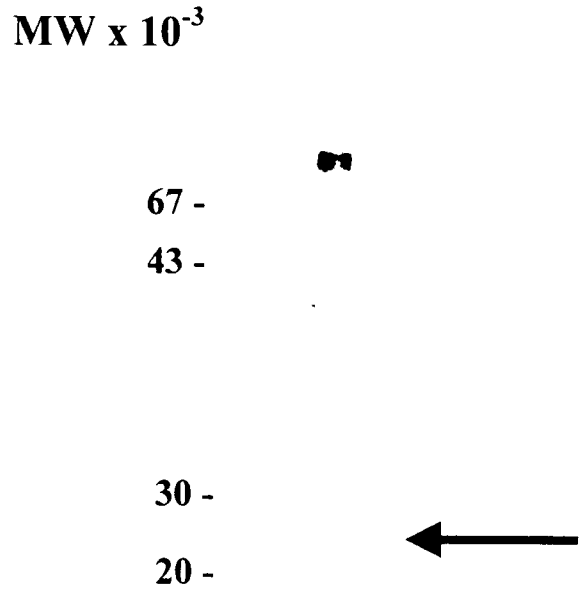

Figure 7. Nod26 is a major symbiosome membrane protein. Coomassie-Blue stained 15% (w/v) SDS-PAGE gel of SM proteins (10 μg total protein). Nod26 is the major 28,000 MW band shown by the arrow. This band was verified as nod26 by western blotting with anti-nod26 IgG (Zhang & Roberts, 1995).

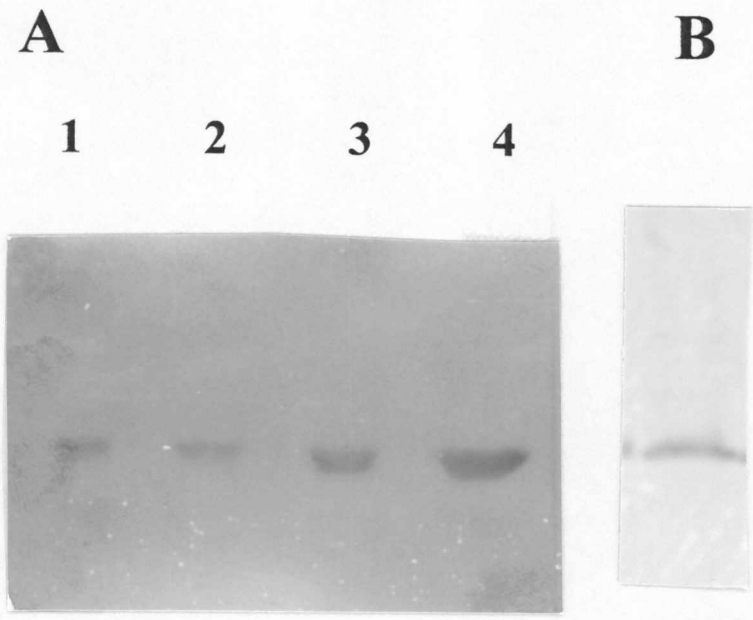

Figure 8. Representative Western blot used for determination of the concentration of nod26 in SM. Purified nod26 standard protein (A) or SM (B) were resolved on SDS-PAGE (15% (w/v)) polyacrylamide gels and were transferred to nitrocellulose and analyzed by Western blot with anti-nod26 IgG (Zhang & Roberts, 1995). **A.** Western blot of purified native nod26. Lanes 1-4 contain 0.64, 1.9, 3.2, and 6.4 μg of nod26 respectively. **B.** Western blot of total SM protein (2 μg total protein). Densitometry was conducted on blots A and B. The values obtained from the purified standard protein shown in A were used to construct a standard curve. The densitometry value from panel B was used to determine the concentration of nod26 within the SM from the standard curve.

Size distribution of SM vesicles.

To carryout a meaningful study of the permeabilities of the SM, a uniform distribution of vesicles must be present and their sizes need to be determined. By using quasielastic light scattering analysis, a uniform population exists and an average diameter of 228 nm was determined (Figure 9). This value was consistent from prep to prep and used for all membrane permeability calculations. Sizing by negative staining followed by visualization by transmission electron microscopy yielded a similar average vesicle diameter (244 nm).

Osmotic water permeability (P_f) of SM vesicles.

SM vesicles were loaded with the fluorescent indicator dye CF (20 mM) and water fluxes were determined by stopped-flow fluorimetery upon rapid injection into a buffer with double the osmolarity (Figure 10). As osmotically driven water efflux occurs, the SM vesicles will shrink increasing the concentration of the entrapped CF. As the CF concentration rises, self-quenching results, which is monitored by a time dependent decrease in fluorescence (Figure 10). Extravesicular CF is quenched using anti-CF antibodies (Kuypers et al., 1984; Lande et al., 1995).

The time course of fluorescence decrease is directly proportional to SM vesicle volume (Lande et al., 1995; Negrette et al., 1996). The curve is fit to a single exponential (see Equation 3, Materials & Methods) generating a rate (s^{-1})

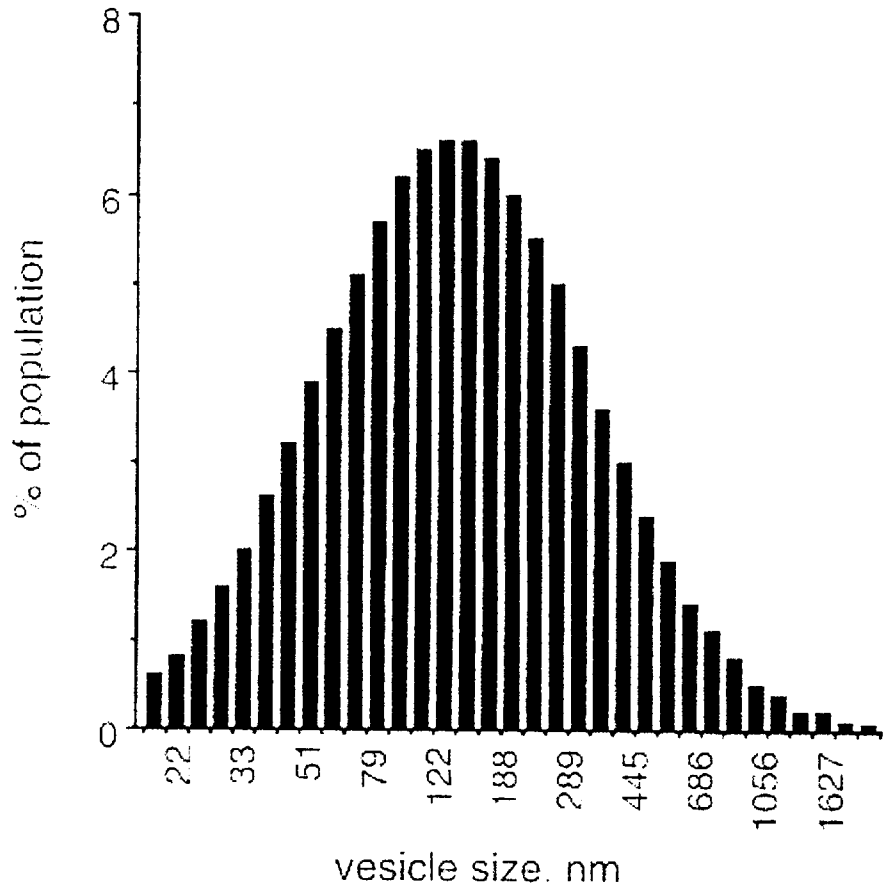

Figure 9. Representative quasielastic light scattering profile of SM vesicles. Plotted are the number of particles (ordinate) verse diameter values (abscissa) showing a uniform population of vesicles.

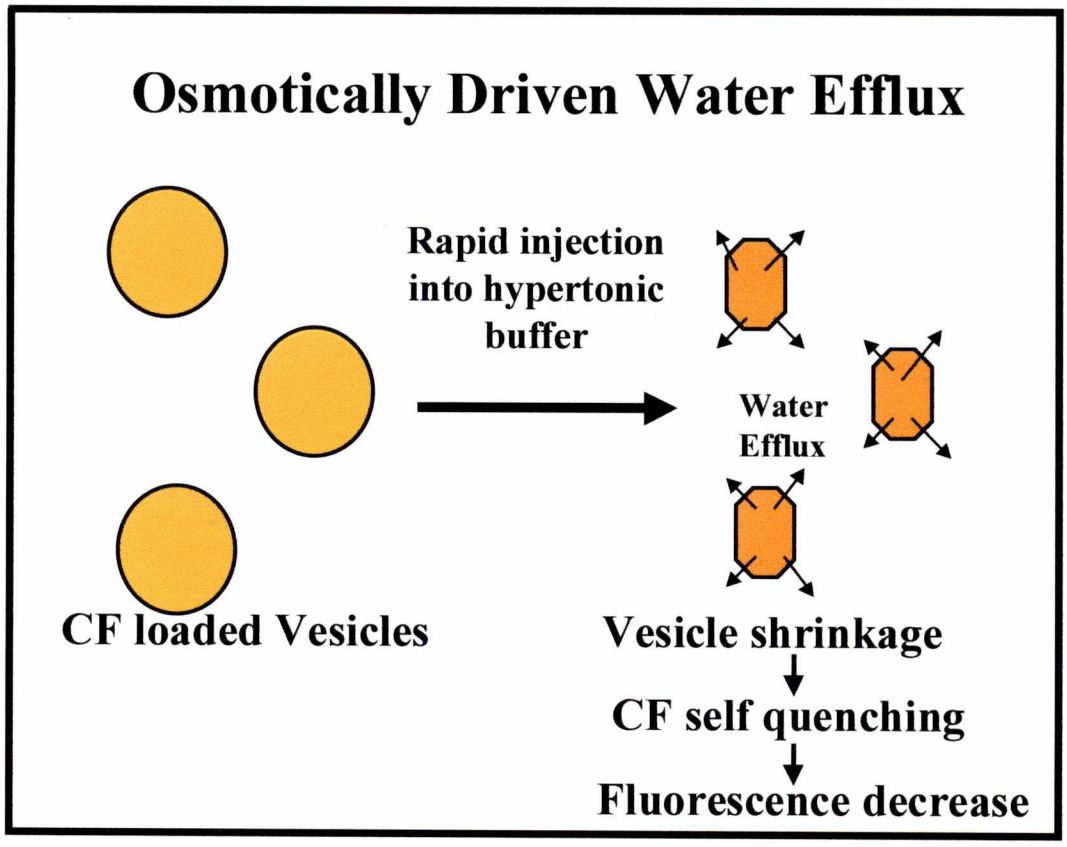

Figure 10. Illustration of stopped-flow fluorimetry technique used to measure water efflux from carboxyfluorescein loaded vesicles. Vesicles loaded with the fluorophore CF are rapidly injected, via stopped flow, into a hypertonic medium with the solute concentration abruptly doubled. Osmotically driven water efflux ensues leading to vesicle shrinkage and an increase in the concentration of the entrapped CF. As the CF concentration rises, self-quenching results, which is monitored spectrofluorimetrically. From the rate of quenching a rate of volume decrease is calculated as described in the Material and Methods.

which is then used, along with the other parameters of the osmotic permeability equation (see Equation 4, Materials & Methods), to calculate an osmotic water permeability coefficient (P_f, cm/s).

Figure 11 shows a representative trace of the time course of osmotic shrinkage of SM vesicles in both the presence and absence of 0.1 mM $HgCl_2$. SM vesicles are highly permeable to water with an average P_f of 0.05 ± 0.003 cm/s at 20°C (n = 15) that is drastically reduced to an average value of 0.00380 ± 0.0006 cm/s (n=7) upon addition of 0.1 mM $HgCl_2$.

Due to the hydrocarbon nature of lipid membranes, a low water permeability results. Water transport across pure lipid membranes is thermodynamically unfavored and is characterized by a high Arrhenius E_a (> 10 kcal/mole) (Finklestein, 1986; Chrispeels & Agre, 1994; Brown et al., 1995; Maurel, 1997). The presence of water channels in a lipid bilayer results in a much decreased E_a (≤ 5 kcal/mole) similar to diffusion of water in a bulk solution (Finklestein, 1986). From an Arrhenius plot constructed from the rates of water flux over a wide temperature range (12-39°C), an E_a of 3.3 ± 0.4 kcal/mole (n=3) was determined (Figure 12). The low E_a and $HgCl_2$ sensitivity of SM water flux suggests a facilitated means of water transport. Based on the results of *Xenopus* oocyte expression experiments, we propose that nod26 is responsible for this facilitated water transport.

From the estimated concentration of nod26 in SM vesicles (Figure 8A & B), the calculated vesicle surface area, and the P_f, a single channel conductance, of

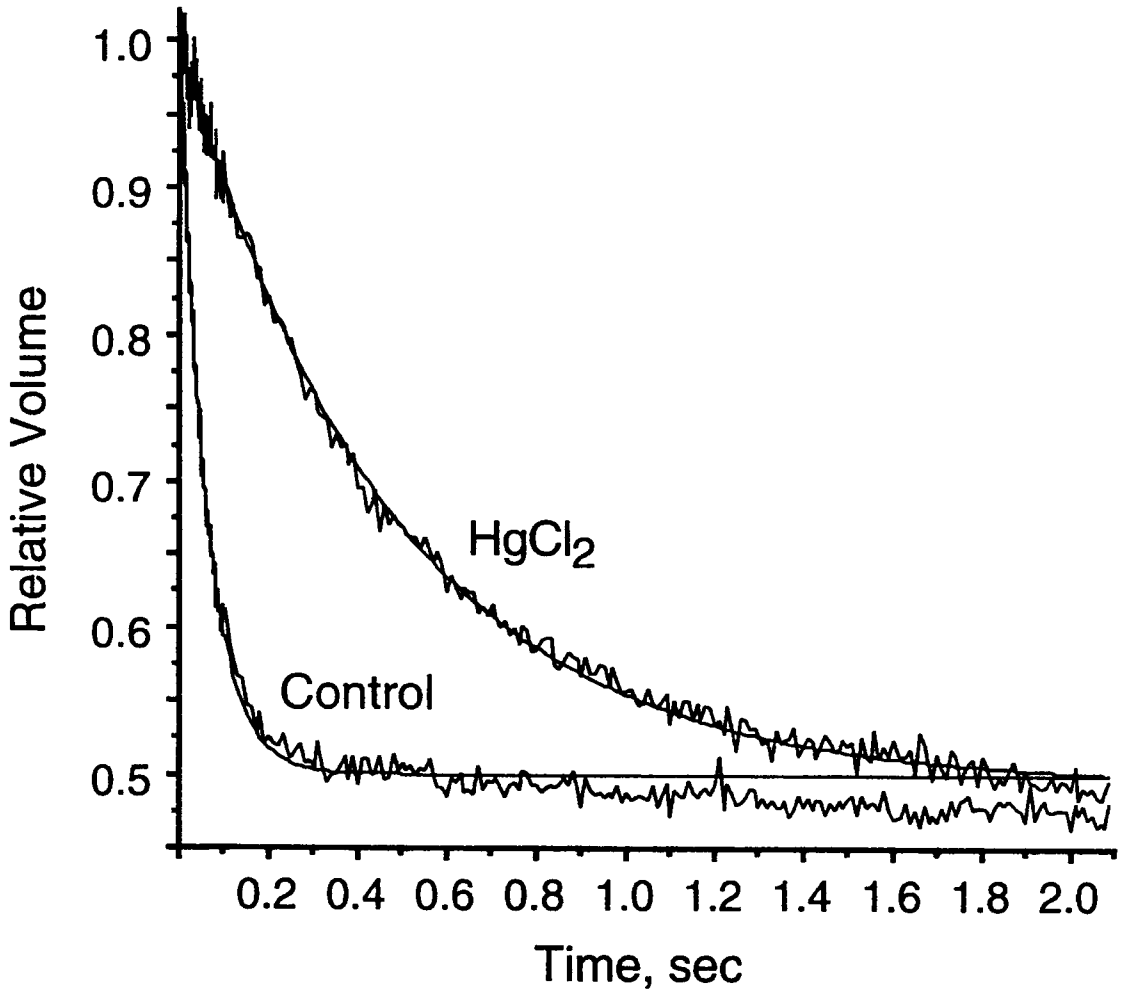

Figure 11. Time course of water efflux from SM vesicles. Water efflux from CF loaded (20 mM) SM vesicles was measured at 20 °C in the absence (control) and presence of 0.1 mM $HgCl_2$. Shown are fitted exponential curves showing the change of relative volume as a function of time. Endpoint for control trace was taken at 0.5 sec. for the single exponential fit.

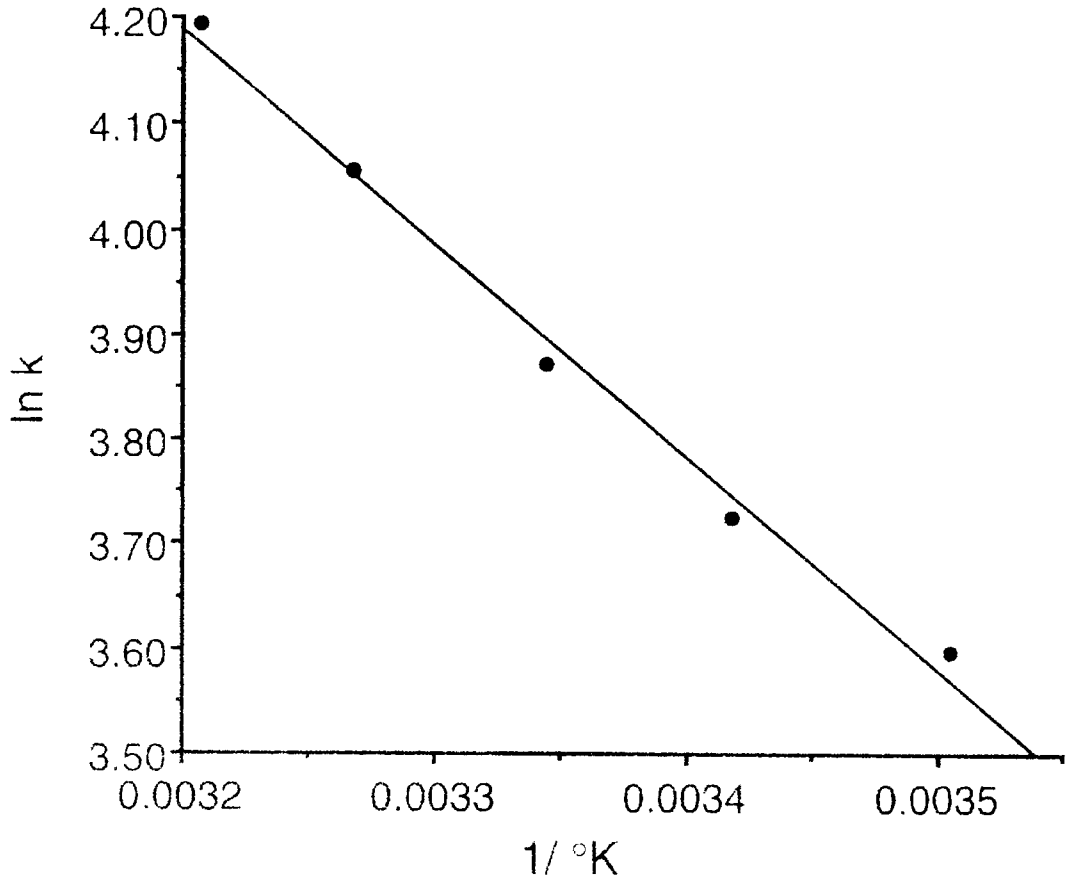

Figure 12. Representative Arrhenius E_a plot of SM water flux as a function of temperature. Plotted are ln k (where k is the rate constant from the single exponential curve fit determined as discussed in the Materials & Methods) on the ordinate and temperature as the inverse of degrees kelvin on the abscissa.

each nod26 monomer, was calculated. This assumes that the measured water flux is largely due to the nod26 channel. Based on our measurements, a single channel conductance of $3.2 \pm 1.3 \times 10^{-15}$ cm^3/s (n=3) was calculated. This value is 30-fold lower than that of the mammalian "archetypal" water channel, AQP1 (Zeidel et al., 1992).

Diffusive water permeability (P_d) of SM vesicles.

Diffusive water permeability (P_d) is a measure of the rate of diffusion of water molecules through the nod26 channel under isotonic conditions. P_d measurements for AQP1 conducted on red blood cells allowed the calculation of the P_f / P_d ratio (Mathai et al., 1996). Based on Finklestein's theory of water transport, the P_f / P_d value is interpreted to be an estimation of the number of water molecules which line up single file within the pore of the channel (Finklestein et al., 1986; Stein, 1990). Additionally a P_f / P_d ratio > 1 is indicative of a water channel while a ratio ≤ 1 is consistent with water flow through pure lipid membranes (Finklestein et al., 1986; reviewed in Brown et al., 1995).

P_d was measured for nod26 in SM vesicles to test the hypothesis that nod26, similar to AQP1, transports water in a a single file fashion. P_d measurements utilize the fluorophore ANTS which shows enhanced fluorescence in the presence of deuterium oxide (D_2O) (Ye & Verkman, 1989). These measurements were carried out under isotonic conditions with the extravesicular buffer contain-

ing 50% D_2O. As D_2O diffuses into the vesicles, ANTS exhibits enhanced fluorescence (Figure 13). From the fluorescent trace (Figure 13), an average P_d of 0.0024 ± 0.0002 cm/s at 12 °C was calculated (n=3). P_f was calculated at the same temperature (P_f = 0.044 ± 0.005 cm/s, n=4), representing a P_f / P_d ratio of 18.3. This ratio multiplied by the diameter of a water molecule (2.72 Å), estimates the length of the nod26 aquaporin at 49.8 Å, similar to the assumed width of a bilayer (50 Å).

Solute permeability (P_{solute}) of SM vesicles.

To determine if nod26 is strictly "water selective" or if it has other transport capabilities, SM vesicles were tested for permeabilty of several uncharged solutes of varying size and flexibility, including formamide, glycerol, acetamide, and urea. SM vesicles were loaded with the respective solute. As illustrated in Figure 14, the solute containing vesicles were then rapidly injected, via stopped flow, into an isotonic buffer (containing the impermeant solute sucrose) lacking the test solute. After mixing, the extravesicular solute concentration was then 50% of its respective concentration inside the vesicle. While at time (t=0) the conditions are isoosmotic a solute gradient is in place. As the test solute is transported out of the vesicles in response to the concentration gradient, an osmotic potential is established driving water efflux. This water efflux leads to vesicle shrinkage

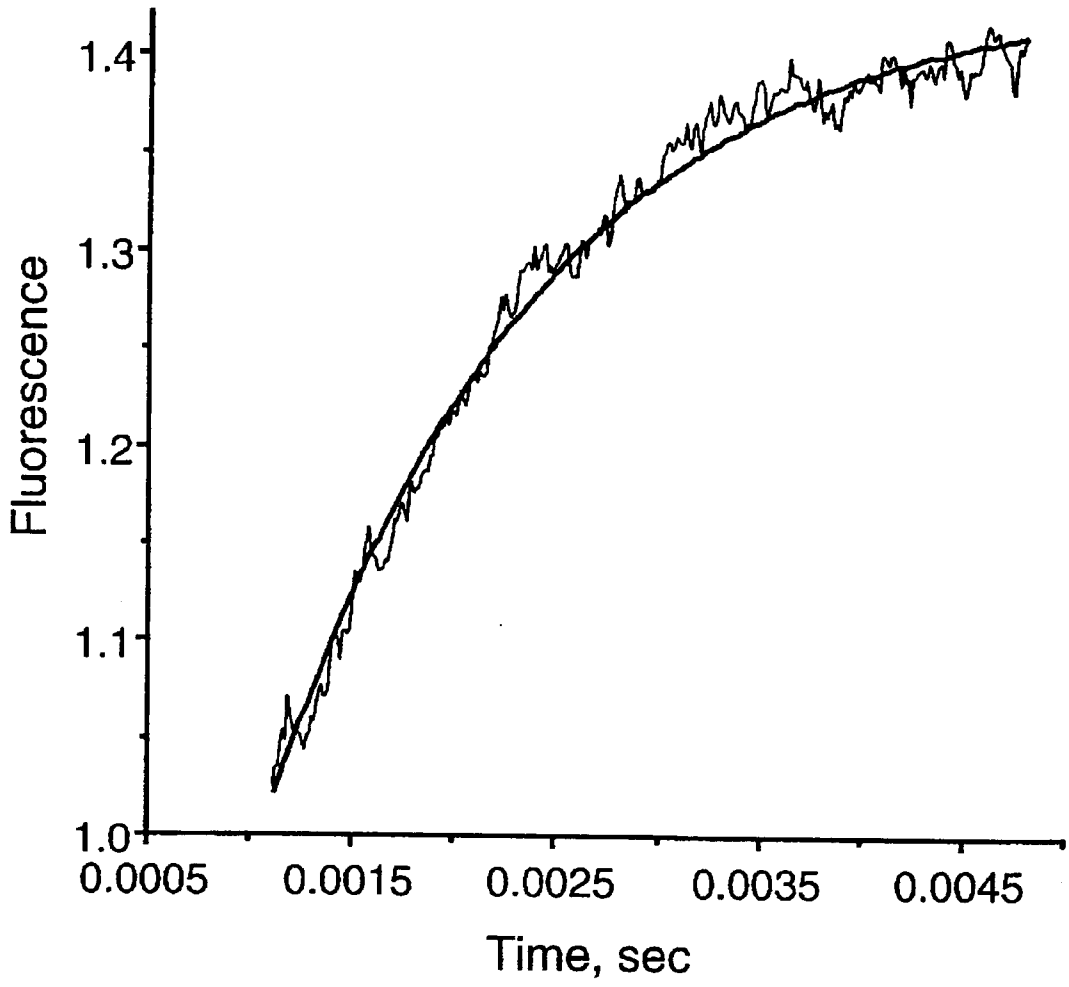

Figure 13. Diffusive water permeability measurements of SM vesicles. SM vesicles loaded with ANTS (10 mM) and equilibrated in a H_2O based buffer (as described in Materials & Methods) were abruptly diluted into a D_2O based buffer at 12 °C. As D_2O replaces H_2O inside the SM vesicle, an enhanced ANTS fluorescence results. ANTS fluorescence and its single exponential fit are plotted on the ordinate verses time on the abscissa. A representative curve is shown.

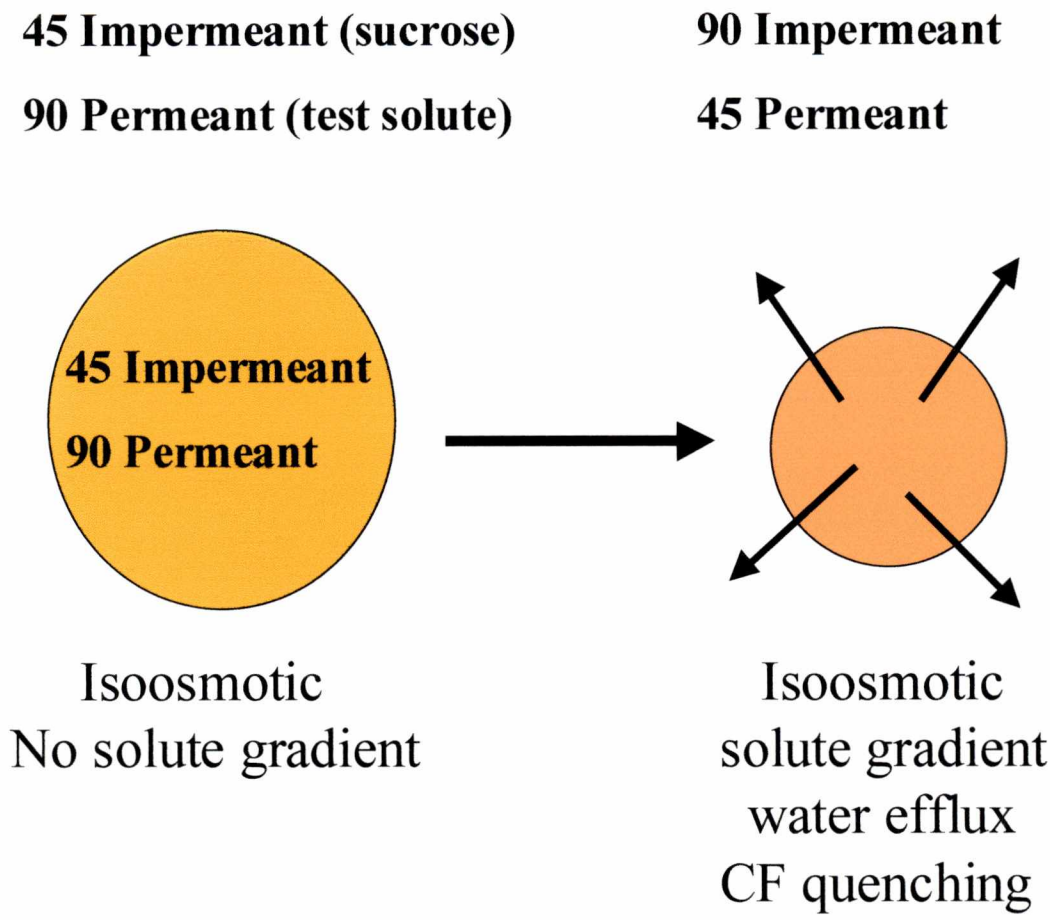

Figure 14. Illustration of stopped-flow fluorimetry technique used to measure solute efflux from carboxyfluorescein loaded vesicles. Vesicles loaded with the test solute are rapidly injected, via stopped-flow, into an isoosmotic buffer lacking the test solute (before mixing). After mixing conditions are isoosmotic but a solute gradient is in place. As the test solute effluxes from the vesicles in response to the solute concentration gradient an osmotic potential is established driving water efflux. Water efflux leads to vesicle shrinkage resulting in CF self-quenching monitored as a time dependent CF quench curve. The values of 45 and 90 for the permeant and impermeant solutes are in mOsm/kg.

and is monitored as a time dependent CF quench curve (Lande et al., 1995; Negrete et al., 1996).

Repesentative traces for the time course of solute flux are shown if Figure 15. The permeability coefficients (P_{solute}) are summarized as a histogram in Figure 16. Permeabilities to formamide and glycerol were high with significant $HgCl_2$ inhibition (85-90%). Acetamide was poorly transported with only a slight inhibition by $HgCl_2$. Facilitated urea transport does not occur.

Water permeability of reconstituted nod26.

The preceding data strongly suggests that nod26 forms a multifunctional aquaporin in the SM. However SM vesicles contain other components beside nod26. To unequivocally establish nod26 as the SM aquaporin, and to carryout a rigorous biochemical characterization of its transport capabilities, we purified native nod26 and reconstituted it into pure lipid vesicles which then were tested for water and glycerol permeability.

Nod26 was purified from isolated soybean SM by solubilization in OG followed by FPLC-anion exchange chromatography on a DEAE Fast Flow column. Elution fractions containing purified nod26 were concentrated on a centricon-10 ultrafiltration device to a final concentration of 0.3-0.5 mg/ml (Figure 17) and Western blotting was done to verify the purified protein was nod26. Nod26 purified by this method was used for all proteoliposome reconstitution studies.

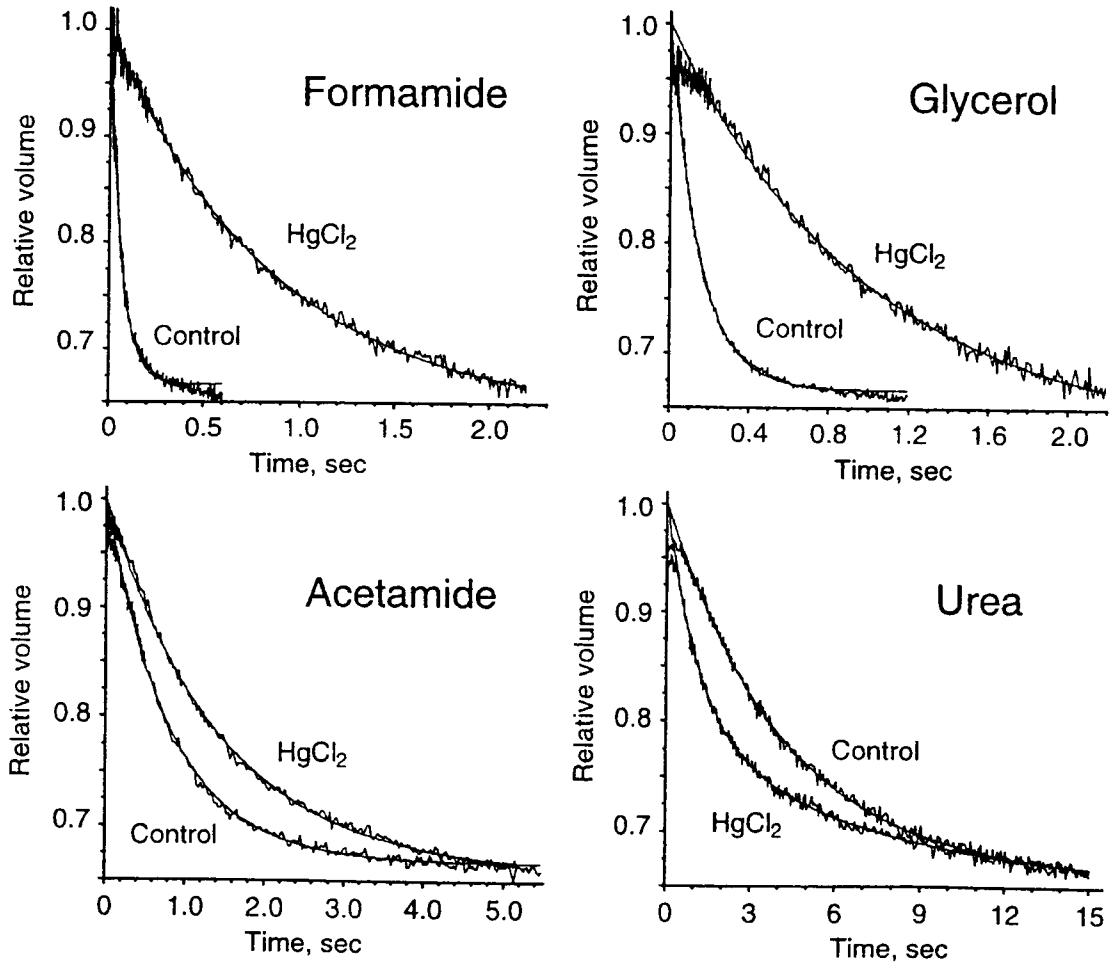

Figure 15. Representative plots of solute efflux from SM vesicles. The time courses of solute efflux for the solutes formamide, glycerol, acetamide, and urea were monitored at 20 °C in both the presence and absence of 0.1 mM $HgCl_2$. Shown are the fluorescence traces and the single exponential fits.

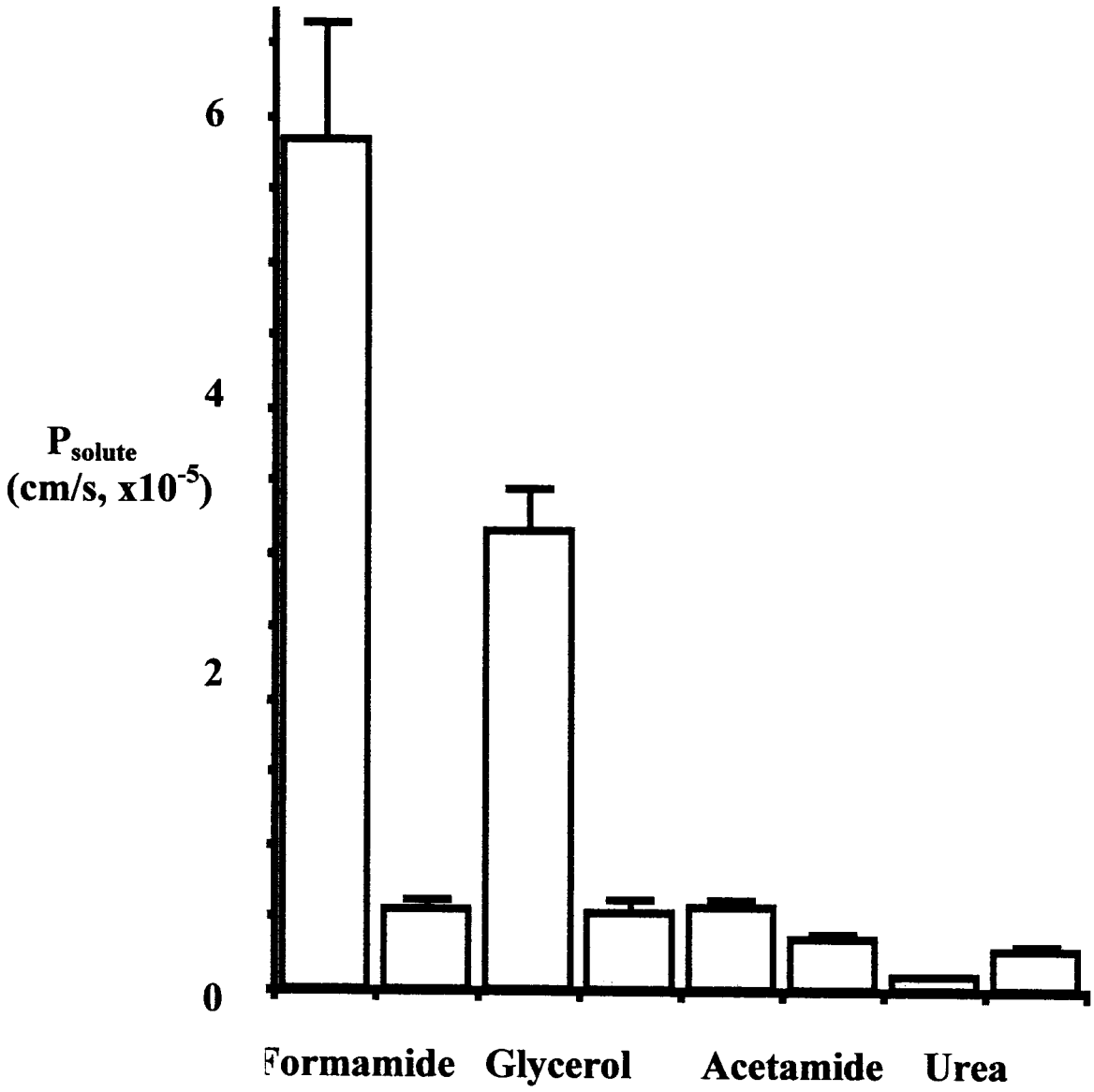

Figure 16. Histogram of solute permeabilities in both the presence (unfilled bars) and absence (dark bars) of 0.1 mM $HgCl_2$. Shown are the mean solute permeabilities ± S.E. for measurements on 4-7 SM vesicle preparations.

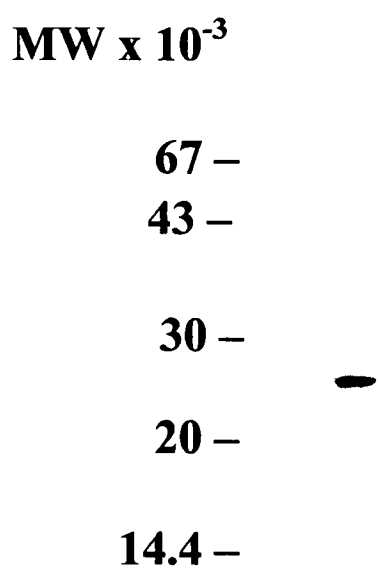

Figure 17. Coomassie-Blue stained gel of purified nod26. Purified and concentrated nod26 (3 μg protein) was resolved by SDS-PAGE on a 15% (w/v) polyacrylamide gel. The band was verified as nod26 by Western blotting (Zhang & Roberts, 1995).

A rapid dilution method (Zeidel et al., 1992) was employed to incorporate nod26 into *E. coli* polar lipids. To test for reconstitution, proteoliposomes recovered by ultracentrifugation were examined by SDS-PAGE (Figure 18). To verify that vesicles were formed, that they are present in a uniform population, and to determine an average vesicle diameter, negative staining of vesicles was done followed by visualization using transmission electron microscopy (Figure 19A & B). From negative staining, an average vesicle diameter of 125 ± 10 nm (n=4) for proteoliposomes (Figure 19A) and 118 ± 14 nm (n=4) for control liposomes (Figure 19B) was determined. Thus both proteoliposomes and control vesicles show similar sizes and are present in a uniform population. The accuracy of the diameter values was supported by quasieleastic light scattering as done above for SM vesicles.

Proteoliposomes and control liposomes are osmotically sensitive.

To verify the osmotic sensitivity and integrity of nod26 proteoliposomes, a simple fluorimetric test was conducted. Osmotically sensitive vesicles will shrink as the concentration of solute increases. Vesicles were diluted into an isotonic buffer and vesicle shrinkage was followed spectrofluorimetricaly upon stepwise additions of 2.0 M sucrose (Figure 20). As a final test to verify CF is trapped within the vesicles, tritonX-100 is added, which lyses the vesicles and releases the entrapped CF. This results in an increased fluorescence signal which is then com-

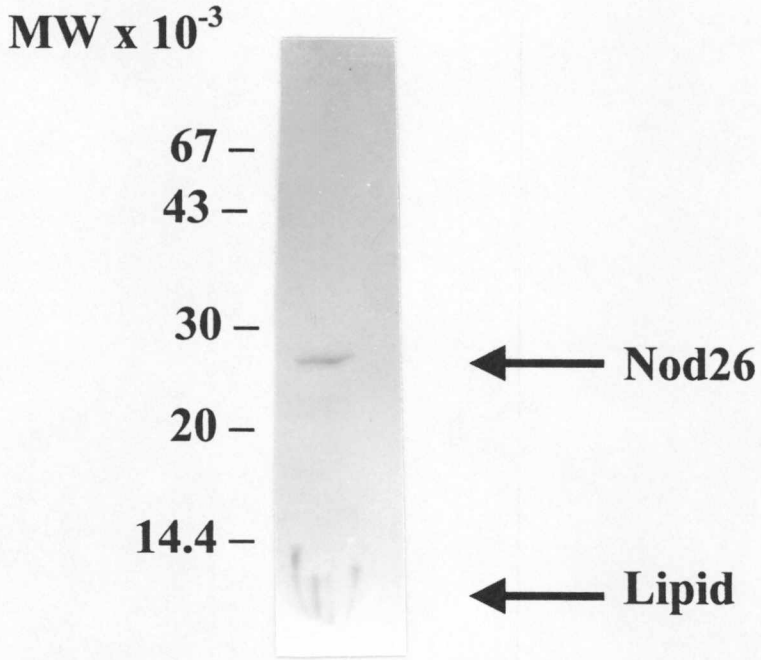

Figure 18. Coomassie-Blue stained gel of a representative nod26 proteoliposome preparation. Nod26 proteoliposomes (1 μg protein) were resolved by SDS-PAGE on a 15% (w/v) polyacrylamide gel and were visualized by Coomassie-blue staining to verify incorporation of nod26 into the vesicles.

A

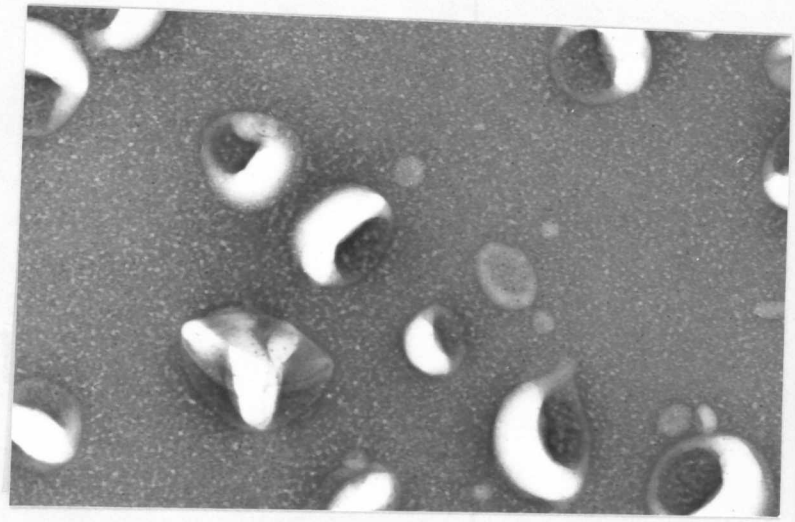

B

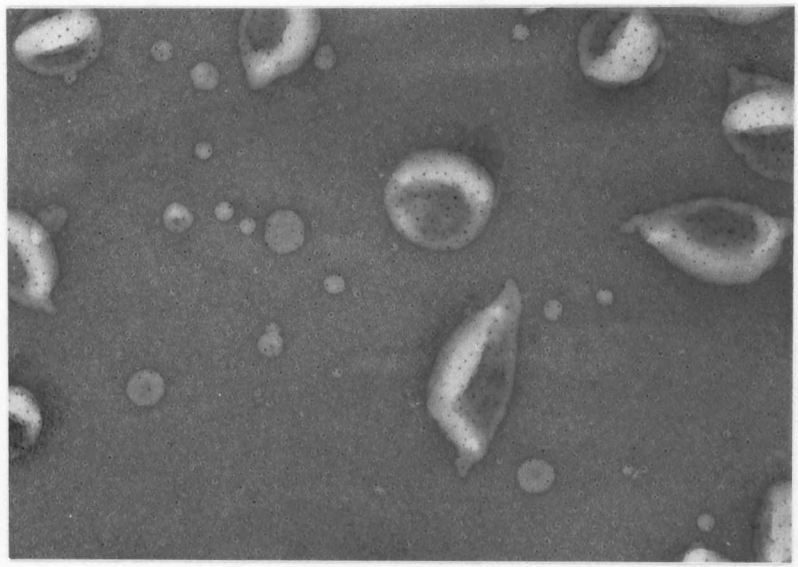

Figure 19. Electron micrographs of representative nod26 proteoliposome and control liposome preparations. Nod26 containing proteoliposomes **(A)** and control liposomes **(B)** were subjected to 1% (w/v) uranyl acetate negative staining and visualized by transmission electron microscopy. Electron micrographs demonstrate both control and proteoliposomes are of similar sizes and are present in a uniform population. Final magnification is 110,000 x.

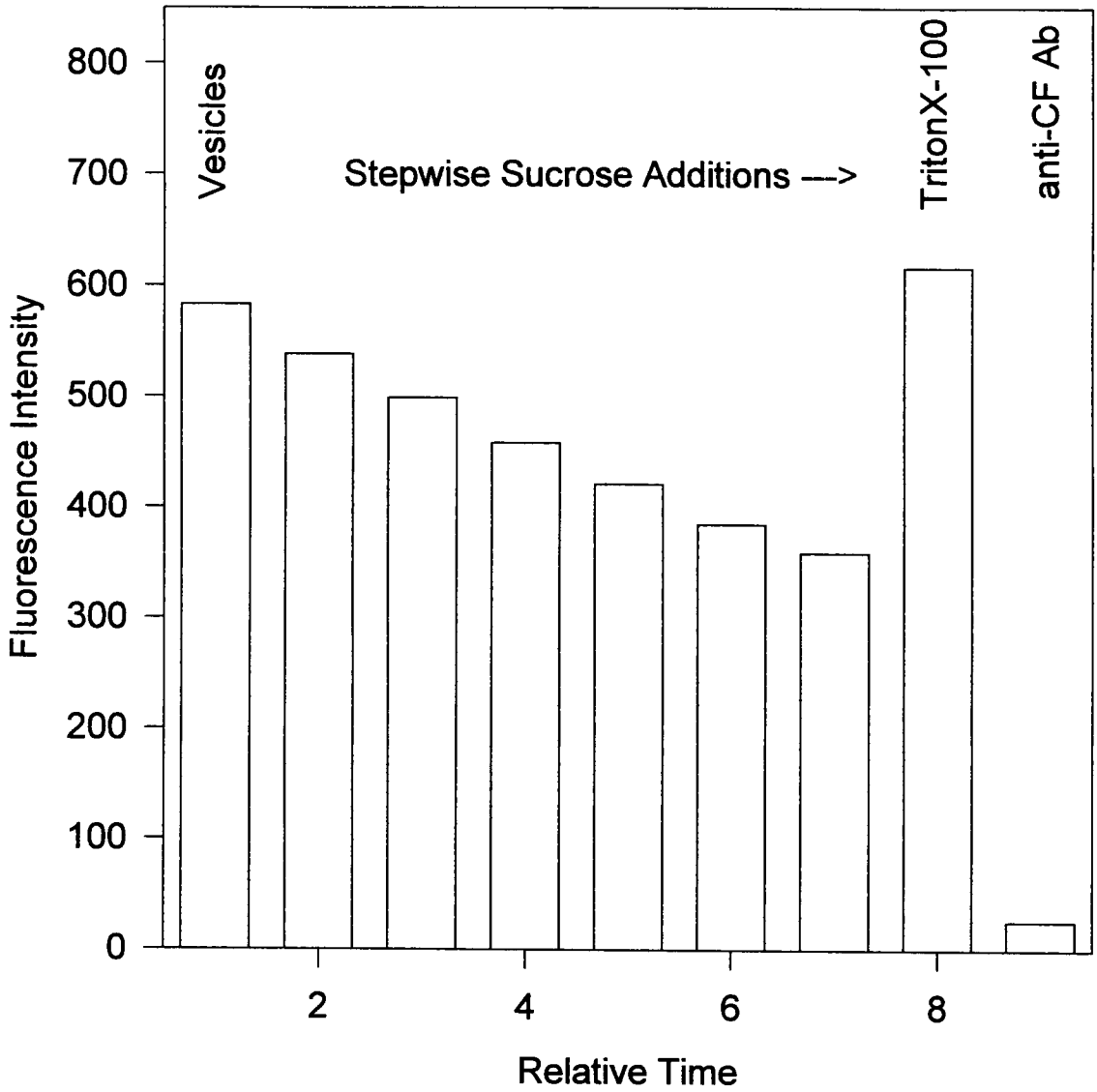

Figure 20. Fluorimeter test to verify integrity of vesicle preparations. CF-loaded vesicles were diluted in an isotonic buffer (3.0 ml) and fluorescence intensity measured spectrofluorimetrically. 73 µl stepwise additions of 2.0 M sucrose (an impermeant solute) cause vesicle shrinkage and CF self-quenching verifying the osmotic sensitivity and integrity of the vesicles. Addtion of TritonX-100 (73 µl) lyses the vesicles releasing the entrapped CF detected as a rise in fluorescent intensity. Anti-CF Ab (10 µl aliquots) is added until a total quenching of the released CF fluorescence occurs. Relative time refers to the aging of the solution in the cuvette prior to the next addition.

pletely quenched by the addition of an anti-CF antibody (Figure 20). The high signal resulting from the entrapped CF release and the sensitivity to sucrose additions are an indication that the vesicles behave as "osmometers" and are not "leaky". These data establish that nod26 was successfully reconstituted into vesicles, that these vesicles were present in a uniform population and that they were osmotically sensitive, and "non-leaky". Thus, the proteoliposomes were suitable for permeability measurements.

Osmotic water permeability determinations of nod26 proteoliposomes.

The P_f of the liposomes were measured after rapidly doubling the extravesicular osmolarity by using the stopped-flow fluorimetric approach described above (Figure 21 and 22). Nod26-containing vesicles are able to facilitate water flux (P_f = 0.012 ± 0.001 cm/s, n=4) approximately 4-fold over control vesicles (P_f = 0.003 ± 0.001cm/s, n=4) and are inhibited approximately 67% by $HgCl_2$ (P_f = 0.004 ± 0.0007 cm/s, n=3).

As discussed earlier, water flux through protein channels are characterized by a reduced E_a. Shown in Figure 23 are representative Arrhenius plots of both nod26 containing vesicles and control pure lipid vesicles. Nod26 proteoliposomes transport water with an E_a of 3.53 ± 1.33 kcal/mole (n=3), a value about 4-fold lower than the value for control liposomes (E_a = 14.8 ± 3.36 kcal/mole, n=4). A

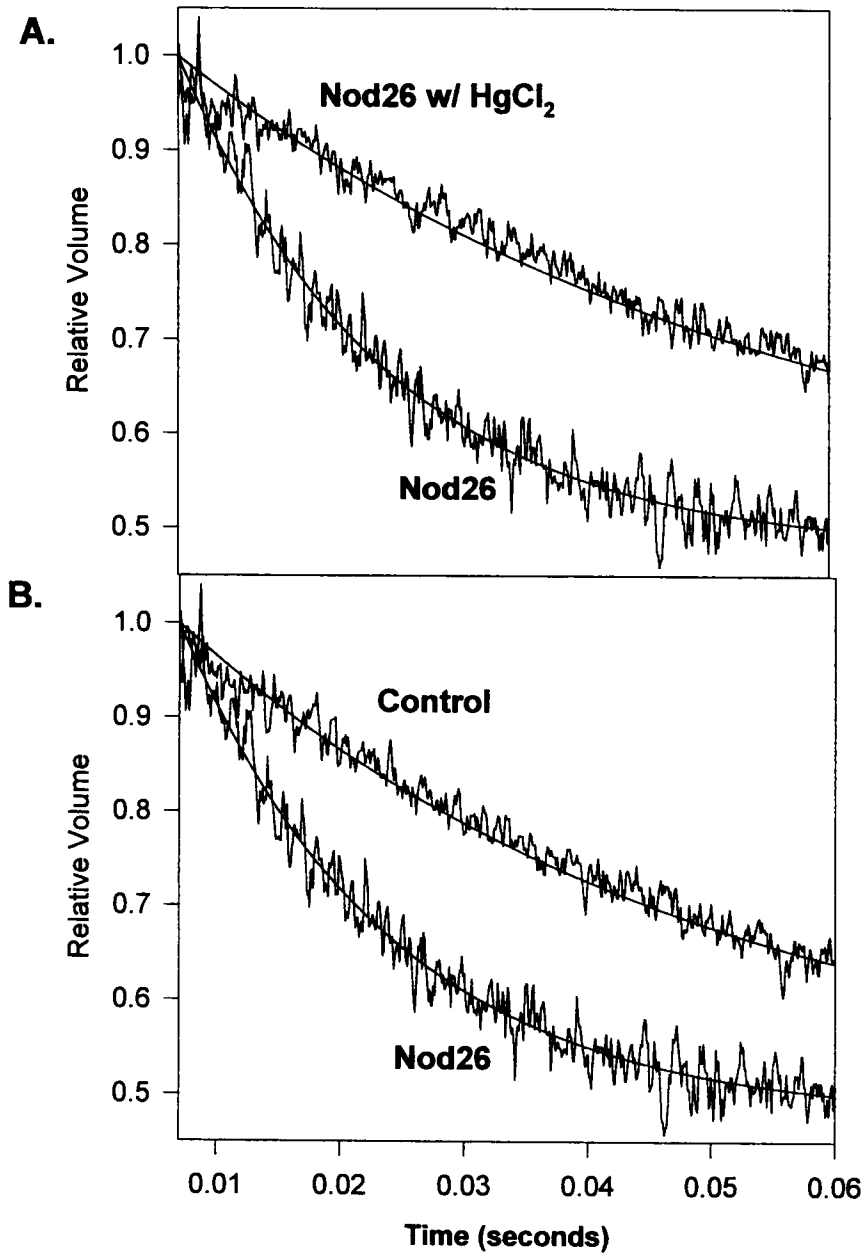

Figure 21. Time course of water efflux from nod26 proteoliposomes and control liposomes. Water efflux from CF-loaded vesicles was monitored at 20 °C as the time course of CF self-quenching. Shown are: **A.** nod26 averaged curves of nod26 proteoliposomes fitted to single exponentials in both the presence and absence of 1.0 mM $HgCl_2$; and **B.** Control pure lipid vesicles recorded under identical experimental conditions as in A. The single exponential fit for each curve is shown. For the sake of illustration the early part of the trace is shown. Full traces are shown in Figure 22.

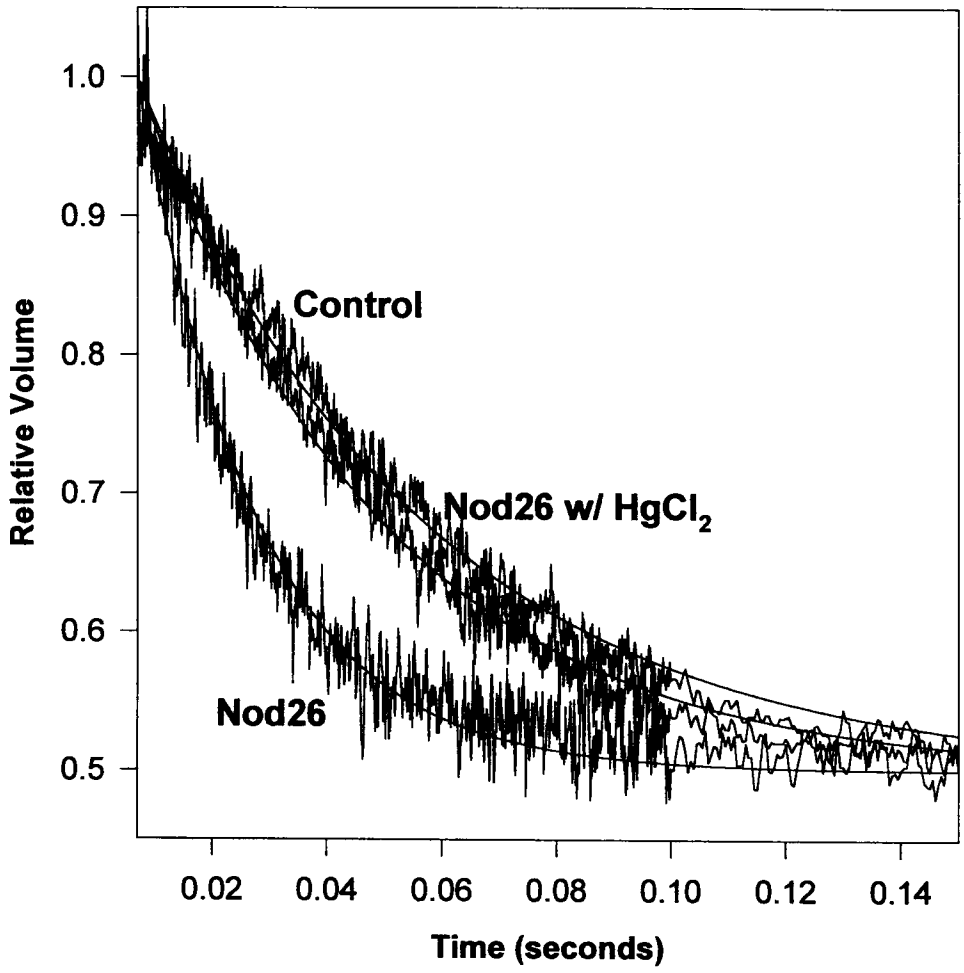

Figure 22. Full time course of water efflux from nod26 proteoliposomes and control liposomes. Water efflux from CF loaded vesicles was monitored at 20 °C as the time course of CF self-quenching. Shown are nod26 proteoliposomes in the presence and absence of 1.0 mM $HgCl_2$ and control pure lipid vesicles. The X-axis was extended to show the full time course of the experiment. The single exponential fit for each curve is shown.

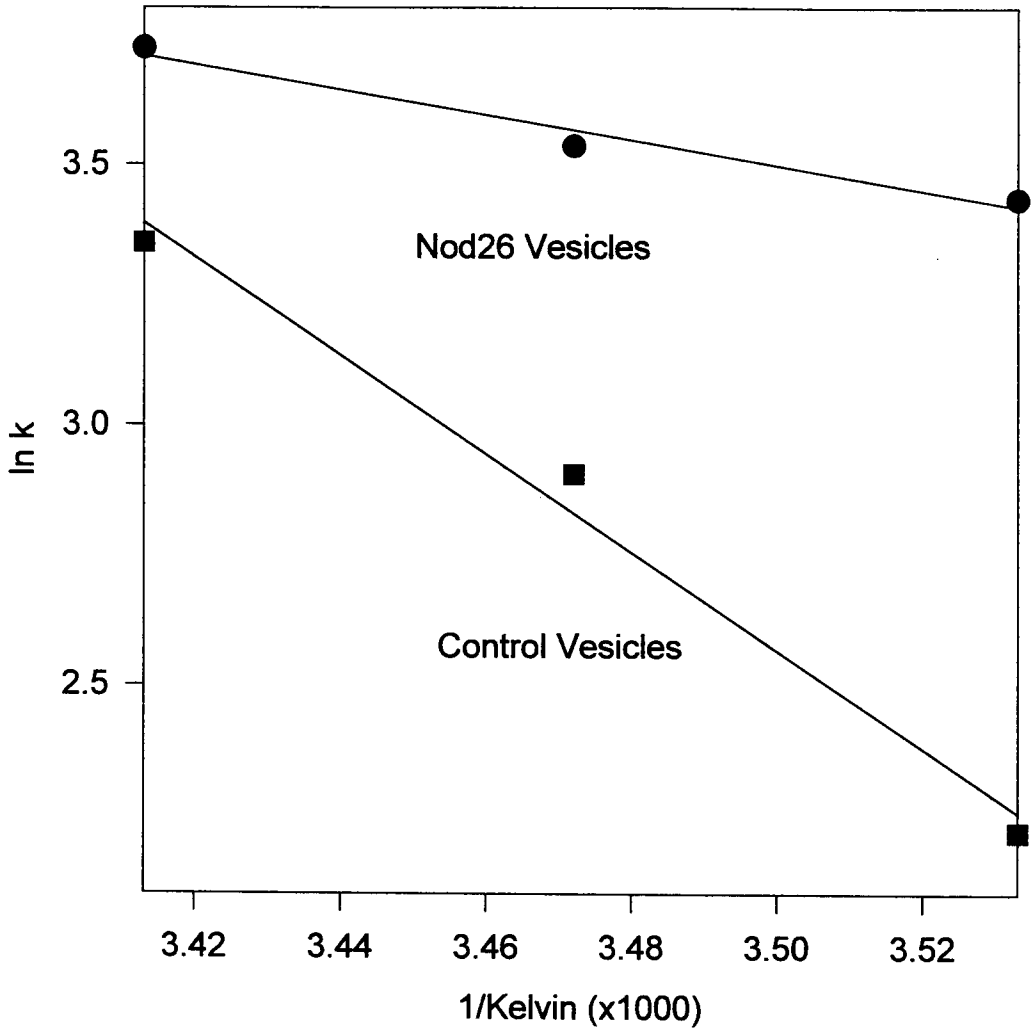

Figure 23. Representative Arrhenius plots for water efflux from nod26 proteoliposomes and control liposomes. Arrhenius activation energy plots for both nod26 proteoliposomes and pure lipid control liposomes with ln k (rate constant determined from the single exponential curve fit) on the ordinate and inverse of temperature as degrees kelvin (x 1000) on the abscissa. The acitvation energy is determined by multiplying the slope of the line by the gas constant.

high rate of water transport and a low E_a for nod26 proteoliposomes suggests nod26 is facilitating water flux as an aquaporin.

Single channel conductance (pf) of nod26 proteoliposomes.

The most quantitative parameter of water flux through an aquaporin is its single channel conductance (pf). This value is an estimation of the amount of water each nod26 channel can transport per unit time assuming, similar to AQP1 (Jung et al., 1994), that each nod26 subunit contains an aqueous pore. To determine this value it was necessary to determine the concentration of nod26 within the proteoliposomes and also the unit surface area of the proteoliposome vesicles.

Shown in Figure 24 are both a representative gel containing increasing amounts of a standard nod26 protein (Figure 24A, lanes 1- 5) and a standard curve (Figure 24B) constructed from the densitometry values of known amounts of the nod26 standard. The concentration of nod26 within proteoliposomes was determined from this standard curve. Nod26 was incorporated into vesicles at a concentration of approximately 2-4 μmolar.

From the diameter of a vesicle, calculated from the negative staining of the proteoliposome preparation (Figure 19), the surface area-to-volume (SAV) ratio was determined. The unit vesicle volume must be determined in order to calculate the unit surface area. Illustrated in Figure 25A is a histogram of the fluorescence intensities of nod26 liposomes and the total CF fluorescence released by lysing the

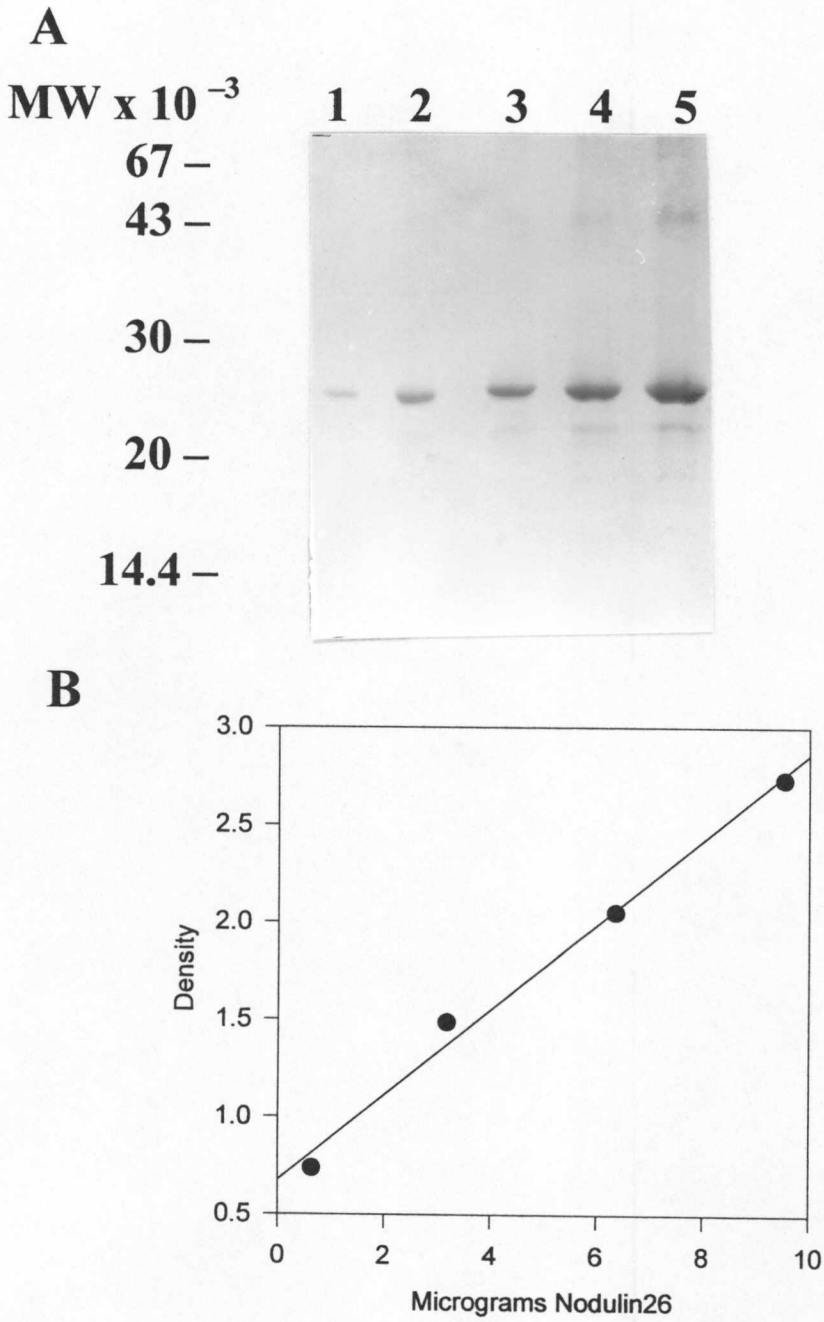

Figure 24. Representative Coomassie-Blue stained gel used for determinations of protein concentrations in nod26 proteoliposomes. **A.** Coomassie-blue stained 15% (w/v) SDS-PAGE gel with purified standard nod26 protein loaded in lanes 1- 5 containing 0.64, 1.9, 3.2, 6.4, 9.5 μg of nod26 respectively. **B.** Standard curve showing densitometry values plotted against μgrams of nod26.

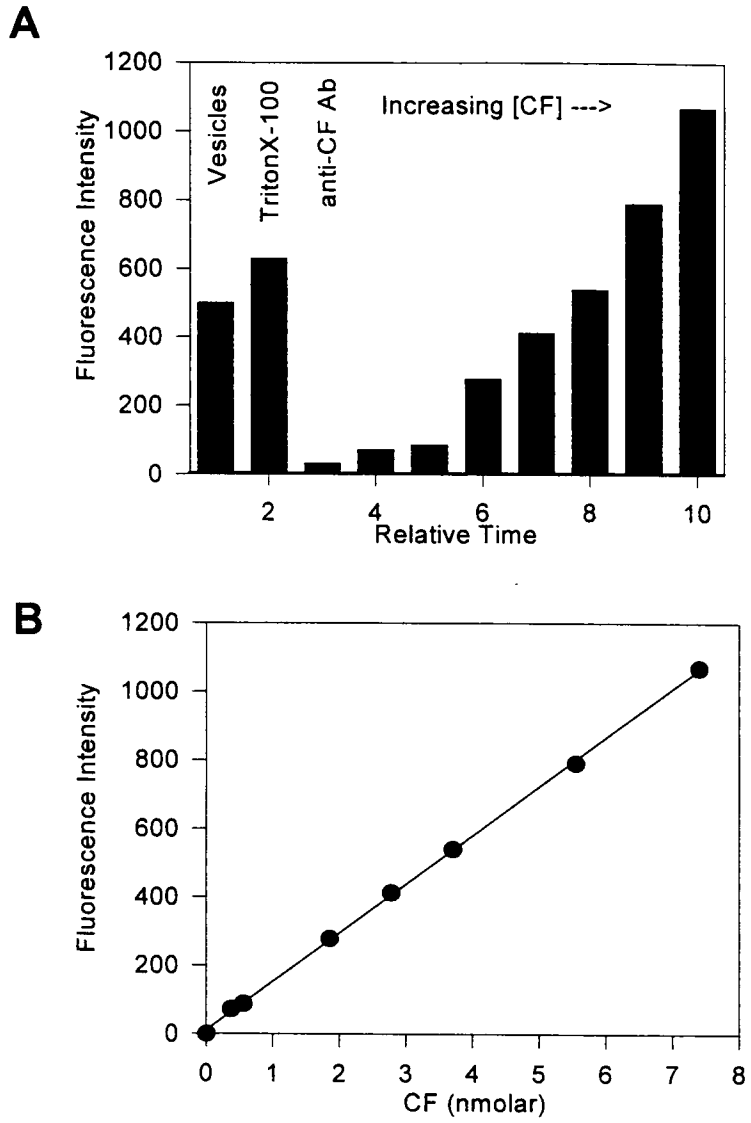

Figure 25. Determination of unit proteoliposome volume. A. Fluorescence intensities for both CF-loaded proteoliposomes diluted in an isotonic buffer and standard CF solutions were determined spectrofluorimetrically. **B.** Standard curve constructed from standard CF solutions. The total nanomoles of CF entrapped within the proteoliposomes were quantitated from the standard curve.

liposomes with TritonX-100. The total fluorescence released by TritonX-100 from the liposomes was corrected for background. The background value was determined by quenching the CF fluorescence with anti-CF antibody (Figure 25A). The concentration of the released CF was determined from a standard curve (Figure 25B) and used to calculate a unit vesicle volume which is then used, along with the SAV ratio, to determine a unit surface area.

From the number of nod26 molecules per unit surface area (SuD), and the P_f value determined on the same proteoliposome preparation a single channel conductance of $3.0 \pm 2.9 \times 10^{-15}$ cm^3/sec (n=2) was obtained. This value is similar to the value of $3.2 \pm 1.3 \times 10^{-15}$ cm^3/sec (n=3) calculated for SM vesicles. These findings suggest that purified nod26 is functionally reconstituted into pure lipid vesicles with water transporting capabilities similar to those measured in the symbiosome membrane.

Glycerol permeability of nod26 proteoliposomes.

We investigated whether purified reconstituted nod26 was capable of facilitating the glycerol efflux similar to that observed in SM vesicles (Figure26). Nod26 (Figure 26A) facilitates a large increase in glycerol transport ($P_{gly} = 0.77 \pm 0.45 \times 10^{-5}$ cm/s, n=3), approximately 40-fold over control vesicles (Figure 26B) ($P_{gly} = 0.02 \pm 0.007 \times 10^{-5}$ cm/s, n=3). Shown in Figue 27 is an expanded time scale of glycerol efflux demostrating the curves reach equilibrium. Consistent

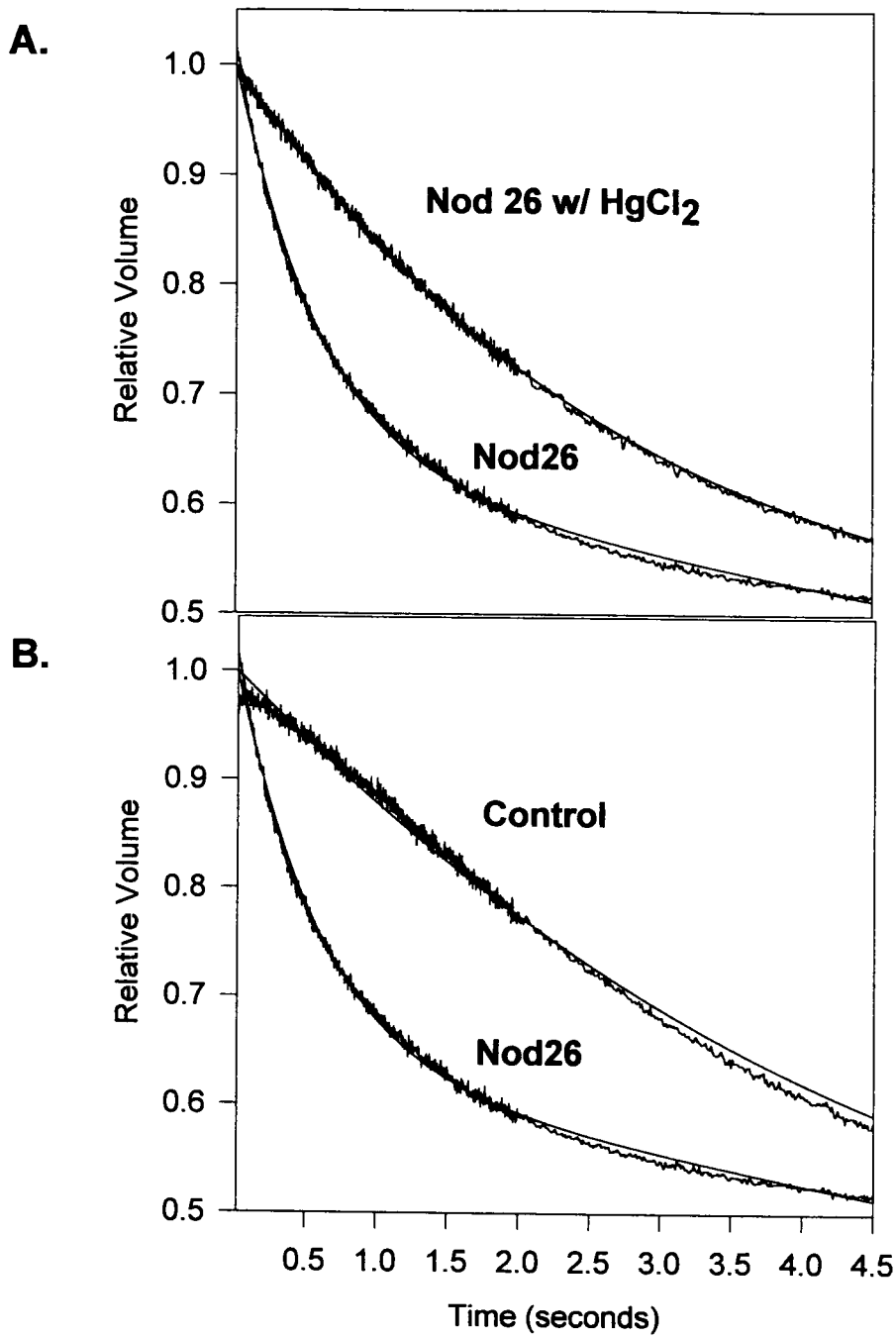

Figure 26. Time course of glycerol efflux from nod26 proteoliposomes and control liposomes. Glycerol efflux from CF loaded vesicles was monitored at 20 °C as the time course of CF self-quenching. **A.** Shown are nod26 proteoliposomes averaged curves fitted to single exponentials in both the presence and absence of 1.0 mM $HgCl_2$. **B.** Control pure lipid vesicles recorded under identical experimental conditions as in A.

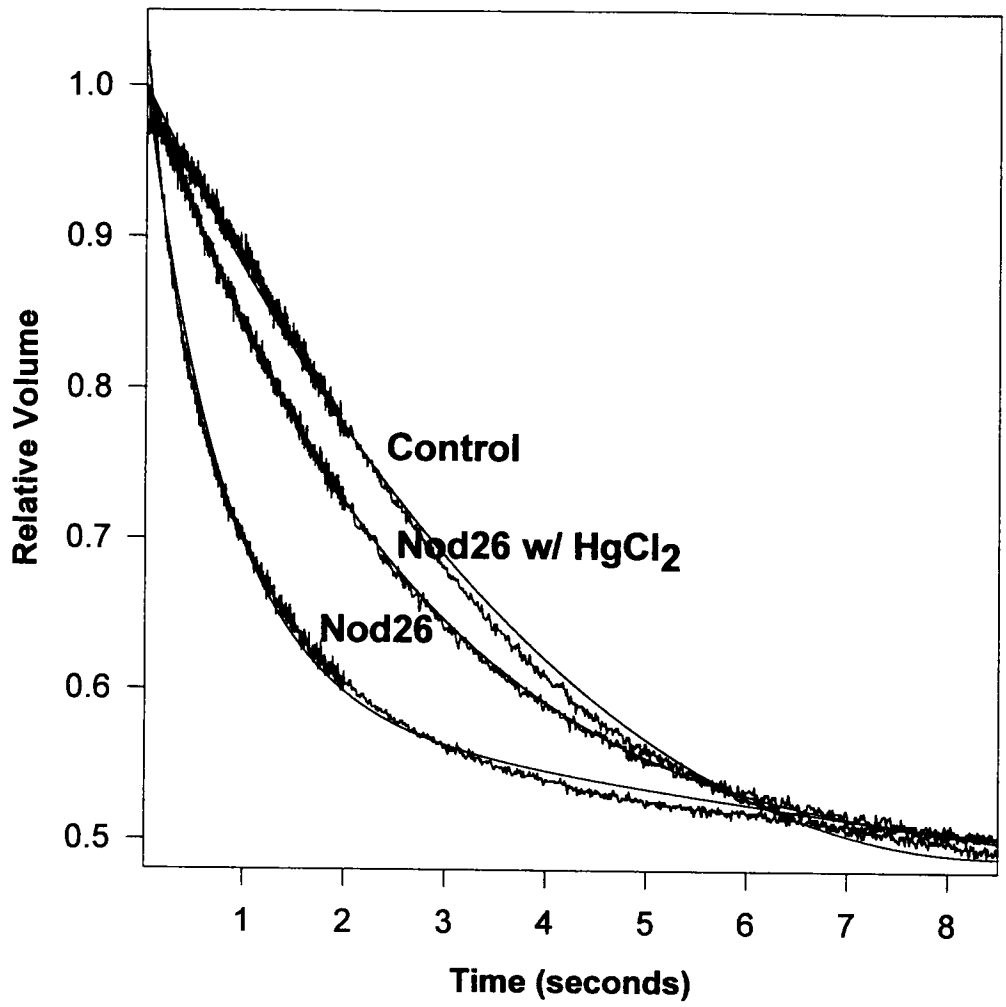

Figure 27. Full time course of glycerol efflux from nod26 proteoliposomes and control liposomes. Glycerol efflux from CF loaded vesicles was monitored at 20 °C as the time course of CF self-quenching. Shown are nod26 proteoliposomes in the presence and absence of 1.0 mM $HgCl_2$ and control pure lipid vesicles. The X–axis was extended to show the full time course of the experiment. The single exponential fit for each curve is shown.

with the SM vesicle results, glycerol transport in nod26 proteoliposomes is inhibited 94% by 1.0 mM $HgCl_2$ (P_{gly} = 0.05 ± 0.03 cm/s, n=2).

CHAPTER IV

DISCUSSION

The present study provides insight into two areas of nod26 function: its potential role in bacteroid / legume host symbioses as well as its characteristics as a member of the aquaporin class of membrane transport proteins. The following observations provide evidence that nod26 possesses water transporting activity and has the capability to be the SM water channel. First, nod26 is a member of the aquaporin class of water transporters of which several show partial or complete inhibition in the presence of $HgCl_2$ (King & Agre, 1997). Second, microinjection of nod26 cRNA confers an enhanced $HgCl_2$ sensitive water permeability to *Xenopus* oocytes. Third, the SM is highly permeable to water characterized by a low E_a and $HgCl_2$ sensitivity indicating this water permeability is facilitated. Fourth, purified native nod26 reconstituted into liposomes is capable of facilitating water flux with a low E_a and a single channel conductance ($3.0 \pm 2.9 \times 10^{-15} cm^3/s$, n=2) similar to that calculated for SM vesicles ($3.2 \pm 1.2 \times 10^{-15}$ cm^3/s, n=3). Additionally, besides water flux, nod26 apparently is multifunctional and also permits the flux of uncharged solutes.

Nod26 and the aquaporin family.

Microinjection of *Xenopus* oocytes with three nod26 cRNAs (w.t., S262A, and S262D) result in an enhanced osmotic water permeability of the oocyte oolemma. This water flux is characterized by $HgCl_2$ inhibition that is reversed by βME. These are hallmarks of the aquaporin class of membrane proteins (King & Agre, 1996).

$HgCl_2$ inhibition was shown for AQP1 to be a result of oxidation of cys-189 thereby implicating it near the pore of the channel (Preston et al., 1993). Nod26 contains two cysteine residues, in sites different from AQP1, located in the first and fourth transmembrane domains respectively (see Figure 4). The $HgCl_2$ sensitivity suggests that one or both of these cysteine residues are located in or near the channel pore and that modification by Hg^{2+} results in channel blockage. Which of these cysteines is responsible for the $HgCl_2$ inhibition is unknown and awaits elucidation by site directed mutagenesis studies.

There appears to be no qualitative difference in P_f upon expression of wild type or phosphorylation site mutants in *Xenopus* oocytes. However, in order to rigorously test this initial finding a quantitative approach must be adopted to critically evaluate these constructs. Similar amounts of cRNA for all three constructs were injected into oocytes, but no determination of the plasma membrane amounts of each construct have yet been performed. Thus, standardization of permeability values to protein amount has not been done. Zampighi et al. (1995) have pub-

lished a method to quantitate the amount of protein targeted to the oocyte plasma membrane utilizing a specialized freeze fracture technique. Also, Yang and Verkman (1997) have recently quantitated the amount of aquaporin protein embedded within the oocyte plasma membrane using epitope-tagged constructs. Similar studies with nod26 will result in a more quantitative evaluation of nod26 wild type and phosphorylation site mutants transport capabilities in the oocyte system. Additionally, previous planar lipid bilayer studies showed phosphorylation modulated ion channel activity only at high membrane potentials (Lee et al., 1995). Further studies of these constructs as a function of voltage potential will show whether phosphorylation also gates water flux. Nonetheless, nod26 and site-directed mutants (S262A & S262D) each show enhanced water flux and mercury inhibition reversed by βME upon *Xenopus* expression suggesting the integrity of the phosphorylation site is not necessary for water flux.

In situ transport studies utilizing isolated SM vesicles as well as proteoliposomes corroborate these studies and lengthen the list of transport activities associated with this protein. SM vesicle studies suggest nod26 may also be multifunctional possessing both water and solute transport capabilities. The significance of these findings are discussed further below.

Table I summarizes the findings of nod26's water transporting properties in both SM vesicles and nod26 proteoliposomes. P_f values determined for both systems are similar with a 92% reduction in P_f seen for SM vesicles as compared to a

Table I. Summary of permeability values for SM vesicles and nod26-containing proteoliposomes.

	SM	Proteoliposomes
Vesicle diameter (nm)	228 (n=2)	125 ± 10[b] (n=4)
P_f, cm/s (20 °C)	0.05 ± 0.003[a] (n=15)	0.012 ± 0.001 (n=4)
P_f, cm/s (20 °C) w/ $HgCl_2$	0.0038 ± 0.006 (n=7)	0.004 ± 0.0007 (n=3)
% Inhibition by $HgCl_2$	92 %	67 %
Unit Cond. (pf, cm^3/s), 20 °C	3.2 ± 1.2 x 10^{-15} (n=3)	3.0 ± 2.9 x 10^{-15} (n=2)
E_a (kcal/mole)	3.3 ± 0.4 (n=3)	3.5 ± 1.3 (n=3)
P_f / P_d	18.3	not determined

[a] ± standard error.
[b] ± standard deviation.

67% reduction observed for nod26 proteoliposomes upon addition of $HgCl_2$. Differences in P_f determinations are a function of protein concentration differences between SM vesicles and nod26 proteoliposomes. The higher P_f value determined for SM vesicles is due to a higher density of nod26 molecules per unit surface area in SM vesicles as compared to proteoliposomes. Single channel conductance measurements, in both systems, show good agreement and establish that purified native nod26 is able to transport water at a similar rate as observed in SM vesicles. Also the unit conductance determinations indicate that nod26 is an aquaporin of modest conductance, transporting water at a rate roughly comparable to AQP0 (Zampighi et al., 1995) and approximately 30-fold less than the archetypal water

channel AQP1 (Zeidel et al., 1992). In both systems a very low E_a results indicating water flux is facilitated.

It is interesting to note that Hg^{2+} does not reduce water permeability coefficients of nod26 proteoliposomes to the extent observed in SM vesicles (e.g. 92 % verses 67 %). This discrepancy may be due to the orientation of the nod26 molecule within the bilayer. The $HgCl_2$ sensitive site may only be accessible to one side of the molecule and the two possible orientations, that the nod26 pore may be inserted into the membrane, may account for the lack of total inhibition to control levels induced by $HgCl_2$. Whereas in SM vesicles, the nod26 channel is present in only one orientation possibly explaining the enhanced mercuric chloride sensitivity. Alternatively, the reaction of $HgCl_2$ with nod26 liposomes may not have occured stochiometrically.

Finklestein (1986) has published a detailed description of the theory and reality of water movement in biological systems. According to Finklestein's theory, the following relationship is proposed for osmotic water permeability (P_f).

$$P_f = v_w kTN / \gamma L^2 \qquad \textit{(Equation 8)}$$

v_w is the volume per water molecule in bulk solution, k is the Boltzmann constant, T is temperature, N is the number of water molecules, γ is frictional coefficient per water molecule, and L is the length of the pore. On the other hand, the following relationship is proposed for diffusive water permeability (P_d).

$$P_d = v_w kT / \gamma L^2 \qquad \textit{(Equation 9)}$$

When Equations 8 is divided by Equation 9, the result is N, the number of water molecules (Finklestein, 1986). For a narrow pore in which water molecules can not pass each other, P_f / P_d equals the number of water molecules which line up single file within the pore (Finklestein, 1986).

The P_f / P_d ratio of 18 suggests that 18 water molecules line up single file within the lumen of the nod26 pore and that the nod26 channel is longer than that of AQP1 which has a lower ratio of 13 (Finklestein et al., 1986; Stein, 1990; Mathai et al., 1996). Additionally, a $P_f / P_d > 1$ is a characteristic of water channels further strengthening the proposed role of nod26 as an aquaporin. Nod26 is only the second aquaporin for which a P_f / P_d ratio has been measured. It is interesting that AQP1 has a higher unit conductance and shorter pore length than nod26, raising the possibility that pore length can influence water permeation rates in this class of aquaporins (Rivers et al., 1997).

Table II summarizes the properties for glycerol transport determined in both SM vesicles and nod26 proteoliposomes. Glycerol flux occurs rapidly in both systems and in nod26 proteoliposomes, glycerol transport occurs at a magnitude 40-fold higher than for control liposomes! $HgCl_2$ drastically inhibits glycerol transport in each system resulting in an 80-90% inhibition.

SM vesicles are readily permeable to water, formamide, and glycerol with the flux of these nonelectrolytes showing $HgCl_2$ sensitivity. In constrast, urea flux

Table II. Summary of glycerol transport values for SM vesicles and nod26-containing proteoliposomes.

	SM	Proteoliposomes
P_{gly} x 10^{-5}, cm/s (20 °C)	3.2 ± 0.29[a] (n=4)	0.77 ± 0.45[b] (n=3)
P_{gly} x 10^{-5}, cm/s (20 °C) w/ $HgCl_2$	0.5 ± 0.088 (n=4)	0.05 ± 0.03 (n=2)
% Inhibition by $HgCl_2$	84 %	94 %

[a] ± standard error.
[b] ± standard deviation.

shows no inhibition by $HgCl_2$ and does not appear to be facilitated. SM is modestly permeable to acetamide showing a weak $HgCl_2$ sensitivity suggesting a weak flux through nod26. Reconstitution of purified nod26 into liposomes demonstrate nod26 can undoubtedly mediate at least the glycerol transport observed in SM vesicles.

The following van der Waal's volumes were found for water and the test solutes: water, 10.6 cm^3/mol; formamide, 24.8 cm^3/mol; urea, 32.8 cm^3/mol; acetamide, 35.9 cm^3/mol; and glycerol, 51.4 cm^3/mole (Maggi & Meli, 1986). The relative permeability of the solutes (formamide > glycerol >> acetamide > urea) suggests the selectivity of nod26 for solutes is not based solely on size. Other parameters that may affect permeability may be the relative flexibility or the relative hydrophobicity of the molecule. Similar to nod26, AQP3 has been

shown to be multiselective. For instance AQP3 mediates high rates of transport for glycerol, urea and water (Ishibashi et al., 1994; Frigeri et al., 1995; Echevarria et al., 1996; Ishibashi et al., 1997). Glycerol transport for AQP3 occurs at a higher rate than urea (Echevarria et al., 1996) and the function of AQP3 *in vivo* as a mutliselective transporter remains unknown. Interestingly, nod26 does not facilitate urea transport so even multifunctional aquaporins are distinct, indicating a functional diversity among members of the aquaporin family.

Although the P_f / P_d ratio for water transport may suggest a single file pathway (Finklestein, 1986; Stein, 1990), the permeability to glycerol, a molecule whose van der Waal's volume is more than twice the size of two water molecules side by side, raise the possibility that solute transport may occur by a pathway distinct from that of water. Also the increased $HgCl_2$ sensitivity (94% inhibition) exhibited for glycerol transport through nod26 as compared to water flux (67% inhibition) may suggest distinct pathways. This conclusion is feasible if one considers the clear cut dissociation in water and solute transport exhibited by MIP family members. AQP1 is readily permeable to water and exhibits no solute transport (Zeidel et al., 1992; Preston et al., 1992; Zeidel et al., 1994), AQP3 is highly permeable to glycerol, urea and water (Ishibashi et al., 1994; Frigeri et al., 1995; Echevarria et al., 1996; Ishibashi et al., 1997). The glycerol facilitator from *E. coli.*, GlpF, is highly permeable to glycerol but exhibits no observed water permeation (Heller et al., 1980; Sweet et al., 1990; Maurel et al., 1994). Interest-

ingly, on a phylogenetic tree nod26, GlpF, and AQP3 developed on a different branches from other aquaporins (Ishibashi et al., 1994) suggesting their shared ability to facilitate glycerol transport may be due to an evolutionary / structural relationship.

Role of nod26 in symbiosis and symbiosome membrane transport.

The transport studies investigated in this report raise the question: in the symbiosome membrane does nod26 function specifically as a water transporter, a solute / metabolite transporter, an ion channel, or a more promiscuous transporter capable of some or all the activities just described?

Previous work has shown nod26 is capable of ion transport in planar lipid bilayers (Lee et al., 1995). This activity is similar to another aquaporin, AQP0, which also forms voltage dependent ion channels with similar properties upon incorporation in planar lipid bilayers (Gorin et al., 1984; Zampighi et al., 1985; Ehring et al., 1990; Shen et al., 1991). However, again similar to nod26, AQP0 shows no detectable ion channel upon expression in *Xenopus* oocytes (Mulders et al., 1995; Zampighi et al., 1995; Chandy et al., 1997). The *Xenopus* oocyte data suggest that the large conductance ion channel activity of AQP0 and nod26 may be solely an *in vitro* phenomena, and that these proteins form aquaporin activities in biological systems. However, *Xenopus* oocytes are a system distinct from the SM and possesses a distinct array of lipid and protein components, including a va-

riety of regulatory components, as well as lacking other potentially crucial components of the SM which may influence nod26 activity. Because of this, studies in heterologous systems must be interpreted with caution. Therefore, *in situ* studies on SM vesicles are crucial for validating nod26 transport activities.

In patch clamp recording of whole symbiosomes, a nonselective voltage dependent channel with a large conductance that could possibly be due to nod26 is occasionally observed (David Day, personal communication). Whether nod26 is capable of mediating ion flux in the SM under certain physiological conditions awaits further investigation.

In the present study nod26 was shown to be capable of facilitating glycerol transport and potentially other solutes in addition to its aquaporin properties. Several other MIP family proteins such as GlpF (Heller et al., 1980; Sweet et al., 1990; Maurel et al., 1994) , FpsI (Van Aelst et al., 1991; Luyten et al., 1995), and AQP3 (Ishibashi et al., 1994; Frigeri et al., 1995; Echevarria et al., 1996; Ishibashi et al., 1997) possess glycerol and / or small nonelectrolyte transport. The solute transporting activities of GlpF, FpsI, and AQP3 indicate that solute transport, while unusual, is not uncommon for MIP family members. However this is the first documented example of a plant aquaporin with multiple functions, and argues for a role of nod26 in solute transport across the SM.

Malate, which was previously shown to be transported across the SM with rates sufficient to support the bacteroid's fixation of nitrogen (Price et al., 1987;

Udvardi et al., 1988; Ou Yang et al., 1990; Li & Day, 1991), is a potentially highly crucial molecule to the maintenance of the symbioses. It has been documented that a dicarboxylate transporter exists within the SM with capabilities of transporting both malate and succinate (Udvardi et al., 1988; Yang et al., 1990; Li & Day, 1991; Streeter, 1995; Udvardi & Day, 1997). Whether the solute transporting properties of the nod26 channel include malate, which can exist in an uncharged protonated form needs to be addressed. Further studies of malate transport studies in purified nod26 containing liposomes as well as radioactive malate uptake studies in *Xenopus* oocytes will likely shed some light on the question of malate transport via nod26. Furthermore, as in a variety of biological membranes, various other metabolites, osmolytes, and regulatory molecules cross the SM (Udvardi & Day, 1997). Whether nod26 facilitates the transport of such molecule(s) needs to be evaluated.

While these observations established that nod26 has the properties to account for the observed water flux seen in isolated SM vesicles, less apparent are the possible roles such a water transporter play in the SM. Infected cells contain a tremendous amount of symbiosomes (Figure 1) that take up the predominant amount of the intracellular space (Roth et al., 1988). Considering the volume of these organelles, it is possible that they may serve an osmoregulatory role within the infected cell in response to stresses. Water flux in and out of these organelles, mediated by nod26, may be important for maintaining osmotic equilibrium and

turgor. As ions and / or metabolites cross the SM this could result in an osmotic gradient that is altered by water flux through nod26.

Also, the integrity of the enclosed endosymbiont is crucial for nitrogen fixation, and it needs to be protected from turgor and drought stress. Many genes are regulated in response to drought and salt stresses such as the *Arabidopsis thaliana* homolog RD28 which is upregulated upon drought treatments (Yamaguchi-Shinozaki et al., 1992; Maurel et al., 1997) and the *Mesembryanthemum crystallinum* (common ice plant) homolog MIPA which is downregulated by salt stress (Yamada et al., 1995; Maurel, 1997). Drought stressed nodules accumulate osmoprotectant metabolites such as proline (Hu et al., 1992), and nod26 could provide the conduit for water flux to maintain water potential under changing environmental conditions. In addition, nodule respiration is highly sensitive to osmotic stresses such as drought and salinity, and respond rapidly and reversibly by lowering O_2 diffusion through intercellular spaces, resulting in the inhibition of nitrogen fixation (Hunt et al., 1993). It has been proposed that these responses may involve changes in osmolyte concentration and water flux (Streeter, 1992; Purcell et al., 1993; Denison et al., 1995), which nod26 could potentially facilitate.

The nod26 aquaporin may be involved in a wide range of functions within the nodule. Whether nod26 mediated water transport serves an osmoregulatory role, a protective response to drought, salinity, or other stresses, or is involved in cell growth / expansion and differentiation are interesting possibilities that await

further investigation. Also, nod26 is a member of a diverse protein family of plant aquaporins and differences in transport rates and selectivities, cellular and subcellular location, and regulation between these proteins may provide a structural and functional diversity to accommodate the multiple cellular roles that these proteins likely play.

LIST OF REFERENCES

LIST OF REFERENCES

Agre, P., Brown, D., & Nielson, S. (1995) *Curr. Opin. Cell Biol.* 7, 472-483.

Agre, P., Douglas, L.D., Devidas, S., & Guggino, W.B. (1997) *Science* **275**, 1490.

Agre, P., Sasaki, S., & Chrispeels, M.J. (1993) *Am. J. Physiol.* **265**, F461.

Bachmann, M., Shiraishi, N., Campbell, K.W.H., Yoo, B.C., Harmon, A.C., & Huber, S. C. (1996) *Plant Cell* **8**, 505-517.

Bai, L., Fushimi, K., Sasaki, S., & Marumo, F. (1996) *J. Biol. Chem.* **271**, 5171-5176.

Bauer, W.D. (1981) *Ann. Rev. Plant Physiol.* **32**, 407-449.

Benzanilla, F., & Armstrong, C.M. (1977) *J.Gen. Physiol.* **70**, 549-566.

Bergmann, H., Preddie, E., & Verma, D.P.S. (1983) *EMBO J.* **2**, 2333-23339.

Bohnert, H.J., Nelson, D.E., & Jensen, R.G. (1995) *Plant Cell* **7**, 1099-1111.

Bolton, E., Higgison, B., Harrington, A., & O'Gara, F. (1986) *Arch. Microbiol.* **144**, 142-146.

Bradford, M.M. (1976) *Anal. Biochem.* **72**, 248-254.

Brown, D., Katsura, T., Kawashima, M., Verkman, A.S., & Sabolic, I. (1995) *Histochem. Cell Biol.* **104**, 1-9.

Calamita, G., Bishai, W.R., Preston, G.M., Guggino, W.B., & Agre, P. (1995) *J. Biol. Chem.* **270**, 29063-29066.

Calvert, H.E., Pence, M.K., Pierce, M., Malik, N.S.A., & Bauer, W.D. (1984) *Can. J. Bot.* **62**, 2375-2384.

Chandy, G., Zamphighi, G.A., Kreman, M. & Hall, J.E. (1997) *J. Membr. Biol.* **159**, 24-39.

Cheng, A., Van Hoek, A.N., Yeager, M., Verkman, A.S., & Mitra, A.K. (1997) *Nature Struct. Biol.* **387**, 627-630.

Chrispeels, M.J. & Agre, P. (1994) *Trends Biochem. Sci.* **19**, 421-425.

Corby, H.D.L., Polhill, R.M., & Sprent, J.I. (1983) *in Nitrogen Fixation: Legumes* (Broughton, W.J. ed) Clarendon Press, Oxford, pp. 1-35.

Daniels, M., Mirkov, T.E., & Chrispeels, M.J. (1994) *Plant Physiol.* **106**, 1325-1333.

Day, D.A., Ou Yang, L.-J., & Udvardi, M.K. (1990) in *Nitrogen Fixation: Achievements and Objectives* (Gresshoff, P.M., Roth, L.E., Stacey, G., & Newton, W.E., eds.) Champman and Hall, New York:London, pp. 219-226.

Day, D.A., Price, G.D., & Udvardi, M.K. (1989) *Aust. J. Plant Physiol.* **16**, 69-84.

Day, D.A. & Udvardi, M.K. (1993) *Symbiosis* **14**, 175-189.

Dean, D.R. & Jacobsen M.R. (1992) in *Biological Nitrogen Fixation* (Stacey, G., Burris, R.H., & Evans, H.J. eds.) Chapman and Hall, New York:London, pp. 349-398.

Deen, P.M.T., Verdijk, M.A.J., Knoers, N.V.A.M., Wieringa, B., Monnens, L.A.H., Van Os, C.H., & Van Oost, B.A. (1994) *Science* **264**, 92-95.

De Lajudie, P., & Huguet, T. (1988) *Plant Molec. Biol.* **10**, 537-548.

Delporte, C., O'Connell, B.C., He, X., Ambudkar, S., Agre, P., & Baum, B.J. (1996) *J. Biol. Chem.* **271**, 22070-22075.

Denison, R.F., & Dinraide, T.B. (1995) *Plant Physiol. (Bethseda)* **84**, 584-592.

Echevarria, M., Erich, W.E., & Frindt, G. (1996) *J. Biol. Chem.* **271**, 25079-25082.

Ehring, G.R., Zampighi, G.A., Horwitz, J., Bok, D., & Hall, J.E. (1990) *J. Gen. Physiol.* **96**, 631-664.

Ehring, G.R., Lagos, N., Zampighi, G.A., & Hall, J.E. (1991) *J. Memb. Biol.* **126**, 75-88.

Faucher, C., Camut, S., Denarie, J., & Truchet, G., (1988) *Mol. Plant-Microbe Interact.* **2**, 291-300.

Faucher, C., Leronge, P., Roche, P., Rosenberg, C., Debelle, F., Vane, J., Cervantes, E., Shanna, S.B., Truchet, G., Prime, J.C., & Denarie, J. (1989) *Signal Molecules in Plants and Plant-Microbe Interactions* NATO ASI Series, 3679-3687.

Finkelstein, A. (1986) *Water Movement Through Lipid Bilayers, Pores, and Plasma Membranes: Theory and Reality*, John Wiley and Sons, New York.

Finan, T.M., Hirsch, A.M., Leigh, J.A., Johansen, E., Kuldau, G.A., Deegan, S., Walker, G.C., & Signer, E.R. (1985) *Cell* **40**, 869-877.

Finan, T.M., Wood, J.M., & Jordan, D.C. (1981) *J. Bacteriol.* **148**, 193.

Fischer, H.M., & Hennecke, H. (1987) *Mol. Gen. Genet.* **209**, 621-626.

Fortin, M.G., Morrison, N.A., &Verma, D.P.S. (1987) *Nucleic Acid Res.* **15**, 813-824.

Franssen, H.J., Nap, J.P., & Bisseling, T. (1992) in *Biological Nitrogen Fixation* (Stacey, G., Burris, R.H., & Evans, H.J. eds.) Chapman and Hall, New York:London, pp. 349-398.

Frigeri, A., Gropper, M.A., Turck, C.W., &Verkman, A.S. (1995) *Proc. Natl. Acad. Sci. USA* **92**, 4328-4331.

Fujita, N., Ishikawa, S., Sasaki, S., Fujisawa, G., Fushimi, K., Marumo, F., & Saito, T. (1995) *Am J. Physiol.* **269**, F926-F931.

Fushimi, K., Sasaki, S., & Marumo, F. (1997) *J. Biol. Chem.* **272**, 14800-14804.

Gloudemans, T., Bhuvaneswari, T.V., Moerman, M., Van Brussel, A.A.N., Van Kammen, A., and Bisseling, T. (1989) *Plant Mol. Biol.* **12**, 157-167.

Golomb, M. & Chamberlain, M. (1974) *J. Biol. Chem.* **249**, 2858.

Gorin, M.B., Yancey, S.B., Cline, J., Revel, J.P., & Horwitz, J. (1984) *Cell* **39**, 49-59.

Govers, F., Gloudemans, T., Moerman, M., Van kammen, A., & Bisseling, T., (1985) *EMBO J.* **4**, 861-867.

Govers, F., Moerman, M., Hooymans, J., Van Kammen, A., & Bisseling, T. (1986) *Planta* 169, 513-517.

Govers, F., Nap, J.P., Van Kammen, A., & Bisseling, T. (1987) *Plant Physiol. Biochem.* **25**, 309-322.

Gunderson, R.E., & Nelson, D.L. (1987) *J. Biol. Chem.* **262**, 4602-4609.

Harmon, A.C., Yoo, B.C., Lee, J.Y., Zhang, Y., & Roberts, D.M. (1997) in *Protein Phosphorylation in Plants* (Shewry, P.R., Halford, N. G., & Hooley, R. eds.) Clarendon Press, Oxford, pp. 267-277.

Harper, J.F., Sussman, M.R., Schaller, E.G., Putnam-Evans, C., Charbonneau, H., & Harmon, A.C. (1991) *Science* **252**, 951-954.

Heller, K.B., Lin, E.C.C. & Wilson, T.H. (1980) *J. Bacteriol.* **144**, 274-278.

Höfte, H., Hubbard, L., Reizer, J., Ludevid, D., & Herman, E.M. (1992) *Plant Physiol.* **99**, 561-570.

Horwitz, J., & Bok, D. (1987) *Biochemistry* **26**, 8092-8098.

Hu, C.A., Delauney, A. J., & Verma, D.P.S. (1992) *Proc. Natl. Academ. Sci. U.S.A.* **89**, 9354-9358.

Huber, S.C. & Huber, J.L. (1995) *Planta* **196**, 180-189.

Ishibashi, K., Sasaki, S., Fushimi, K., Yamamoto, T., Kuwahara, M., & Marumo, F. (1997) *Am. J. Physiol.* **272**, F325-F241.

Ishibashi, K., Sasaki, S., Fushimi, K., Uchida, S., Kuwahara, M., Saito, H., Furukawa, T., Nakajima, K., Yamaguchi, Y., Gojobori, T., & Marumo, F. (1994) *Proc. Natl. Acad. Sci.* USA **91**, 6269-6273.

Jacobs, F.A., Zhang, M., Fortin, M.G., & Verma, D.P.S. (1987) *Nucleic Acids Res.* **15**, 1271-1280.

Jap, B.K. & Lee, H. (1995) J. Mol. Biol. 251, 413-420.

Jo, I., Harris, W.H., Amendt-Raduege, A.M., Majweski, R.R., & Hammond, T.G. (1995) *Proc. Natl. Acad. Sci. USA* **92**, 1876-1880.

Johnson, K.D., Herman, E.M. & Chrispeels, M.J.(1989) *Plant Physiol.* **91**, 1006-1013

Johansson, I., Larsson, C., Ek, B., & Kjellbom, P. (1996) *Plant Cell* **8**, 1181-1191.

Jung, J.S., Bhat, R.V., Preston, G.M., Guggino, W.B., Baraban, J.M., & Agre, P. (1994) *Proc. Natl. Acad. Sci. USA* **91**, 13052-13056.

Jung, J.S., Preston, G.M., Smith, B.L., Guggino, W.B., & Agre, P. (1994) *J. Biol. Chem.* **269**, 14648-14654.

Kaldenhoff, R., Kolling, A., Meyers, J., Karmann U, & Ruppel, G. (1995) *Plant J.* **7**, 87-95.

Kaldenhoff, R., Kolling, A., & Richter, G. (1993) *Plant Mol. Biol.* **23**, 1187-1198.

Kaldenhoff, R., Kolling, A., & Richter, G. (1997) *J. Photobiol. Photobiochem.* In press.

Kasahara, M. & Hinkle, P.C. (1977) *J. Biol. Chem.* **252**. 7384-7390.

Katsura, T., Ausiello, D.A., & Brown, D. (1996) *Am. J. Physiol.* **270**, F548-F533.

Kijne, J.W. (1992) in *Biological Nitrogen Fixation* (Stacey, G., Burris, R.H., & Evans, H.J. eds.) Chapman and Hall, New York:London, pp. 349-398.

King, L.S. & Agre, P. (1996) *Annu. Rev. Physiol.* **58**, 619-648.

Knepper, M.A. (1997) *Am. J. Physiol.* **272**, F3-F12.

Kuwahara, M., Fushimi, K., Terada, Y., Bai, L., Marumo, F., & Sasak, S. (1995) *J. Biol. Chem.* **270**, 10384-10387.

Kuypers, F.A., Roelofsen, B., Berendsen, W., Op Den Kamp, J.A.F., & Van Deenen, L.L.M. (1984) *J. Cell Biol.* **99**, 2260-2267.

Kyte, J. & Doolittle, R.F. (1982) *J. Mol. Biol.* **157**, 105-132.

Laemmli, U.K. (1970) *Nature* **227**, 680-685.

Lampe, P.D. & Johnson, R.G. (1990) *Eur. J. Biochem.* **156**, 541-547.

Lande, M.B., Donovan, J.M., & Zeidel, M.L. (1995) *J. Gen. Physiol.* **106**, 67-84.

Lande, M.B., Jo, I., Zeidel, M.L., Somers, M., & Harris, W.H., Jr. (1996) *J. Biol. Chem.* **271**, 552-557.

Lee, D.M., Bhakta, K.Y., Raina, S., Yonescu, R., Griffin, C.A., Copeland, N.G., Gilbert, D.J., Jenkins, N.A., Preston, G.M., & Agre, P. (1996) *J. Biol. Chem.* **271** 8599-8604.

Lee, J.W., Zhang, Y., Weaver, C.D., Shomer, N.H., Louis, C.F., and Roberts, D.M.(1995) *J. Biol. Chem.* **270**, 27051-27057.

Lee, J.W. (1995) Thesis for M.S., Univ. of Tennessee at Knoxville.

Legocki, R.P., and Verma, D.P.S. (1980) *Cell* **20,** 153-163.

LeVier, K., Day, D.A., & Guerinot, M.L. (1996) *Plant Physiol.* **111**, 893-900.

Li, Y. & Day, D.A. (1991) *J. Exp. Bot.* **42**, 1325-1329.

Libbenga, K.R. & Harkes, P.A.A. (1973) *Planta* **114**, 17-28.

Long, S.R., (1992) in *Biological Nitrogen Fixation.* (Stacey, G., Burris, R.H., & Evans, H.J. eds.) Chapman and Hall, New York:London, pp. 560-597.

Long, S.R. (1996) *Plant Cell* **8**, 1885-1898.

Ludevid, D. Höfte, H., Himelblau, E., & Chrispeels, M.J. (1992) *Plant Physiol.* **100**,1633-1639.

Luyten, K., Albertyn, J., Skibbe, F.W., Prior, B.A., Ramos, J., Thevelein, J.M., & Hohmann, S. (1995) *EMBO J.* **14**, 1360-1371.

Maggi, C.A. & Meli, A. (1986) *J. Auton. Pharmacol.* **6**, 133-162.

Mathai, J.C., Mori, S., Barbara, S.L., Preston, G.M., Mohandas, N., Collins, M., van Zijl, P.C.M., Zeidel, M.L., & Agre, P. (1996) *J. Biol. Chem.* **271**, 1309-1313.

Maurel, C. (1997) *Annu. Rev. Plant Physiol. Plant Mol. Biol.* **48**, 399-429.

Maurel, C., Kado, R.T., Guern, J., Chrispeels, M.J. (1995) *EMBO J.* **14**, 3028-3035.

Maurel, C., Reizer, J., Shroeder, J.I., Chrispeels, M.J., & Saier, M.H., Jr. (1994) *J. Biol. Chem.* 269, 11869-11872.

Mellor, R.B., Christensen, T.M.I.E., & Werner, D. (1986) *Proc. Natl. Acad. Sci. USA* **83**, 659-663.

Mellor, R.B. & Werner, D. (1990) in *Biological Nitrogen Fixation.* (Stacey, G., Burris, R.H., & Evans, H.J. eds.) Chapman and Hall, New York:London, pp. 349-398.

Melroy, D.L. & Herman, E.M. (1991) *Planta* **184**, 113-122.

Miao, G.-H., Hong, Z., & Verma, D.P.S. (1992) *J. Cell Biol.* **118**, 481-490.

Miao, G.-H., & Verma, D.P.S. (1993) *Plant Cell* **5**, 781-794.

Minami, E., Kouchi, H., Cohn, J.R., Tomoya, O., & Stacey, G. (1996) *Plant J.* **10**, 32-32.

Mitra, A.K. & Yeager, M. (1994) *Biochemistry* **33**, 12735-12740.

Moreau, S., Meyer, J.-M., & Puppo, A. (1995) *FEBS Lett.* **361**, 225-228.

Morrison, N. & Verma, D.P.S., (1987) *Plant Mol. Biol.* **9**, 185.

Mulders, S.M., Preston, G.M., Deen, P.M.T., Guggino, W.B., van Os, C.H., & Agre, P. (1995) *J. Biol. Chem.* **270**, 9010-9016.

Mylona, P., Pawlowski, K., & Bisseling, T. (1995) *Plant Cell* 7, 869-885.

Negrette, H., Rivers, R., Gough, A.H., Colombini, M., & Zeidel, M.L. (1996) *J. Biol. Chem.* **271**, 11627-11630.

Newcomb, W. (1976) *Can J. Bot.* **54**, 2163-2186.

Newcomb, W. (1981) in *Nodule Morphogenesis and Differentiation* (Giles, K.L., & Athereley, A.G., eds.) Academic Press, New York: New York, pp.247-297.

Newcomb, W., Sippel, D., & Peterson, R.L. (1979) *Can. J. Biol.* **57**, 2603-2616.

Nielsen, S., Marples, D., Frokiaer, J., Knepper, M., & Agre, P. (1996) *Kidney International* **49**, 1718-1723.

Nielsen, S., Smith, B.L., Christensen, E.I., & Agre, P. (1993) *Proc Natl Acad Sci USA* **90**, 7275-7279.

Opperman, C.H., Taylor, C.G. & Conkling, M.A. (1994) *Science* **263**, 221-223.

Ou Yang, L.-J., Udvardi, M.K., & Day, D.A. (1990) *Planta* **182**, 437-444.

Ou Yang, L.-J., Whelan, J., Weaver, C.D., Roberts, D.M., & Day, D.A. (1991) *FEBS Lett.* **293**, 188-190.

Pao, G.M., Wu, L.-F., Johnson, K.D., Höfte, H., Chrispeels, M.J., Sweet, G., Sandal, N.N., & Saier, M.H., Jr. (1991) *Mol. Microbiol.* **5**, 33-37.

Park, J.H. & Saier, M.H., Jr. (1996) *J. Membrane Biol.* **153**, 171-180.

Preston, G.M. & Agre, P. (1991) *Proc. Natl. Acad. Sci.* USA **88**, 11110-11114.

Preston, G.M., Carroll, T.P., Guggino, W.B., & Agre, P. (1992) *Science* **256**, 385-387.

Preston, G.M., Jung, J.S., Guggino, W.B., & Agre, P. (1993) *J. Biol. Chem.* **268**, 17-20.

Preston, G.M., Jung, J.S., Guggino, W.B., & Agre, P. (1994) *J. Biol. Chem.* **269**, 1668-1673.

Price, G.D., Day, D.A., & Gresshoff, P.M. (1987) *J. Plant Physiol.* **130**, 157-164.

Purcell, L.C., & Sinclair, T.R. (1994) *Plant Cell Environ.* **17**, 837-843.

Raina, S., Preston, G.M., & Agre, P. (1995) *J. Biol. Chem.* **270**, 1908-1912.

Rao, Y., Jan, L.Y., & Jan, Y.N. (1990) *Nature* **345**, 163-167.

Regensburger, B., Meyer, L., Filser, M., Weber, J., Studer, D., Lamb, J.W., Fischer, H.-M., Hanh, N., & Hennecke, H. (1986) *Arch. Microbiol.* **144**, 355-366.

Reizer, J., Reizer, A., & Saier, M.H. (1993) *Crit. Rev. Biochem. Mol. Biol.* **28**, 235-257.

Rivers, R.L., Dean, R.M., Chandy, G., Hall, J.E., Roberts, D.M., & Zeidel, M.L. (1997) *J. Biol. Chem.* **272**, 16256-16261.

Roberts, D.M., Brooks, K.P., & Dean, R.M. *Proceedings of the 2nd European Symposium on Protein Phosphorylation in Plants*. In Press.

Roberts, D.M., & Harmon, A.C. (1992) *Annu. Rev. Plant Physiol. Plant Mol. Biol.* **43**, 375-414.

Roberts, D.M., (1993) *Curr. Op. Cell Biol.* **5**, 242-246.

Robinson, D.G., Sieber, H., Kammerloher, W., & Schaffner, A.R. (1996) *Plant Physiol.* **111**, 645-649.

Ronson, C.W. & Astwood, P.M. (1985) in *Nitrogen Fixation Research Progress*. (Evans, H.J., Bottomley, PlJ., & Newton, W.E. eds) Manrtius Nijhoff Dordrecht p. 201.

Ronson, C.W., Lyttleton, P., & Robertson, J.G. (1981) *Proc. Natl. Acad. Sci. USA* **78**, 4284-4288.

Roth, E., Jeon, K., & Stacey, G. (1988) in *Molecular Genetics of Plant Microbe Interactions* (Palcios, R. and Verma, D.P.S., eds.) pp. 220-225, ADS Press, St. Paul, MN.

Roth, L.E. & Stacey, G. (1989) *Eur. J. Cell Biol.* **49**, 24-32.

Sabolic, L., Katsura, T., Verbavatz, J.-M., & Brown, D. (1995) *J. Memb. Biol.* **143**, 165-175.

Saier, M.H., Jr. (1994) *Bioessays* **16**, 23-29.

Sambrook, J., Fritsch, E.F. II, & Maniatis, T. (1989) *Molecular Cloning a Laboratory Manual, 2nd addition.* Cold Springs Harbor Laboratory Press, USA.

Sandal, N.N. & Marcker, K.A. (1988) *Nucl. Acids Res.* **16**, 9347.

Sheehy, J.E., Minchein, F.R., & Witty, J.F. (1985) *Ann. Bot.* **55**, 549-562.

Shen, L., Shrager, P., Girsch, S.J., Donaldson, P.J. & Peracchia, C. (1991) *J. Memb. Biol.* **124**, 21-32.

Shi, L.-B. & Verkman, A.S. (1996) *Biochemistry* **35**, 539-544.

Shiels, A., Kent, N.A., McHale, M., & Bangham, J.A. (1988) *Nucleic Acids Res.* **16**, 9348.

Smith, B.L., & Agre, P. (1991) *J. Biol. Chem.* **266**, 6407-6415.

Son, M., Gunderson, R.E., & Nelson, D.L. (1993) *J. Biol. Chem.* **268**, 5940-5948.

Stacey, G., Burris, R.H., & Evans, H.J. eds. (1992) *Biological Nitrogen Fixation.* Chapman and Hall, NewYork:London.

Stein, W.D. (1990) *Channels, Carriers, and Pumps: An Introduction to Membrane Transport*, pp. 66-69, Academic Press, San Diego.

Streeter, J.G. (1992) *Plant Physiol.* **84**, 584-592.

Streeter, J.G. (1995) *Symbiosis* **19**, 175-196.

Stokkermans, T.J.W., Ikeshita, S, Cohn, J., Carlson, R.W., Stacey, G., Ogawa, T., & Peters, K.N. (1995) *Plant Physiol.* **108**, 1587-1595.

Steudle, E. & Henzler, T. (1995) J. Exp. Bot. 46, 1067-1076.

Sweet, G., Gandor, C., Voegele, R., Beuerle, J., Truniger, V., Lin, E.C.C., & Boos, W. (1990) *J. Bacteriol.* **172**, 424-430.

Takemoto, L. & Hansen, J. (1981) *Biochem. Biophys. Res. Commun.* **99**, 324-331.

Terris, J., Ecelbarger, C.A., Marples, D., Knepper, M.A., & Nielson, S. (1995) *Am. J. Physiol.* **269**, F775-F785.

Thummler, F. & Verma, D.P.S. (1987) *J. Biol. Chem.* **262**, 14730-14736.

Tjepkema, J.D., & Yocum, C.S. (1974) *Planta* **119**, 351-360.

Turgeon, B.G. & Bauer, W.D. (1982) *Can. J. Bot.* **60**, 152-161.

Turgeon, B.G. & Bauer, W.D. (1985) *Planta* **163**, 328-349.

Tyerman, S.D., Whitehead, L.F., & Day, D.A. (1995) *Nature* **378**, 629-632.

Udvardi, M.K. & Day, D.A. (1989) *Plant Physiol.* **90**, 982-987.

Udvardi, M.K. & Day, D.A. (1990) *Plant Physiol.* **94**, 71-76.

Udvardi, M.K. & Day, D.A. (1997) *Annu. Rev. Plant Physiol. Plant Mol. Biol.* **48**, 493-523.

Udvardi, M.K., Lister, D.L. & Day, D.A. (1991) *Arch. Mirobiol.* **156**, 362-366.

Udvardi, M.K., Ou Yang, L.-J., Young, S., & Day, D.A. (1990) *Plant Mol. Biol. Microbe Interact.* **3**, 334-340.

Udvardi, M.K., Price, G.D., Gresshoff, P.M., & Day, D.A. (1988) *FEBS Lett.* **231**, 36-40.

Valenti, G., Frigeri, A., Ronco, P.M., D'Ettorre, & Svelto, M. (1996) *J. Biol. Chem.* **271**, 24365-24370.

Van Aelst, L., Hohman, S., Zimmerman, F.K., Jans, A.W.H., & Thevelein, J.M. (1991) *EMBO J.* **10**, 2095-2014.

Van de Sande, K., Pawlowski, K., Czaja, I., Wieneke, U., Schell, J., Smidt, J., Walden,R., Mativienko, M., Wellink, J., Van Kammen, A., Franssen, H., & Bisseling, T. (1996) *Science* **273**, 370-373.

Van de Wiel, C., Scheres, B., Franssen, H., Van Lierop, M.J. Van Lammeren, A., Van Kammen, A., & Bisseling, T., (1990) *EMBO J.* **9**, 1-7.

Van Hoek, A.N., Wiener, M., Bickenese, S., Mircke, L., Biwersi, J. & Verkman, A.S. (1993) *Biochemistry* **32**, 11847-11856.

Van Kammen, A. (1984) *Plant Mol. Biol. Rep.* **2**, 43-45.

Van Lieburg, A.F., Verdijk, M.A.J., & Knoers, N.V.A.M. (1994) *Am. J. Hum. Genet.* **55**, 648-652.

Verbavatz, J.-M., Brown, D., Sabolic, I., Vlaenti, G., Ausiello, D.A., Van Hoek, A.N., & Verkman, A.S. (1993) *J. Cell Biol.* **123**, 605-618.

Verma, D.P.S. (1992) in *Transport and Receptor Proteins of Plant Membranes* (Cooke, D.T. & Clarkson, D.T., eds.) pp. 113-117, Plenum Press, New York.

Walz, T., Smith, B.L., Agre, P., & Engel, A. (1994) *EMBO J.* **13**, 2985-2993.

Walz, T., Hiral, T., Murata, K., Heymann, J.B., Mitsuoka, K., Fujiyoshi, Y., Smith, B.L., Agre, P., & Engel, A. (1997) *Nature Struct. Biol.* **387**, 624-626.

Weaver, C.D., Crombie, B., Stacey, G., & Roberts, D.M. (1991) *Plant Physiol.* **95**, 222-227.

Weaver, C.D. & Roberts, D.M. (1992) *Biochemistry.* **31**, 8954-8959.

Weaver, C.D., Shomer, N.H., Louis, C.F., & Roberts, D.M. (1994) *J. Biol. Chem.* **269**, 17858-17862.

Weig, A., Deswarte, C., & Chrispeels, M.J. (1997) *Plant Physiol.* **114**, 1347-1357.

Werner, D. (1992) in *Biological Nitrogen Fixation.* (Stacey, G., Burris, R.H., & Evans, H.J. eds.) Chapman and Hall, New York:London, pp. 399-431.

Werner, D., Morschel, E., Dort, R., Mellor, R.B. & Bassarab, S., (1984) *Planta.* **162**, 8-16.

Werner, D., Mellor, R.B., Hahn, M.G. & Grisebach, H., (1985) *Zeitschrift fur Naturforschung.* **40c**, 179-181.

Whitehead, L.F. & Day, D. A. (1997) *Physiol. Plant.* In press.

Whitehead, L.F., Tyerman, S.D., Salom, C.L., & Day, D.A. (1995) *Symbiosis* **19**, 141-154.

Wittenberg, J.B., Bergersen, F.J., Appleby, C.A., & Turner, G.L. (1974) *J. Biol. Chem.* **249**, 4057-4066.

Wittenberg, J.B., Wittenberg, B.A., Day, D.A., Udvardi, M.K., & Appleby, C.A. (1996) *Plant and Soil Sci.* **178**, 161-169.

Witty, J.F., Minchin, F.R., Shot, L., & Sheehy, J.E., (1986) in *Nitrogen Fixation and Oxygen in Legume Root Nodules*. Oxford Surveys of plant and cellular biology, **3**, pp. 275-315.

Yamada, S., Katsuhara, M., Kelly, W.B., Michalowski, C.B., & Bohnert, H.J. (1995) *Plant Cell* 7, 1129-1142.

Yamaguchi-Shinozaki, K., Koizumi, M., Urao, S., & Shinozaki, K. (1992) *Plant Cell Physiol.* **33**, 217-224.

Yasui, M., Zelenin, S.M., Celsi, G., & Aperia, A. (1997) *Am. J. Physiol.* **272**, F443-F450.

Ye, R., & Verkman, A. S. (1989) *Biochemistry* **28**, 824-829.

Yool, A.J., Stamer, D.W., & Regan, J.W. (1996) *Science* **273**, 1216-1218.

Zaat, S.A.J., Wiffelman, C.A., Spaink, H.P., Ban Brussel, A.A.N., Okker, R.J.H., & Lugtenberg, B.J.J. (1987) *J. Bacteriol.* **169**, 198-204.

Zagotta, W.N., Hoshi, T., & Aldrich, R.W. (1990) *Science* **250**, 568-571.

Zampighi, G.A., Hall, J.E., Ehring, G.R., & Simon, S.A. (1989) *J. Cell Biol.* **108**, 2255-2275.

Zampighi, G.A., Hall, J.E., & Kreman, M. (1985) *Proc. Natl. Acad. Sci. USA* **82**, 8468-8472.

Zampighi, G.A., Kreman, M., Boorer, K.J., Loo, D.D.F., Benzanilla, F., Chandy, G., Hall, J.E., & Wright, E.M. (1995) *J. Memb. Biol.* **148**, 65-78.

Zeidel, M.L., Ambudkar, S.V., Smith, B.A., & Agre, P. (1992) *Biochemistry* **31**, 7436-7440.

Zeidel, M.L., Nielson, S., Smith, B.L., Ambudkar, S.V., Maunsbach, A.B., & Agre, P. (1994) *Biochemistry* **33**, 1606-1615.

Zhang, Y. & Roberts, D.M. (1995) *Mol. Biol. Cell* **6**, 109-117.

VITA

Robert Michael Dean was born in Cleveland, Ohio on September 15, 1971. He graduated from St. Edward High School in Lakewood, Ohio in May of 1989. In the fall of 1989 he enrolled as an undergraduate student at Bowling Green State University (BGSU) in Bowling Green, Ohio. While attending BGSU he developed a keen interest in science reflected in his double major of Chemistry and Biology. His senior year he worked on an undergraduate biochemistry research project under the supervision of Dr. Neocles Leontis. In May of 1994 he graduated from BGSU with a dual Bachelor of Science degree in Chemistry and Biology.

To pursue his interests in biochemistry he enrolled into the Department of Biochemistry at The University of Tennessee, Knoxville in the fall of 1994. He completed his graduate study in December of 1997 and was awarded a Master of Science degree.

While completing his graduate studies he was employed as a graduate teaching assistant (GTA) from January of 1995 until December of 1997. During the time of his graduate study he presented his research data at departmental seminars and was an author on several presentations and poster sessions presented at scientific meetings. Finally, as a result of his graduate research he published several papers and abstracts (see below for details).

Published papers and abstracts.

Rivers, R.L., Coury, L.A., **Dean, R.M.**, Roberts, D.M., & Zeidel, M.L. (1996) Functional analysis of the nodulin 26 aquaporin in symbiosome membranes. *Molecular Biology of the Cell (suppl)* **7**, 253a.

Rivers, R.L., **Dean, R.M.**, Roberts, D.M., & Zeidel, M.L. (1997) Permeabilities of the nodulin 26 aquaporin of soybean symbiosome vesicles. *FASEB Journal* **11** (3), A22.

Rivers, R.L., **Dean, R.M.**, Chandy, G., Hall, J.E., Roberts, D.M., & Zeidel, M.L. (1997) Functioanl analysis of nodulin 26, an aquaporin in soybean root nodule symbiosomes. *The Journal of Biological Chemistry* **272** (26), 16256-16261.

Roberts, D.M., **Dean, R.M.**, Rivers, R.L., & Zeidel, M.L. (1997) Water permeability of the symbiosome membrane: functional analysis of nodulin 26 aquaporin activity. *Plant Physiology (suppl)* **279**, 114.

Roberts, D.M., Brooks, K.P., & **Dean, R.M.** (1997) Phosphorylation of the soybean nodulin 26 aquaporin channel by a membrane-associated CDPK. *Proceedings of the 2nd European Symposium on Protein Phosphorylation in Plants,* In Press.

Work in preparation.

Dean, R.M. & Roberts, D.M. Water and solute permeabilities of the functionally reconstituted aquaporin nodulin 26. Work in preparation.